

AD-A077 867

WASHINGTON UNIV SEATTLE DEPT OF OCEANOGRAPHY

F/G 8/10

COLUMBIA RIVER EFFLUENT IN THE NORTHEAST PACIFIC OCEAN, 1961, 1--ETC(U)

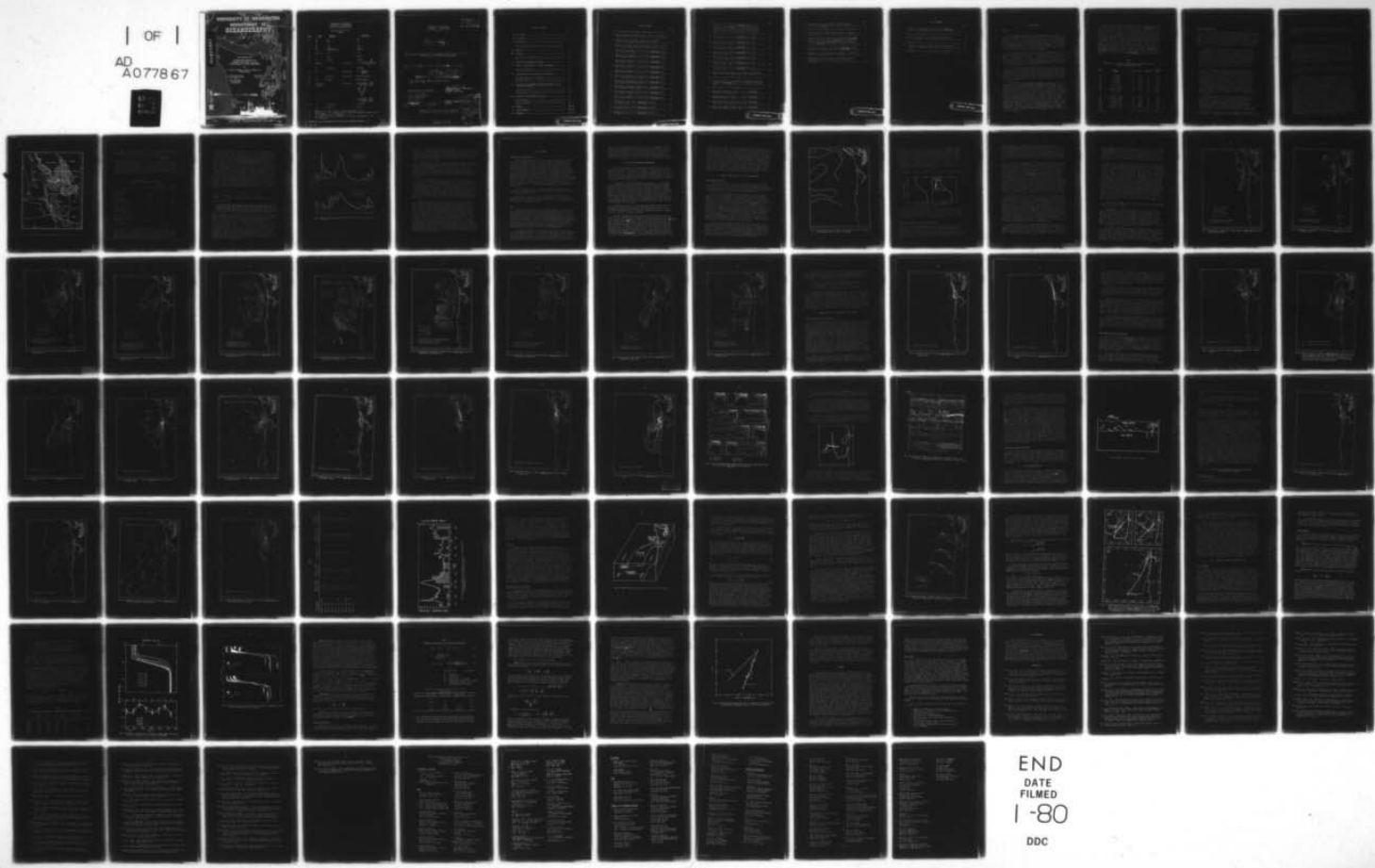
FEB 64 T F BUDINGER , L K COACHMAN

NONR-477(10)

UNCLASSIFIED TR-99

NL

| OF |  
AD  
A077867



END  
DATE  
FILED  
1-80  
DDC

ADA077867

# UNIVERSITY OF WASHINGTON

## DEPARTMENT OF OCEANOGRAPHY

UNIVERSITY  
WASSEN LABORATORIES  
CONTACT Nonr-266(84)

Technical Report No. 99

COLUMBIA RIVER EFFLUENT IN THE  
NORTHEAST PACIFIC OCEAN, 1961, 1962:  
SELECTED ASPECTS OF PHYSICAL OCEANOGRAPHY

by

Thomas F. Budinger, Lawrence K. Coachman, and  
Clifford A. Barnes

U.S. Atomic Energy Commission  
Contract AT(45-1)-1385 AT(45-1)-1725  
and

Office of Naval Research  
Contract Nonr 477(10)  
Project NR 083 012

Reference M63-18  
February 1964



FILE COPY

DDC

APPROVED FOR PUBLIC RELEASE; DISTRIBUTION UNLIMITED

SEATTLE, WASHINGTON 98105 MAY 25 1964

UNIVERSITY OF WASHINGTON  
DEPARTMENT OF OCEANOGRAPHY  
Seattle, Washington 98105

Technical Report No. 99  
ERRATA

<u>PAGE</u>	<u>LINE</u>	<u>ORIGINAL</u>	<u>CORRECTED</u>
iii	29	66	69
	30	68	71
	31	68	71
11	36	sea	river
	37	river	sea
	44	...measurements...	(delete)
14	bottom	cn	cm
30	9	then	there
43	15	mising	mixing
	equation		should read $H = \frac{32.5 Z^* - S}{32.5} dz$
41		approval	approach
54	(1)		should read $V = \frac{0.0127}{\sqrt{\sin Q}} V$
55	23	...charts...	...pressure charts...
64	39	...Okubo.	...Okubo (1962).
66	lower half of page		should read $\dots \exp \left\{ \frac{-U}{4X} \left( \frac{Y^2}{K_y} + \frac{Z^2}{K_z} \right) \right\}$ $\frac{\left\{ \frac{Y^2}{K_y} + \frac{Z^2}{K_z} \right\}}{\frac{X^2}{K_x}}$ $\dots \exp \left\{ \frac{-U}{4X} \left( \frac{Y^2}{K_y} + \frac{Z^2}{K_z} \right) \right\}$
67	7	32.% °/oo	32.5 °/oo
	13	...(2.6)	...L <sup>2.6</sup> )
71		"Barnes, C. A., and C. M. Love" should read "Love, C. M."	
73		"Gross, M. G., J. S. Creager, and D. A. McManus" should read "Gross, M. G., D. A. McManus, and J. S. Creager"	
75		"Richards, F. A., and U. Stefansson" should read "Stefansson, U., and F. A. Richards"	

CORRECTIONS HAVE BEEN ENTERED IN MOST COPIES OF TECHNICAL REPORT NO. 99.

COLUMBIA UNIVERSITY  
H. S. N LABORATORIES  
CONTRACT Nonr-266(84)

UNIVERSITY OF WASHINGTON  
DEPARTMENT OF OCEANOGRAPHY  
Seattle, Washington 98105

⑨ Technical Report No. 99

⑥ COLUMBIA RIVER EFFLUENT IN THE NORTHEAST PACIFIC OCEAN, 1961, 1962:  
SELECTED ASPECTS OF PHYSICAL OCEANOGRAPHY

by

⑩ Thomas F. Budinger, Lawrence K. Coachman, Clifford A. Barnes

⑯ ⑮ NONR-477(10),  
AT(45-1)-1385

APPROVED FOR PUBLIC RELEASE; DISTRIBUTION UNLIMITED

⑭ TR-99, REF-M63-18

U.S. Atomic Energy Commission  
Contract AT(45-1)-1385 AT(45-1)-1725  
and  
Office of Naval Research  
Contract Nonr 477(10)  
Project NR 083 012

Reference M63-18  
Feb 1964

⑯ ⑫ 86

*Clifford A. Barnes*  
CLIFFORD A. BARNES  
PRINCIPAL INVESTIGATOR

RICHARD H. FLEMING  
CHAIRMAN

Accession For	
NTIS	GRA&I
DDC TAB	<input checked="" type="checkbox"/>
Justification _____	
By _____	
Distribution _____	
Availability Codes _____	
Distr	Avail and/or special
A	<input checked="" type="checkbox"/>

Reproduction in whole or in part is permitted  
for any purpose of the United States Government

370280

*Done*

## TABLE OF CONTENTS

	Page
LIST OF FIGURES .....	v
LIST OF TABLES .....	xi
I. INTRODUCTION .....	1
Purpose .....	1
Previous Investigations .....	3
II. HYDROLOGY .....	4
III. WEATHER .....	10
Precipitation and Evaporation .....	10
Wind .....	10
IV. ESTUARY AND NEARSHORE ENVIRONMENT .....	11
V. PHYSICAL CHARACTERISTICS OF THE OCEAN REGIME .....	12
Ambient Water Features .....	12
Geostrophic Currents .....	14
VI. CHARACTERISTICS OF THE EFFLUENT IN THE OCEAN .....	27
Areal Distribution of the Effluent .....	27
Depth Distribution of the Effluent .....	30
Freshwater Budget.....	43
VII. MAJOR PHYSICAL PHENOMENA AFFECTING DISPERSION OF THE EFFLUENT IN THE SEA .....	45
General Description .....	45
Currents .....	52
Wind Transport of the Plume .....	52
VIII. DIFFUSION OF RIVER WATER IN THE SEA .....	59
General Remarks .....	59
Vertical Mixing .....	60
Horizontal Mixing .....	62
IX. SUMMARY .....	66 69
X. ACKNOWLEDGMENTS .....	68 71
XI. REFERENCES .....	68 71

## LIST OF FIGURES

	Page
1. Columbia River drainage basin and adjacent sea .....	5
2. Daily discharge from Columbia River, 1961-62, in thousands of ft <sup>3</sup> sec <sup>-1</sup> .....	8
3. Salinity ( <sup>0</sup> /oo) at bottom of upper zone, June 1962. (Pacific Oceanographic Group Circular 22, 1962).....	13
4. Salinity structure of the oceanic regime, and the influence of the Columbia River effluent on this structure.....	14
5. Geopotential topography, <sup>0</sup> /1000 decibars, <u>Brown Bear Cruise</u> 275, 10-27 January 1961.....	17
6. Geopotential topography, <sup>0</sup> /1000 decibars, <u>Brown Bear Cruise</u> 280, 7-24 March 1961.....	18
7. Geopotential topography, <sup>0</sup> /1000 decibars, <u>Brown Bear Cruise</u> 287, 8-24 May 1961.....	19
8. Geopotential topography, <sup>0</sup> /1000 decibars, <u>Brown Bear Cruise</u> 288, 9-19 June 1961.....	20
9. Geopotential topography, <sup>0</sup> /1000 decibars, <u>Brown Bear Cruise</u> 290, 6-25 July 1961.....	21
10. Geopotential topography, <sup>0</sup> /1000 decibars, <u>Brown Bear Cruise</u> 293, 14 September-20 October 1961.....	22
11. Geopotential topography, <sup>0</sup> /1000 decibars, <u>Brown Bear Cruise</u> 297, 28 November-18 December 1961.....	23
12. Geopotential topography, <sup>0</sup> /1000 decibars, <u>Brown Bear Cruise</u> 299, 23 January-7 February 1962.....	24
13. Geopotential topography, <sup>0</sup> /1000 decibars, <u>Brown Bear Cruise</u> 304, 27 March-12 April 1962.....	25
14. Geopotential topography, <sup>0</sup> /1000 decibars, <u>Brown Bear Cruise</u> 308, 7-19 June 1962.....	26
15. Salinity ( <sup>0</sup> /oo) at surface, <u>Brown Bear Cruise</u> 275, 10-27 January 1961.....	28
16. Salinity ( <sup>0</sup> /oo) at surface, <u>Brown Bear Cruise</u> 280, 7-24 March 1961.....	29
17. Salinity ( <sup>0</sup> /oo) at surface, <u>Brown Bear Cruise</u> 287, 8-24 May 1961.....	31

	Page
18. Salinity ( $^{\circ}$ /oo) at surface, <u>Brown Bear</u> Cruise 288, 9-19 June 1961 and <u>Acona</u> Cruise 6106, 19-29 June 1961 (dashed). The distributions for these two cruises are shown together to illustrate the effect after about 10 days of a strong northerly wind ( $16 \text{ m sec}^{-1}$ ) on plume movement.....	32
19. Salinity ( $^{\circ}$ /oo) at surface, <u>Brown Bear</u> Cruise 290, 6-25 July 1961.....	33
20. Salinity ( $^{\circ}$ /oo) at surface, <u>Brown Bear</u> Cruise 291, 28 July-13 August 1961.....	34
21. Salinity ( $^{\circ}$ /oo) at surface, <u>Brown Bear</u> Cruise 293, 14 September-20 October 1961.....	35
22. Salinity ( $^{\circ}$ /oo) at surface, <u>Brown Bear</u> Cruise 297, 28 November-18 December 1961.....	36
23. Salinity ( $^{\circ}$ /oo) at surface, <u>Brown Bear</u> Cruise 299, 23 January-7 February 1962.....	37
24. Salinity ( $^{\circ}$ /oo) at surface, <u>Brown Bear</u> Cruise 304, 27 March-12 April 1962.....	38
25. Salinity ( $^{\circ}$ /oo) at surface, <u>Brown Bear</u> Cruise 308, 7-19 June 1962.....	39
26. Density and salinity profiles along axis of Columbia River plume for the various Brown Bear cruises, 1961-62.....	40
27. Location of profile shown in Figure 28.....	41
28. Vertical distribution of temperature, salinity, oxygen, and chlorophyll, <u>Brown Bear</u> Cruise 312, 14 September-9 October 1962.....	42
29. Model studies of vertical mixing.....	44
30. Equivalent height of freshwater in meters, <u>Brown Bear</u> Cruise 275, 10-27 January 1961.....	46
31. Equivalent height of freshwater in meters, <u>Brown Bear</u> Cruise 290, 6-25 July 1961.....	47
32. Equivalent height of freshwater in meters, <u>Brown Bear</u> Cruise 293, 14 September-20 October 1961.....	48
33. Equivalent height of freshwater in meters, <u>Brown Bear</u> Cruise 304, 27 March-12 April 1962.....	49

	Page
34. River discharge curve ( $10^8 \text{m}^3 \text{day}^{-1}$ ) and plume volume ( $10^{10} \text{m}^3$ ) for <u>Brown Bear</u> Cruises 275-308, 1961-62.....	51
35. Major physical phenomena affecting effluent dispersion.....	53
36. Monthly averages of Ekman transport, 1961, converted to velocity ( $\text{cm sec}^{-1}$ ) of the water column 0 to 40 meters.....	56
37. Predicted axis and outward extent of plume: A) <u>Brown Bear</u> Cruise 288, 9-19 June 1961, and <u>Acona</u> Cruise 6106, 19-29 June 1961 (dashed); B) <u>Brown Bear</u> Cruise 290, 6-25 July 1961; C) <u>Brown Bear</u> Cruise 293, 14 September-20 October 1961.....	58
38. Vertical distributions of salinity at <u>Brown Bear</u> drifting station 47 during Cruise 309, 20 June-9 July 1962.....	62
39. Normalized salinity distributions of Figure 38 showing salt gain and loss between successive stations.....	63
40. Relationship between the ratio of horizontal to vertical eddy coefficients of diffusion and the scale of the phenomenon.....	68

PRECEDING PAGE BLANK

## LIST OF TABLES

	Page
1. Summary of 1961 and 1962 cruises of R. V. <u>Brown Bear</u> in the Columbia River effluent area.....	2
2. Mean annual discharge of coastal rivers.....	6
3. Correction factors for computing daily discharge at the river mouth.....	7
4. Freshwater budget.....	50
5. Computation of vertical eddy coefficient from drifting station 47 BB Cruise 309.....	61
6. Computation of vertical velocities from continuity.....	65

PRECEDING PAGE BLANK

## I. INTRODUCTION

### Purpose

The Columbia River, which drains a large portion of the Pacific Northwest, discharges a mean annual average of  $257,000 \text{ ft}^3 \text{ sec}^{-1}$  ( $7,300 \text{ m}^3 \text{ sec}^{-1}$ ) of fresh water into the northeast Pacific Ocean at  $46^\circ 20' \text{N}$ . This amounts to 14 percent of the total annual discharge from the United States of America as estimated by Langbein (1949). The flow is seasonal in nature, with a maximum in June and a secondary maximum in January. It never drops below approximately half of its average rate and the River at all seasons contributes the majority of freshwater discharged from the Pacific coast between southern California and southeastern Alaska.

The area of the Pacific Ocean into which the Columbia River discharges is characterized by weak and poorly defined currents (Barnes and Paquette 1957). The west-wind drift of the North Pacific Ocean sets eastward and on approaching the continent of North America, diverges well offshore near  $45^\circ \text{N}$ . The northern branch feeds a gyre in the Gulf of Alaska and the southern branch turns southward, forming the California Current. The Columbia enters the Pacific from a straight North-South coast line and can disperse through an arc of 180 degrees.

The low salinity water associated with the river discharge is distributed in the form of a plume. This plume extends from the river mouth over many tens of thousands of square miles and remains identifiable for long periods of time. The discharge of the Columbia River into the northeast Pacific therefore provides a good system for the study of the nature, movement, dispersion and related effects of river effluent in the ocean, as well as a very good natural system for studying the effects of wind on ocean surface waters.

The Department of Oceanography, University of Washington, under contract with the Atomic Energy Commission from 1961 to the present, has intensified its studies in the area of Columbia River discharge. The first objectives were to determine the gross features of the movement and dispersion of the effluent water in the open sea, and ultimately to ascertain the probable fate of any radioactive material that might be associated with river effluent or river-borne materials. Studies of the physical, chemical, geological and biological properties of the effluent water and ambient ocean water were undertaken with these objectives in mind. This paper reports the gross features of the plume as they were observed in 1961 and 1962 and describes quantitatively certain features of the dispersion of the plume water; other results of this continuing study will be reported when analyses are completed. The intense sampling program which commenced in January 1961 has formed the basis for investigations of chemical properties by Richards and Stefansson (1963) and Stefansson and Richards (1964); biological studies by Anderson (1964); and geological studies by Gross and co-workers (1963).

The observations and descriptions presented in this paper are based on the 1961 and 1962 results of 17 cruises of the R. V. Brown Bear to the area occupied by the effluent of the Columbia River. Twelve of these cruises were designed specifically to delineate the extent of effluent dispersion. Cruises since 1962 have investigated some of the finer detail. In addition to the measurements of temperature, salinity, and oxygen, made routinely at each oceanographic station, continuous measurements of surface salinity and temperature by means of a salinity-temperature deviation recorder were made while underway. At many stations samples were collected for phosphate, nitrate, silicate, productivity and chlorophyll a measurements. The observations for the cruises from January to June 1961 are given by Barnes and Love (1963). The information gathered on these cruises was supplemented by data from the Oregon State University's research vessels R. V. Kiska and Acona, the Canadian Naval Vessels C.N.A.V. St. Anthony and Whitethroat operating with the Pacific Naval Laboratories and the Pacific Oceanographic Group, and the M. V. John N. Cobb of the U.S. Fish and Wildlife Service. A summary of the R. V. Brown Bear's cruises is presented in Table 1.

TABLE 1

## SUMMARY OF 1961 AND 1962 CRUISES OF R. V. BROWN BEAR IN THE COLUMBIA RIVER EFFLUENT AREA

Cruise No.	Period	Days	Miles	Stations	Salinity Samples
1961					
275	10-27 Jan	18	1685	67	958
280	7-24 Mar	17	1585	74	987
282	3- 7 Apr	4	765	6	80
287	8-24 May	16	1762	82	1093
288	9-19 Jun	10	960	47	645
290	6-25 Jul	19	2300	77	1134
291	28 Jul - 13 Aug	16	1700	28	521
292	14-20 Aug	6	700	9	147
293	14 Sep - 20 Oct	36	4155	131	2872
297	28 Nov - 18 Dec	20	2122	73	1613
1962					
299	23 Jan - 7 Feb	15	1644	97	1509
304	27 Mar - 12 Apr	16	1775	89	1693
308	7-19 Jun	13	959	79	1277
309	20 Jun - 9 Jul	19	702	89	1108
310	10-23 Jul	13	1506	31	647
311	24 Jul - 14 Aug	21	2300	15	242
312	14 Sep - 9 Oct	25	3840	158	2887
TOTALS		284	30460	1152	19413

Previous Investigations

Conventional mapping and scientific investigations of rivers have in the past been confined to hydrological studies of the drainage system on land, with little attention given to the effluent characteristics in the open sea. However, in recent years, interest in the problems associated with the disposal of radioactive waste and sewage in the open seas has given impetus to scientific studies both descriptive and theoretical (e.g., NASS-NRC, 1957, 1962; Pearson 1960; Waldichuk 1963). The descriptive studies, although limited in number and detail, suggest the following characteristics:

(1) The fresh river water, after entering the sea, is confined to a relatively thin surface layer, less than 50 meters thick, with the horizontal distribution, usually in the shape of a plume, spreading over a large area. Chau (1959) showed that Pearl River water contributed as much as 20 percent of the water in the upper 20-meter layer of the South China Sea 185 km from the River mouth. Bates (1953) found that the Mississippi River flowed from Southwest Pass like a two-dimensional jet. The distinguishable effluent was confined to the upper 6 meters, 8 km from the mouth. Ichiye (1960) found traces of Mississippi water in the surface layer 740 to 925 km from the delta.

(2) The horizontal distribution of the effluent water at sea appears to be governed by a combination of the offshore circulation and the local prevailing wind. Bol'shakov (1958) observed the direction of the plume of water from the Dnieper-Bug estuary to conform with the wind direction. The direction taken by the southeast branch of the Kuri River was found to change from south to northeast within a few days, apparently in response to a wind shift from northeast to southeast (Dobrovolskii, et al., 1961). Scruton and Moore (1953) found a significant correlation between the Mississippi River plume orientation and wind direction when the currents were weak and sporadic. They concluded that the wind stress was of primary importance in distributing the plume during these periods. Henry and Elder (1958) found both the wind and prevailing current to have important effects on the Mississippi plume orientation.

(3) Although Ichiye (1960) concluded that river drainage has relatively small influence on the dynamics and water budget of the adjacent ocean, there are certain marked influences on sedimentation and biological properties directly attributable to river effluent. Bates (1953) has documented the role played by the Mississippi River in sedimentation near its mouth. Riley (1937) reported a sizeable increase in phosphate and an associated increase in plant biomass within surface waters off the Mississippi.

This report introduces the results of physical oceanographic investigations of the Columbia River effluent dispersion during 1961 and 1962.

The hydrology, weather and background ocean water characteristics are discussed first to lay a foundation for the description of the effluent. Quantitative estimates are made of the major physical phenomena affecting the dispersion, and the elements of a dispersion prediction system are discussed.

## II. HYDROLOGY

The watershed of the 1930-km (1,200-mile) long Columbia River comprises approximately  $670,000 \text{ km}^2$  (259,000 square statute miles). Eighty-five percent or about  $570,000 \text{ km}^2$  (220,000 square miles), is within the United States and constitutes about 7 percent of the nation's area. The drainage basin (Bureau of Reclamation, 1947) includes nearly all of Idaho, most of Washington, Oregon and western Montana, and smaller areas in Wyoming, Nevada and Utah (Fig. 1). The source of the main stem of the river is in a mountain lake of British Columbia, 808 meters (2,650 feet) above sea level. The River flows 749 km (465 miles) through Canada and, after entering the northeast corner of the State of Washington, continues southward through the state to the Washington-Oregon boundary where it turns westward and eventually discharges into the Pacific Ocean.

The River's largest tributary is the Snake River, which enters from the east. Other major tributaries are the Cowlitz River from the north and the Willamette River from the south. These latter two tributaries are west of The Dalles, the point at which the Columbia penetrates the Cascade Mountain range.

The annual mean discharge of the Columbia River at its mouth is  $7.3 \times 10^3 \text{ m}^3 \text{ sec}^{-1}$  ( $257,000 \text{ ft}^3 \text{ sec}^{-1}$ ) by computations reported here and  $7.2 \times 10^3 \text{ m}^3 \text{ sec}^{-1}$  estimated by Leopold (1962). This runoff of over 186 million acre-feet per year represents 77 percent of the total gauged and ungauged freshwater discharged into the Pacific Ocean south of the Strait of Juan de Fuca to and including the Rogue River at  $42^\circ 30' \text{N}$  lat or about 66 percent of the total gauged and ungauged discharge to but excluding the effluent of San Francisco Bay. These percentages are valid only when considered for an average yearly period. Differences in seasonal phasing between the peak runoff of the coastal rivers and that of the Columbia River result in marked fluctuations in the relative contributions of freshwater. The maximum discharge of the Columbia River occurs in late May or June responding to snow melt, whereas the maxima for the small coastal rivers south to the Rogue River normally occur during the heavy precipitation period from November through February. The latter period is one of minimum flow for the upper basin and part of the lower basin of the Columbia River. During the winter months, the Columbia River contributes about 60 percent of the fresh water added to the Pacific Ocean in this region, but during the late summer-early fall period, when the coastal rivers are at minima it contributes as much as 95 percent. The maximum winter runoff from some coastal rivers is often 25 times greater than their summer minimum. During the winter the Columbia River effluent mixes with the maximal flow from the coastal rivers and it becomes difficult to distinguish as a separate entity.

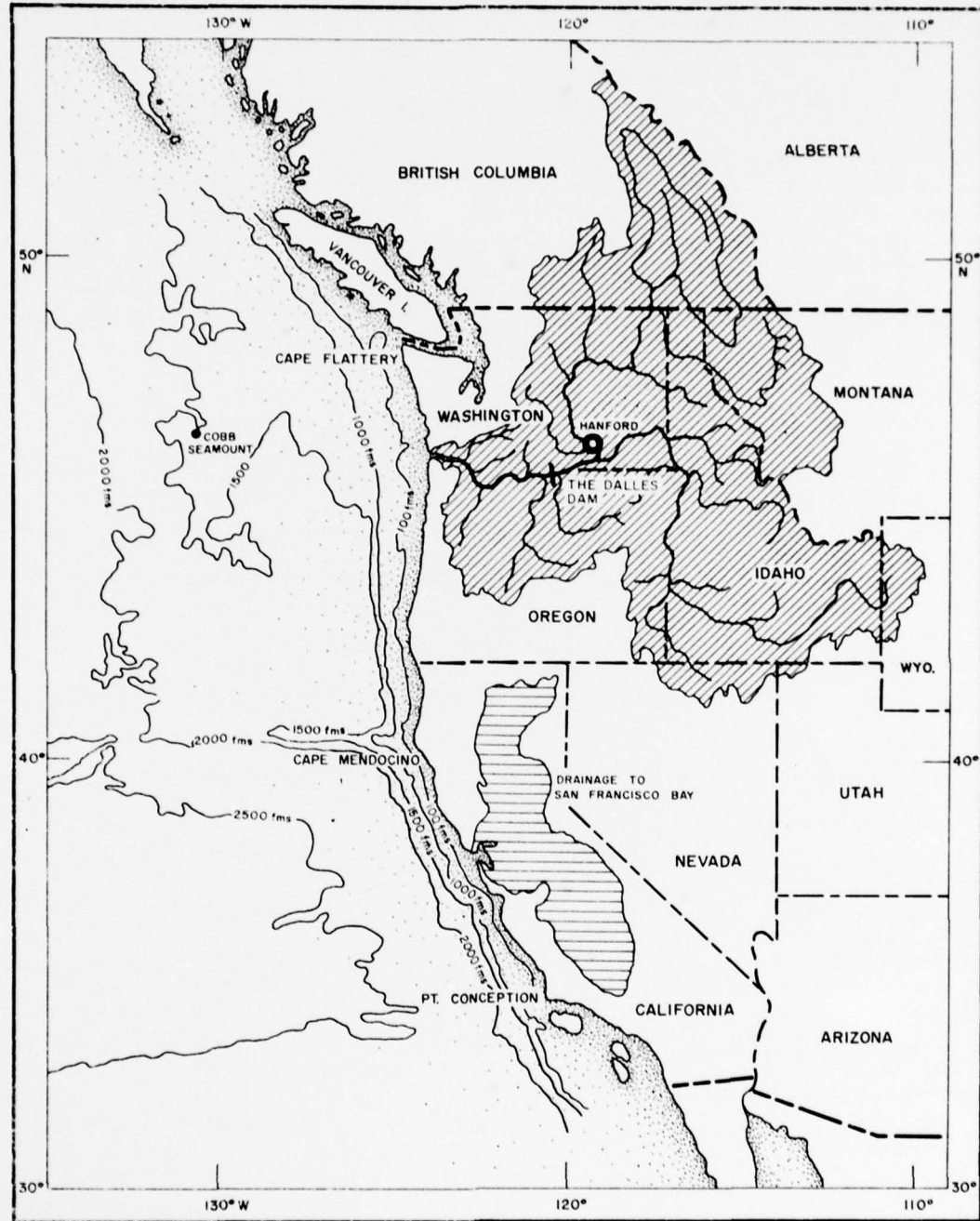


Fig. 1--Columbia River drainage basin and adjacent sea.

Table 2 shows the computed total discharge for the major rivers and the drainage basin between those rivers from the Strait of Juan de Fuca to San Francisco Bay. The values shown were computed from:

$$\text{Total Discharge} = \text{Gauged Discharge} \left[ 1 + \frac{(Pu)(DA_u)}{(Pg)(DA_g)} \right]$$

where  $P_u$  and  $P_g$  are the precipitation in the ungauged and gauged areas, respectively; and  $D_{Au}$  and  $D_{Ag}$  are the ungauged and gauged drainage areas, respectively. The precipitation figures were taken from Normal Annual Isohyetal Maps supplied by U.S. Army Corps of Engineers. The gauged area is about 75 percent of the total area. Gauged discharge figures were taken from the 10- to 30-year averages reported in Surface Water Supply of the United States (U.S. Geological Survey, 1955-1961). Areas were planimetered from large scale U.S. Geological Survey maps.

TABLE 2  
MEAN ANNUAL DISCHARGE OF COASTAL RIVERS

	<u>Area (mi<sup>2</sup>)</u>	<u>Discharge (ft<sup>3</sup> sec<sup>-1</sup>)</u>	<u>Runoff (inches)</u>
Strait of Juan de Fuca to Grays Harbor	2,520	20,658	111
Grays Harbor	2,636	12,713	66
Willapa Bay	942	5,075	73
COLUMBIA RIVER	259,000	257,000	39
From Columbia River to Umpqua River Basin	4,371	20,554	64
Umpqua River Basin	4,397	9,582	30
From Umpqua Basin to Rogue-Illinois Basins	2,149	9,497	60
Rogue and Illinois Rivers	5,737	16,198	38
From Rogue-Illinois Basins to San Francisco Bay	17,772	37,472	29

The data used to compute the percentage contribution by the Columbia River to the freshwater runoff were obtained from several sources. Daily discharge figures for the Willamette, Cowlitz, Hood, Klickitat and the Columbia River at The Dalles gauging station, are published in Weekly Report, Pacific Northwest Resources (U.S. Geological Survey, 1961-1963). Statistics for the other gauged streams below The Dalles are found in Geological Water Papers. Below The Dalles the Columbia is not gauged and only

50 percent of the drainage basin runoff into the lower Columbia River is gauged on a regular basis. However, a good estimate of the total Columbia discharge was achieved by combining the figures for the discharge at The Dalles with the adjusted discharge (25 percent of the total) of the tributaries entering the River between The Dalles and Astoria. Based on data of past years presented in Water-Supply Paper No. 1318 (U.S. Geological Survey, 1958) an estimate was made of average monthly discharge during earlier gauging periods of minor streams. A relation was derived between the flow of streams all gauged in the past and those gauged on a continuing basis. This procedure accounted for all but 14 percent of the drainage basin below The Dalles. The watersheds of gauged and ungauged rivers and streams below The Dalles were estimated by planimetry large area topographic sheets. By taking into account the mean monthly runoffs of gauged streams and the areas of gauged and ungauged drainage basins a series of correction factors was derived. The first set of derived factors related the runoff of streams in the coastal maritime regime of two peak runoff periods to that of the Willamette and Cowlitz Rivers. The second set of correction factors applies to rivers in the mountain regime with a spring snow-melt peak. This factor is applied to the discharge from the Hood and Klickitat rivers. The correction factors and equation used to compute the daily total discharge of the Columbia River at Astoria are presented in Table 3.

TABLE 3

$$\text{Astoria discharge} = \frac{\text{The Dalles discharge}}{\text{Willamette plus Cowlitz discharge}} + \left\{ \begin{array}{l} \text{Willamette plus Cowlitz discharge} \\ \text{Hood plus Klickitat discharge} \end{array} \right\} F_1 + \left\{ \begin{array}{l} \text{Hood plus Klickitat discharge} \\ \text{Cowlitz discharge} \end{array} \right\} F_2$$

where  $F_1$  and  $F_2$  are:

	Jan	Feb	Mar	Apr	May	June	July	Aug	Sept	Oct	Nov	Dec
$F_1$	1.95	2.05	1.85	2.12	1.87	1.80	1.79	1.72	1.60	2.06	1.88	1.87
$F_2$	2.20	2.13	1.68	1.92	1.84	2.07	2.08	2.06	1.95	1.97	1.91	1.93

Direct measurements at the mouth of the Columbia River for parts of May, June, and September (a total of 50 days) are available for 1959 (U.S. Army Engineers, 1960). A comparison of the daily discharge computed as described above with that measured by the U.S. Army Corps of Engineers shows good agreement. If a 5-day lag period is applied to measurements made at the lowest available gauging stations, the computed daily discharge at the mouth is within 3 percent of that reported by the Army Engineers. The ranges used in the comparison varied between  $4.25$  and  $16.7 \times 10^3 \text{ m}^3 \text{ sec}^{-1}$  ( $150,000 \text{ ft}^3 \text{ sec}^{-1}$  and  $590,000 \text{ ft}^3 \text{ sec}^{-1}$ , respectively). The Dalles is 342 km from the river mouth and the 5-day lag would suggest a mean flow of  $71 \text{ cm sec}^{-1}$ ; however, the apparent 5-day lag is in part an artifact created by the technique of applying correction factors for the lower basin. Reliance may be placed in the daily discharge if a 5-day lag is applied; however, the difference is insignificant for our purposes, and this lag is not incorporated in the daily discharge tabulations shown in Figure 2.

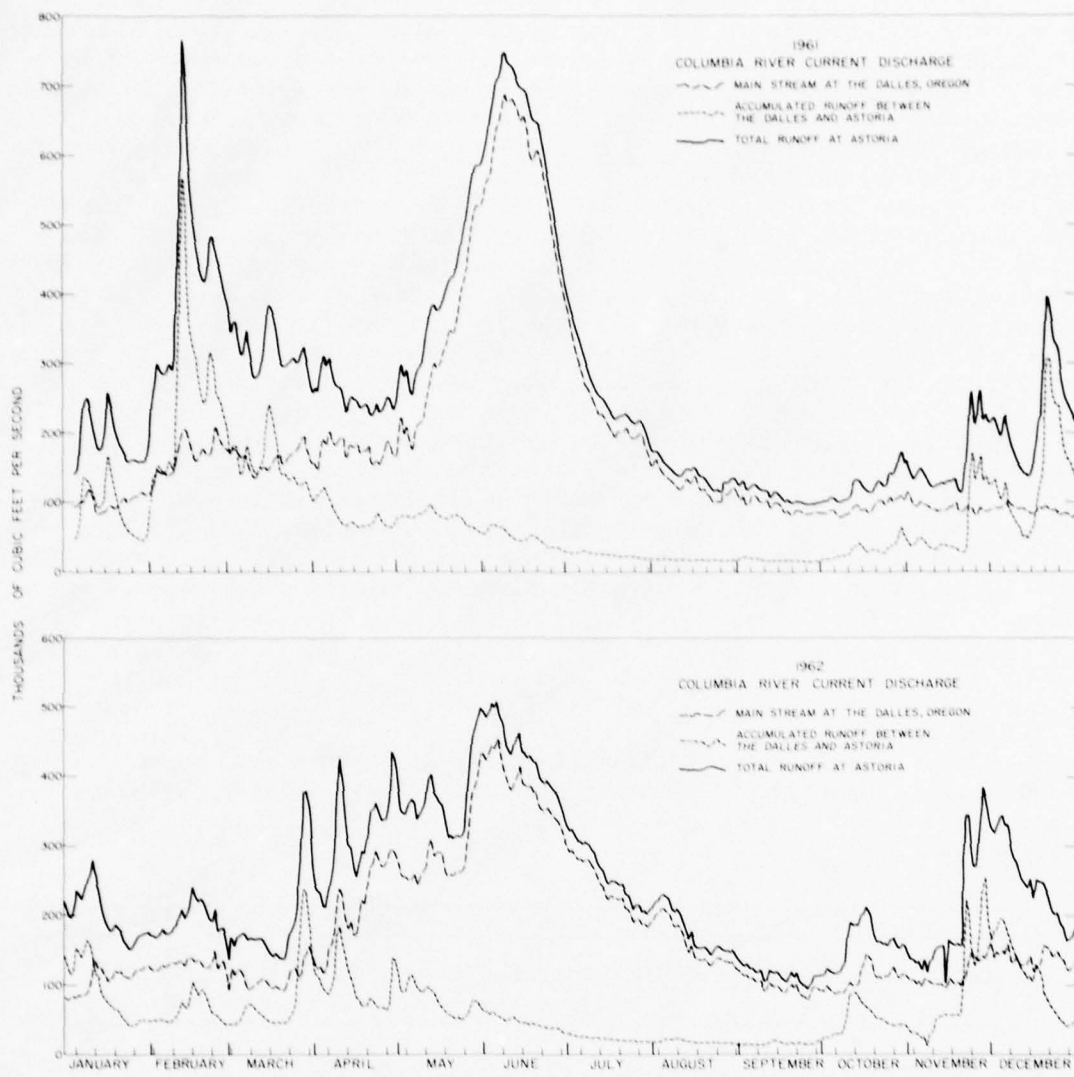


Fig. 2--Daily discharge from Columbia River, 1961-62, in thousands of  $\text{ft}^3 \text{ sec}^{-1}$ .

The results of the discharge computations for 1961 and 1962 are shown in Figure 2. The major peak in June of both years is associated with snow melt from the interior mountains, while the minor peak in February represents the winter rainy season along the coastal area. The discharge of the coastal rivers (dashed curve in Figure 2) is directly related to the local coastal rainfall. The extended periods of low discharge during the dry season of summer and early fall are apparent.

According to the estimates made by the Geological Survey (Langbein, et al., 1949) the average runoff between The Dalles and Astoria is 30 inches. This is in fair agreement with the figure of 39 inches obtained from the computations described above. The total drainage area including the Columbia River basin from the Strait of Juan de Fuca to and including the Rogue River is  $734,000 \text{ km}^2$  ( $283,000 \text{ mi}^2$ ). The computed annual discharge from this area is  $9.95 \times 10^9 \text{ m}^3 \text{ sec}^{-1}$ . This figure agrees with the estimate of Langbein and co-workers (1949) of  $9.76 \times 10^9 \text{ m}^3 \text{ sec}^{-1}$  based on runoff maps.

The role of ground water is believed to be of little importance in the quantity of daily discharge; however, the level fluctuation, dissolved solids composition, and circulation of ground water are significant variables affecting the quality of the water along the reaches of the River, particularly in the lowland areas. From the oceanographic standpoint leaching by ground water may contribute trace substances necessary for the intermediary metabolism of plants and animals. The relatively low productivity during the winter rapid runoff season may be due, in part, to a lower concentration in winter than in summer of trace substances which catalyze growth and production. The correlation between freshwater and high productivity in the sea is discussed by Anderson (1964) in a companion volume of this report.

The Washington (State) Pollution Control Commission, the Department of Conservation and the U.S. Geological Survey (1961) jointly report the mean discharge of dissolved solids at The Dalles to be 94 ppm. The two major components of the dissolved material are bicarbonates, comprising about 57 percent of the total, and calcium, making up about 14.3 percent. Because the ratio of dissolved constituents in the river differ from those in the sea, the apparent value of salinity determined from conductivity will be inaccurate, but this error is negligible except in areas of low salinity along the lower river course. The month-to-month changes in concentration of the dissolved solids are out of phase with the river stage; i.e., the higher concentrations of total dissolved solids occur when the discharge is low, but the ratios of the individual dissolved solids appear to remain rather constant throughout the year. Nitrate is twice as abundant in the river water during the late winter and early spring than it is in summer and fall. A discussion of the relation between river water nutrients and ambient ocean water nutrients is given by Stefansson and Richards (1963), and the analyses of nutrients and other constituents in the River are given by Sylvester and Carlson (1961).

### III. WEATHER

#### Precipitation and Evaporation

The mean annual precipitation in the coastal and immediate offshore areas of the northeast Pacific Ocean influenced by the Columbia River effluent is estimated to exceed  $120 \text{ cm yr}^{-1}$ . Most of the precipitation falls during the winter season, the summer months being generally dry. Precipitation exceeds evaporation and essentially the entire ocean area under consideration is one of net dilution. The surplus of precipitation is least in the west and south, and increases to a maximum of more than  $90 \text{ cm yr}^{-1}$  off the coast of British Columbia and southeastern Alaska. South of the Columbia River the surplus decreases to near zero at San Francisco Bay (Jacobs, 1951). The precipitation over the Columbia River drainage basin and contiguous coastal drainage basins is as variable as the topography. In the Columbia River Basin alone, the yearly average varies from less than 20 to over 300 cm, depending on location. The mountainous areas receive generally heavy precipitation, much of it in the form of snow, whereas the plateaus lying in the rain shadow of the Cascade Mountains receive little rain or snow.

On the average, during the summer the surplus precipitation at sea is about  $0.1 \text{ cm day}^{-1}$  and during the winter, about  $0.3 \text{ cm day}^{-1}$ , according to estimates by Jacobs (1951).

The surface exchange of water by precipitation and evaporation in the Columbia River effluent area should differ but little from that of the ambient ocean water and can probably be neglected in the first approximation of the budget of river water at sea.

#### Wind

Winds on a regional basis affect the general water circulation in an area and, on a local basis, both the movement and mixing of surface waters. The seasonal cycle of winds over the northeast Pacific Ocean is largely determined by the circulation about the North Pacific high pressure area and the Aleutian low pressure area. During the summer months the high reaches its greatest development. In July, the center of highest pressure (approximately 1,025 millibars) is located near  $30^\circ\text{N}$ ,  $150^\circ\text{W}$ ; and an average pressure in excess of 1,015 millibars prevails over most of the northeast Pacific Ocean. During this period, the Aleutian low is almost nonexistent. This pressure distribution favors predominantly northwest and north winds over the coastal and near offshore areas of Oregon and Washington.

In October, the Pacific high extends from the United States coast across the Pacific Ocean and onto the Asiatic Continent, reaching a maximum of 1,020 millibars pressure in the vicinity of  $30^\circ\text{-}35^\circ\text{N}$  and  $135^\circ\text{-}140^\circ\text{W}$ . The high weakens with the approach of the winter season and by November it is little more than a weak belt of high pressure lying between the Aleutian low and the equatorial belt of low pressure. The Aleutian low, with pressures

lower than 1,002 millibars, appears on the charts as a permanent system located near  $50^{\circ}$ N,  $180^{\circ}$ W, but in reality is a system of migratory lows frequently moving through the area during the winter season. These traveling depressions moving eastward cause considerable day-to-day variation in pressure, particularly in the area north of  $40^{\circ}$ N. The winter winds are frequently of gale force (5 to 8 percent of the observations) and range in direction from southeast at the coast to southwest in the offshore region.

#### IV. ESTUARY AND NEARSHORE ENVIRONMENT

The initial mixing of the river water with seawater occurs in the estuary and nearshore environment where tidal, surf, and hydraulic processes prevail. The relative importance of the mixing, sedimentation, and biological processes in the estuary and nearshore environments were not studied in 1961 and 1962 by the University of Washington. Model studies are being conducted by the U.S. Army Corps of Engineers and the U.S. Geological Survey at Vicksburg, Mississippi. These studies include movements of dissolved solids and bed load in the estuary.

A study of the salinity, temperature, and velocity of the Columbia River between Beaver Army Terminal (mile 52) and the River mouth was made by the North Pacific Division of the U.S. Army Corps of Engineers (1960). Data were collected in 1959 from a number of cross sections at different depths and under conditions of low, medium and high river flow. According to these measurements the River hydraulic current is reversed on flood tide during all seasons of the year up to 40 km from the mouth. During the September low discharge period of 1959, flood tide reversed the River flow at the highest upriver measuring section, 84 km (mile 52). The intrusion of salt water extended upriver past 21 km (Tongue Point) but less than 32 km during September 1959 and not past 19 km (Astoria, Oregon) during the high discharge period of May and June.

The Pacific Ocean tides can be measured upstream as far as Bonneville Dam where the diurnal range is 0.2 m. The tidal prism volume for the Columbia River from the mouth to Bonneville Dam ( $23\frac{1}{4}$  km upriver) is about  $0.85 \text{ km}^3$ . Columbia River water enters the nearshore environment in 12-hour pulses as clouds of low salinity effluent.

In 1963, examination was begun of physical processes and the scale of phenomena in the nearshore environment. The observations indicate large tidal influence and an initial mixing in the estuary of about one part ~~river~~ water with two parts ~~sea~~ water. The currents near the mouth of the river directly affect the local transport and mixing. At the mouth, midway between north and south jetties, the measured currents near the surface were about  $300 \text{ cm sec}^{-1}$  seaward on ebb and  $120 \text{ cm sec}^{-1}$  upriver on flood during June and  $240 \text{ cm sec}^{-1}$  seaward on ebb and  $180 \text{ cm sec}^{-1}$  upriver on flood in September (U.S. Army Corps of Engineers, 1960). From 5 years of discontinuous measurements (1915 to 1920, with 1915, 1919, and 1920 nearly complete) of surface current measurements by drift pole (Marmer, 1926) it was possible to resolve the hourly observations into tidal and nontidal components at the

Columbia River Lightship located 9 km southwest of the south jetty. The tidal current is clockwise rotary, semidiurnal with little diurnal inequality. Strength of flood ( $13 \text{ cm sec}^{-1}$ ) comes about one hour before low water. Flood sets northeasterly and ebb southwesterly. The nontidal current setting westerly and southerly ranged from a monthly average of  $15 \text{ cm sec}^{-1}$  in March to  $38 \text{ cm sec}^{-1}$  in June. There is some correlation between discharge and speed of current at the lightship. The yearly average set was west and the average of all measurements (over 20,000) is  $19 \text{ cm sec}^{-1}$ . Hydraulic currents are considered by Takano (1954) to diminish by an order of magnitude at a distance seaward equal to several times the width of a river mouth. This concept is supported by these measurements off the Columbia, and hence beyond 40-50 km from the river mouth geostrophic currents, wind stress, diffusion and biological transport are probably the most important processes affecting dispersion of river water and river borne materials.

#### V. PHYSICAL CHARACTERISTICS OF THE OCEAN REGIME

##### Ambient Water Structure

The northeast Pacific Ocean is a region of net dilution, in which the precipitation on the sea surface and adjacent land masses exceeds the evaporation. The land runoff acts as a line source of freshwater extending from southern Alaska to the coast of northern California. Along this line the Columbia River is by far the largest single contributor.

The area of the northeast Pacific Ocean subject to the greatest influence by the Columbia River outfall is bounded by latitudes  $40^\circ$  and  $50^\circ\text{N}$  from the coast ( $124^\circ\text{W}$ ) west to  $132^\circ\text{W}$ , and is subarctic in character. Reviews of the oceanography of the subarctic region have been given by various authors and most recently by Dodimead, Favorite, and Hirano (1963) and Uda (1963). In the upper kilometer, the vertical thermohaline structure is characterized by three layers or zones (cf. Doe 1955, Dodimead 1958, Fleming 1958). The first of these zones, the surface zone of 75-100 meters thickness, is somewhat diluted because of the runoff and net precipitation; the dilution is not, however, accompanied by large changes of salinity with depth in the zone. The temperature within the layer decreases markedly with depth in summer, but in winter is nearly uniform. The second zone, a quasi-isothermal halocline, shows a marked increase of salinity with the depth, and falls approximately within the 100-200 meter depth increment. In the deeper waters, which comprise the third zone, the temperature slowly decreases and the salinity slowly increases with depth.

Tully and other investigators (Doe 1955, Tully and Dodimead 1957, Dodimead 1958, Tully and Barber 1960) have shown that the salinity at the bottom of the halocline is very nearly constant ( $33.8 \pm 0.1 \text{ }^{\circ}/\text{o}$ ) throughout the year. The values at the upper boundary of the halocline (which varies in depth from 75 m to 150 m) change throughout the year  $0.2 \text{ }^{\circ}/\text{o}$  or less at any given location. In the area affected by Columbia River discharge the salinity at the upper halocline boundary is approximately  $32.7 \text{ }^{\circ}/\text{o}$ , but increases toward the west and decreases toward the north (Figure 3).



Fig. 3--Salinity ( $^{\circ}/oo$ ) at bottom of upper zone, June 1962. (Pacific Oceanographic Group Circular 22, 1962).

Within the area, the variation of freshwater contribution with time is small (Tully and Barber 1960). Although there is a net upward transfer of salt across the halocline, the constant salinity at the upper boundary suggests that a dynamic balance is maintained with water added by precipitation and runoff. The upper boundary of the halocline may be considered the lower limit of the penetration of seasonal effects. Immediately along the Washington-Oregon coast is located a continental shelf of 30 to 70 kilometers width. The water lying over the shelf and the adjacent continental slope undergoes somewhat greater fluctuations in temperature and salinity than the water farther offshore. Upwelling of deeper water along the continental slope and tidal or hydraulic forces nearshore help create the rapid changes which are found in this area.

The basic structure described above is modified by the Columbia effluent as shown in Figure 4. The base of the upper halocline was identified

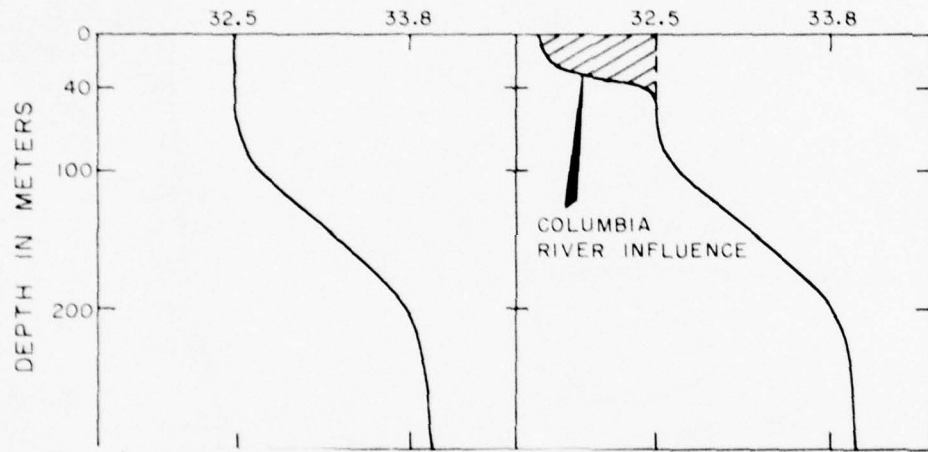


Fig. 4. Salinity structure of the oceanic regime, and the influence of the Columbia River effluent on this structure.

on plots of salinity versus logarithm of depth by a sharp change in slope at a salinity between 32.4 ‰ and 32.7 ‰. The change in slope in this salinity range, together with the fact that the surface water salinity of the area immediately affected by the plume falls in approximately the same range, suggest that 32.5 ‰ is a good index salinity for ascertaining the horizontal and vertical extent of the River effluent.

#### Geostrophic Currents of the Investigation Area

Past studies of geostrophic currents include those of Tully (1938, 1942), Doe (1955), Fleming (1955), Barnes and Paquette (1957), Dodimead (1961), and Dodimead and co-workers (1963). Their observations show that the entire area is characterized by poorly defined currents which are influenced significantly by changing wind patterns and local bathymetric features. The currents computed from the dynamic topography of the sea surface have an average value of about  $5 \text{ cm sec}^{-1}$  and maxima up to  $20 \text{ cm sec}^{-1}$ .

(10 miles per day), setting south in spring and summer. Drift bottle studies by Thompson and Van Cleve (1936), Dodimead and Hollister (1962), Reid (1960), and Wyatt and Kujala (1962) corroborate the pattern depicted by the dynamic studies. The drift bottle studies of Thompson and Van Cleve (1936) and dynamic calculations by Tully (1938, 1941) showed a flow which was northerly in the spring and southerly in the summer, probably related to the seasonal change in the wind pattern. Dodimead (1961) has discussed the year-to-year variations in the geostrophic circulation from 1955 to 1959.

In the present study a dynamical analysis has been made of the waters adjacent to the coasts of Washington, Oregon, and Northern California and the resulting topographies are shown in Figures 5 to 14. Geostrophic currents (the water movements associated with the internal distribution of mass) were deduced from calculations of topography of the sea. The 1000-decibar surface was chosen as the reference level (level of assumed no motion). Calculations were made for all Brown Bear cruises during 1961 and 1962 except Cruise 291 (geology cruise) and Cruise 309 (biology cruise). The topographies shown are deviations from the geoid surface and neglect the effect of atmospheric pressure. These charts represent the first season-to-season dynamical analysis of the offshore areas adjacent to the Washington, Oregon and Northern California coasts. Throughout this analysis standard techniques of computing dynamic height anomalies were used. Values for the shallow inshore stations were computed by a method of extrapolation (Helland-Hansen 1934) or by the technique of plotting the specific volume anomaly versus the logarithm of depth, as described by Bennett (1959), or by both methods. Those stations deeper than 1,000 meters are circled on the charts. Stations of less than 300 meters depth were not used in the extrapolation.

The contour interval, 2 dynamic centimeters, used in contouring the topographic charts may be open to criticism in view of the probable errors in measurements and the technique employed (cf. Reid 1959, Leipper 1959). Large fluctuations can also occur in individual dynamic height calculations because of local short-term fluctuations in the distribution of mass in the water column. It has been found that these fluctuations are often of the same magnitude as the contour interval. The probable error of  $\pm 2$  dyn. cm is based on repetitious sampling during these observations and the results of repetitious measurements at station PAPA (Fofonoff, personal communication). The short-term fluctuations were probably due to the passage of intense storms and internal waves as well as errors in measurement. Defant (1950), in examining a series of geopotential topographic charts prepared by Scripps Institute of Oceanography for an area off the coast of California, found that many of the highs and lows could be attributed to internal waves. Wooster and Taft (1958) have shown that a probable error of  $\pm 1$  dyn. cm can be expected considering the precision of measurement only.

The reference level of 1,000-decibars was chosen because of the limited number of observations in deeper water. Reid (1961), Dodimead (1961), and Bennett (1959) have suggested that 1,000-decibar level is adequate for showing the direction of flow in the eastern subarctic. It is improbable that a uniform reference level exists in a north-south direction in the subarctic. Neumann (1955) has shown that the reference level rises from the

Equator toward the Poles in the Atlantic Ocean. Drogue measurements made by the Brown Bear in 1961 in the effluent area indicate a current at 1,000 meters of  $2 \text{ cm sec}^{-1}$ . In view of this discussion, charts of dynamic topography 0 over 1,000 decibars are probably slightly in error in some parts of the area; but it is felt that they adequately depict the gross features of the speed and direction of water movement. A constant 1,000-decibar reference level is inadequate for computations of mass transport in this area.

During January 1961, a current was observed to set northward at approximately  $10 \text{ cm sec}^{-1}$  (Fig. 5). This flow intensified to greater than  $20 \text{ cm sec}^{-1}$  during March (Fig. 6), and reversed direction during May (Fig. 7). The radical change in current set is associated with a shift in the predominant wind from southerly to northerly and during the summer a southerly current averaging  $8 \text{ cm sec}^{-1}$  predominated. The current pattern change from winter to summer is complicated by cyclonic and anticyclonic eddies. There is a suggestion of a cyclonic eddy in the topography of Figure 6 and this eddy appears better developed in Figure 7. The anticyclonic eddy or high near  $46^\circ \text{N}$  shown in Figures 7 to 10 is well documented by numerous observations and appears rather consistently throughout the summer and autumn, hence is probably not an artifact associated with the lack of synopticity in sampling and/or internal waves (Defant, 1950). Reid, Schwartzlose, and Brown (1963) confirmed the existence of a permanent eddy off the California coast using parachute drogues. The drogue movements agree with what might be expected from dynamic topography, which suggests that the eddies are geostrophically in balance. Reid and co-workers suggested that the eddies probably result from the horizontal shear between two currents. McEwen (1948) studied the dynamics of similar eddies and concluded that the decrease in velocity and increase in size noted on successive cruises are probably successive stages of decay from an initial state of maximum intensity and small extent.

The dynamic topography derived from the early fall cruise (September-October 1961) is shown in Figure 10. Velocities as high as  $20 \text{ cm sec}^{-1}$  are evident in the cyclonic eddies.

The response of the distribution of mass to the autumnal shift in winds from predominantly north to predominantly south is shown in the geopotential topography for December 1961 (Fig. 11). The northward setting Davidson Current appears to be in an early stage of development but the isopleths inshore are based on Helland-Hansen (1934) extrapolation over large distances, hence the depiction may not be accurate. The circulation pattern of the surface water is less complex in mid-winter as shown by Figure 12. Here a trough is evident about 130 to 185 kilometers offshore, with a northerly current inshore and a southerly current seaward. The speeds of the two opposing flows are about equal at  $10 \text{ cm sec}^{-1}$ .

The southerly winds persisted until after the next sampling in April, 1962. Figure 13 shows the northerly (Davidson) current fully developed along the coast. During May and June, 1962, the winds shifted from southerly to northerly and the spring conditions again appeared with a nearshore southerly current and an offshore northerly current (Fig. 14). Thus, in general, the average surface current pattern along the coasts of Washington and Oregon is northerly at  $10$  to  $20 \text{ cm sec}^{-1}$  in the winter and southerly at  $5$  to  $20 \text{ cm sec}^{-1}$  in the summer.



Fig. 5--Geopotential topography, 0/1000 decibars, Brown Bear Cruise 275, 10-27 January 1961.

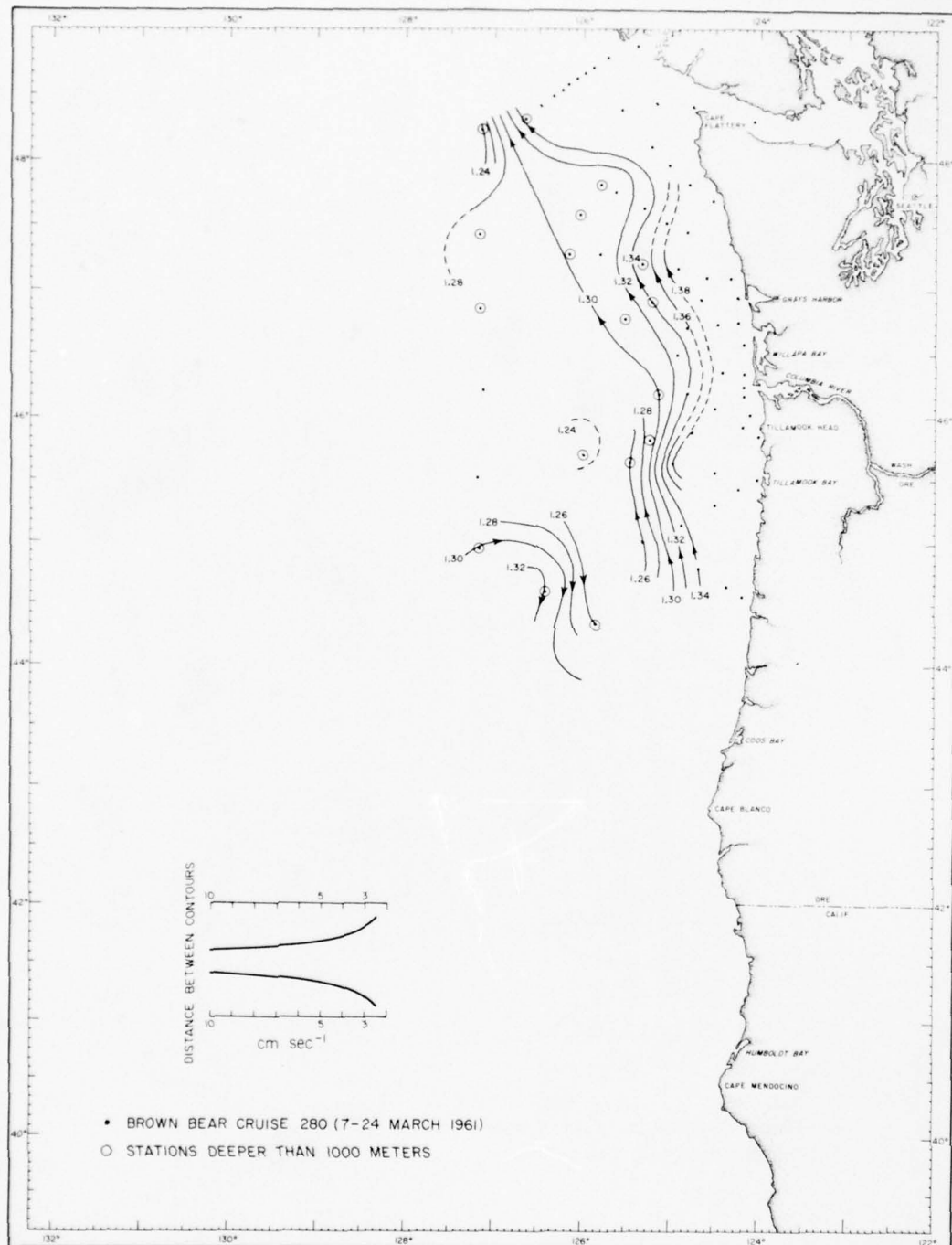


Fig. 6--Geopotential topography,  $^0/1000$  decibars, Brown Bear Cruise 280, 7-24 March 1961.

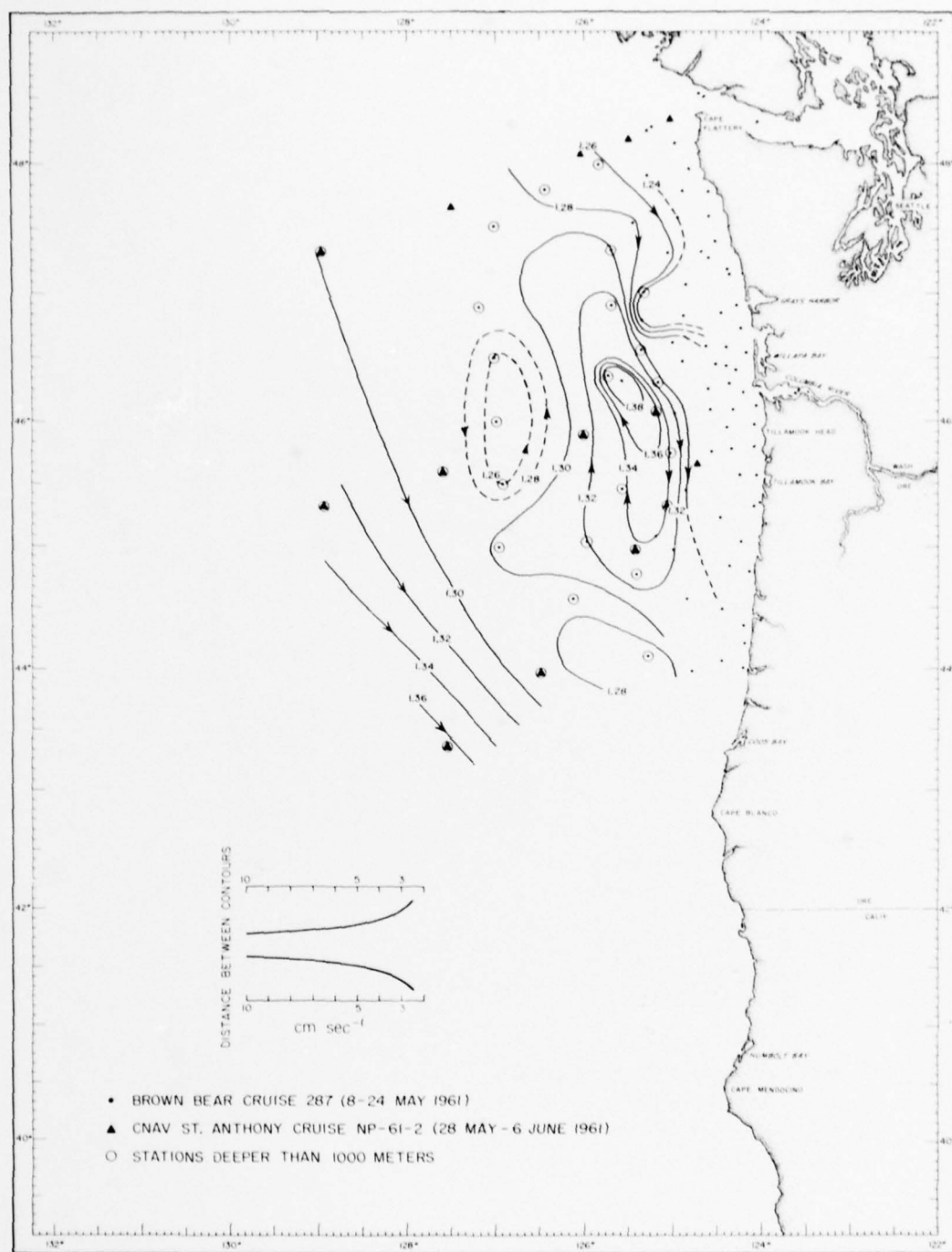


Fig. 7--Geopotential topography,  $^0/1000$  decibars, Brown Bear Cruise 287, 8-24 May 1961.

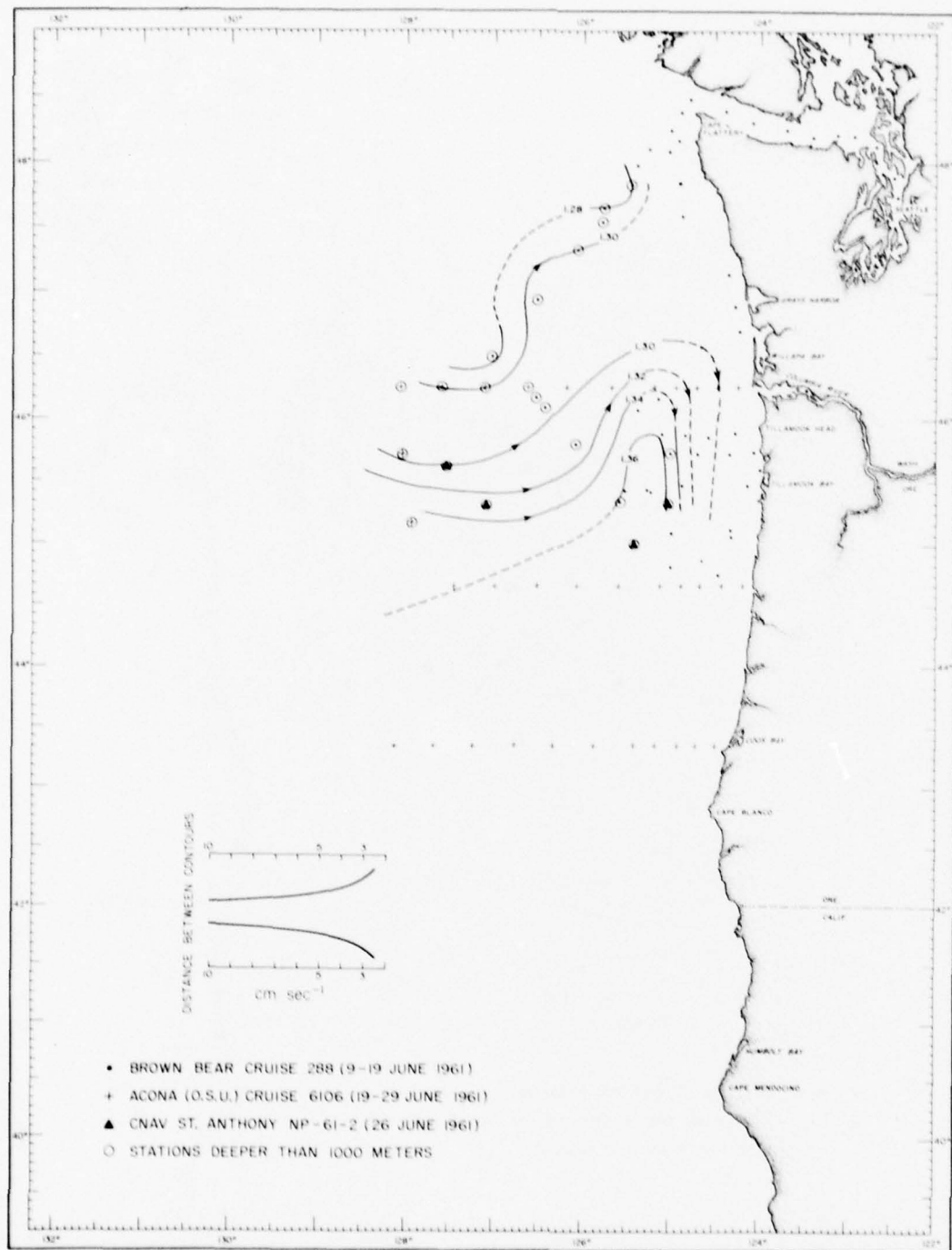


Fig. 8--Geopotential topography,  $^0/1000$  decibars, Brown Bear Cruise 288, 9-19 June 1961.

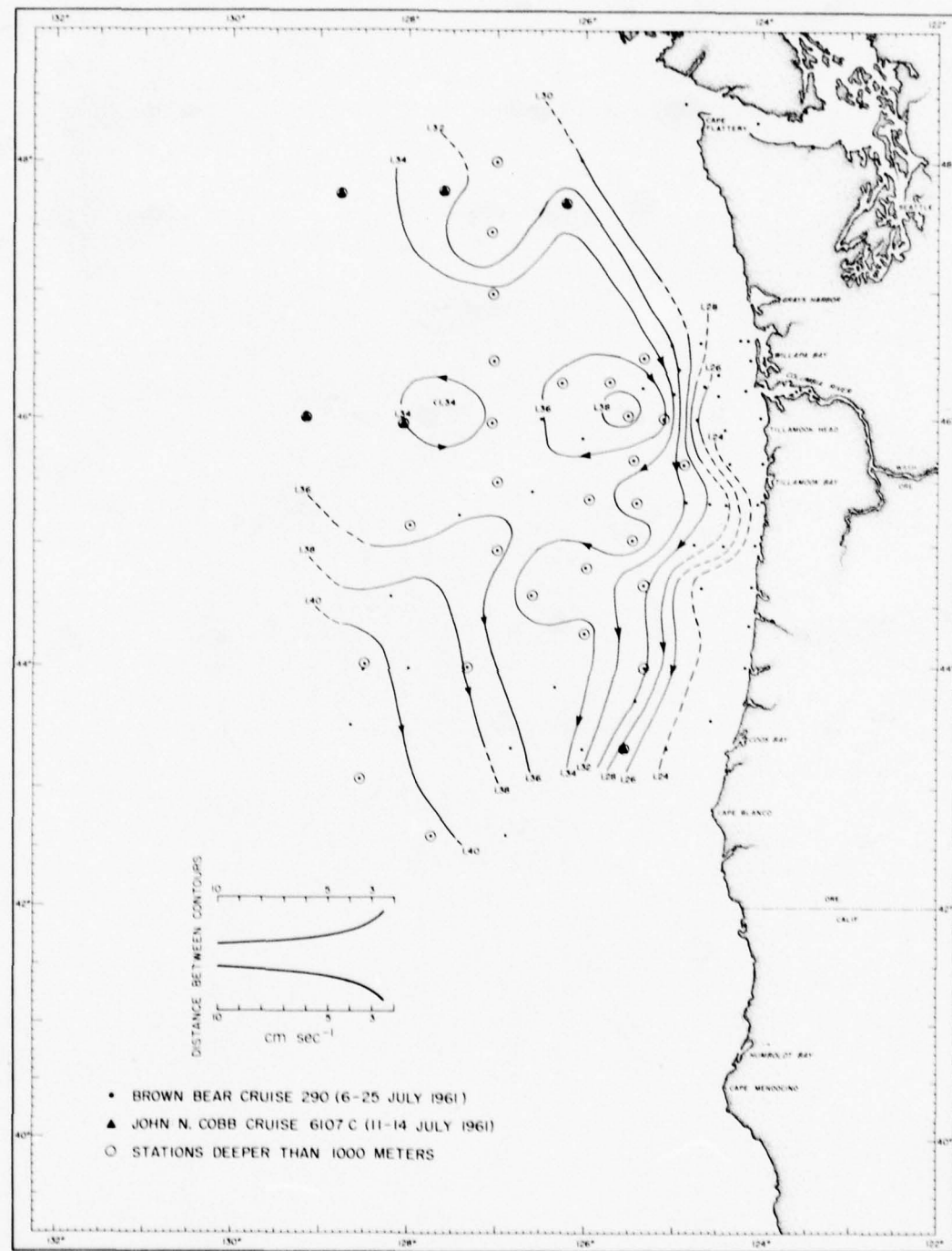


Fig. 9--Geopotential topography,  $^0/1000$  decibars, Brown Bear Cruise 290, 6-25 July 1961.

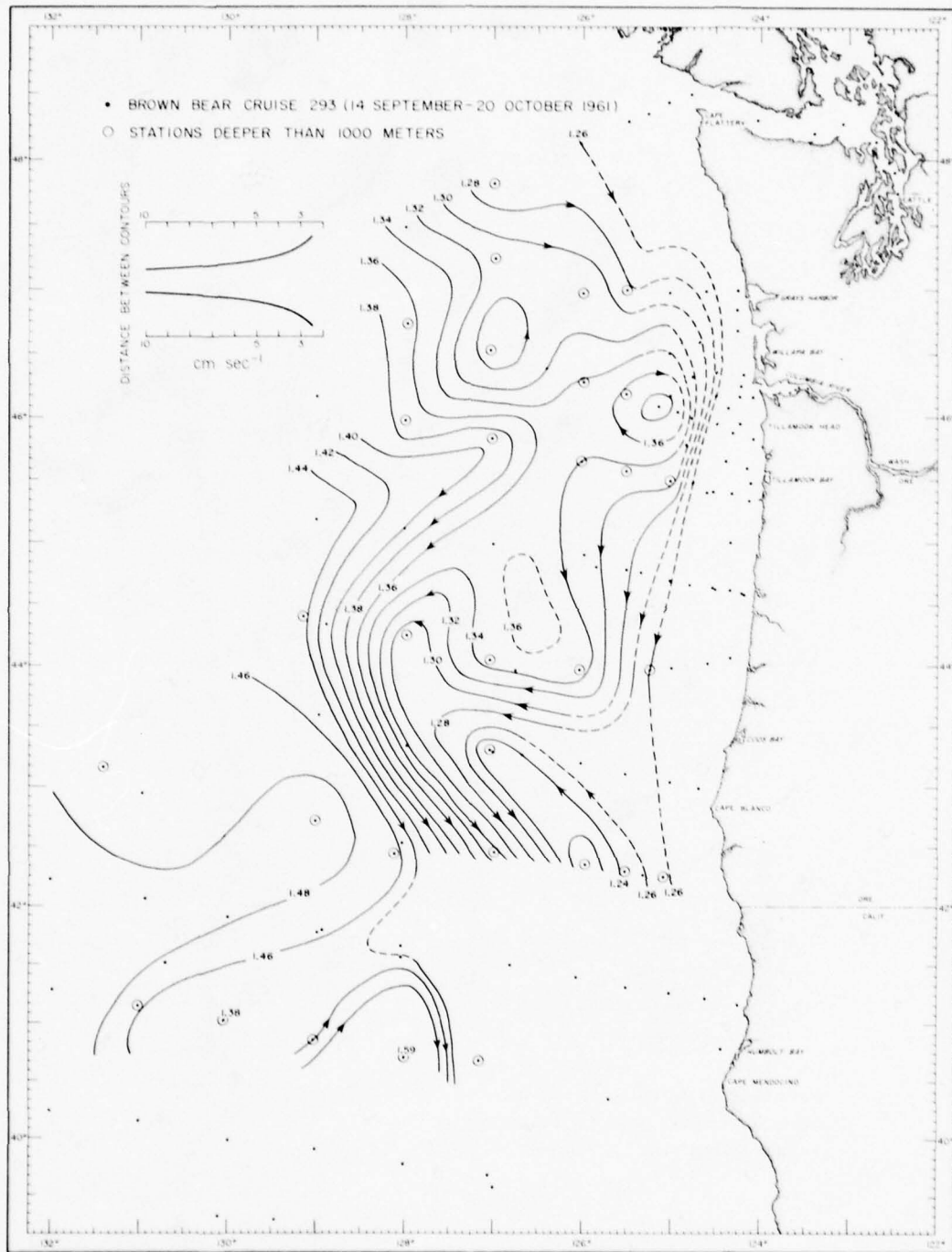


Fig. 10--Geopotential topography, 0/1000 decibars, Brown Bear Cruise 293,  
14 September-20 October 1961.

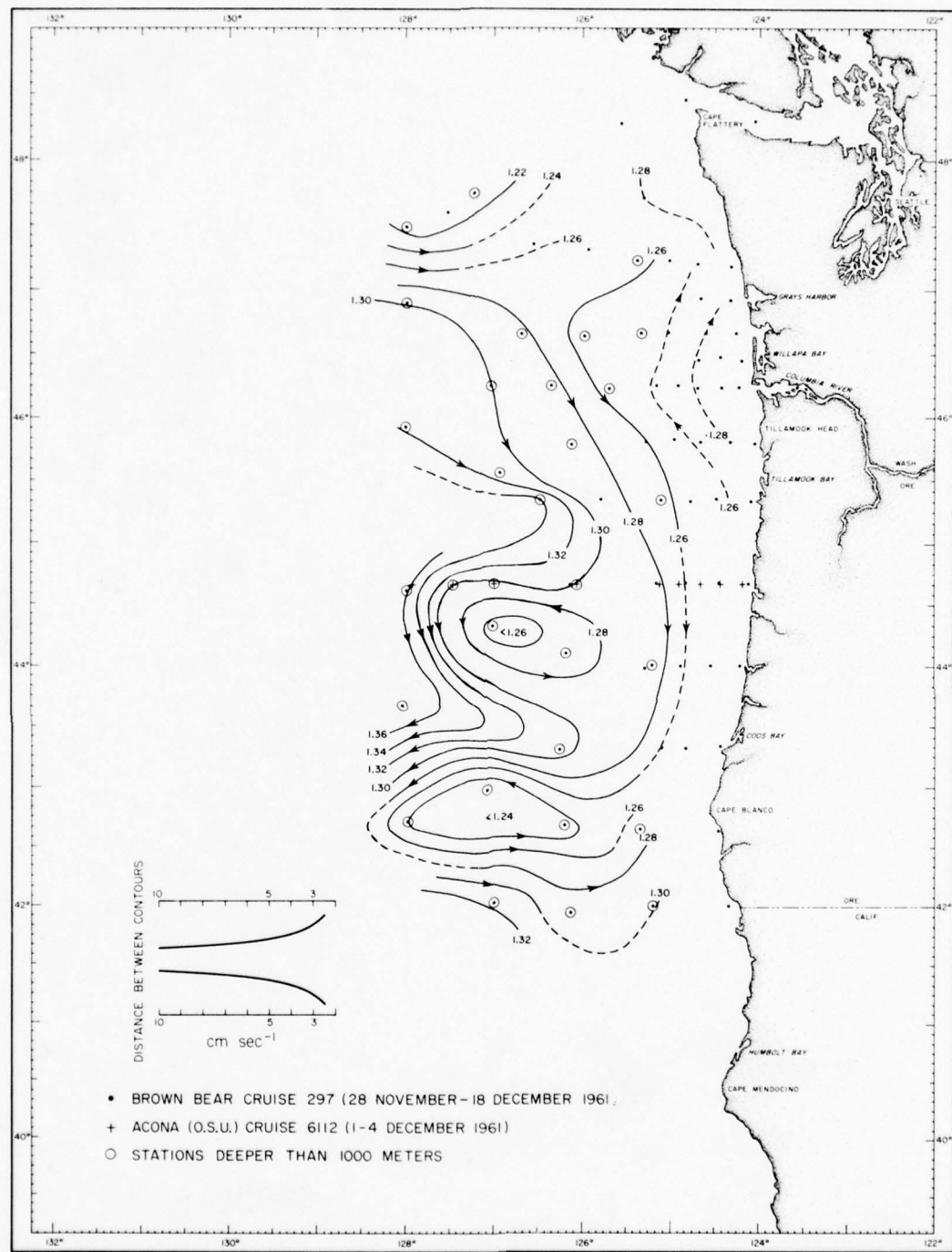


Fig. 11--Geopotential topography,  $^0/1000$  decibars, Brown Bear Cruise 297,  
28 November-18 December 1961.

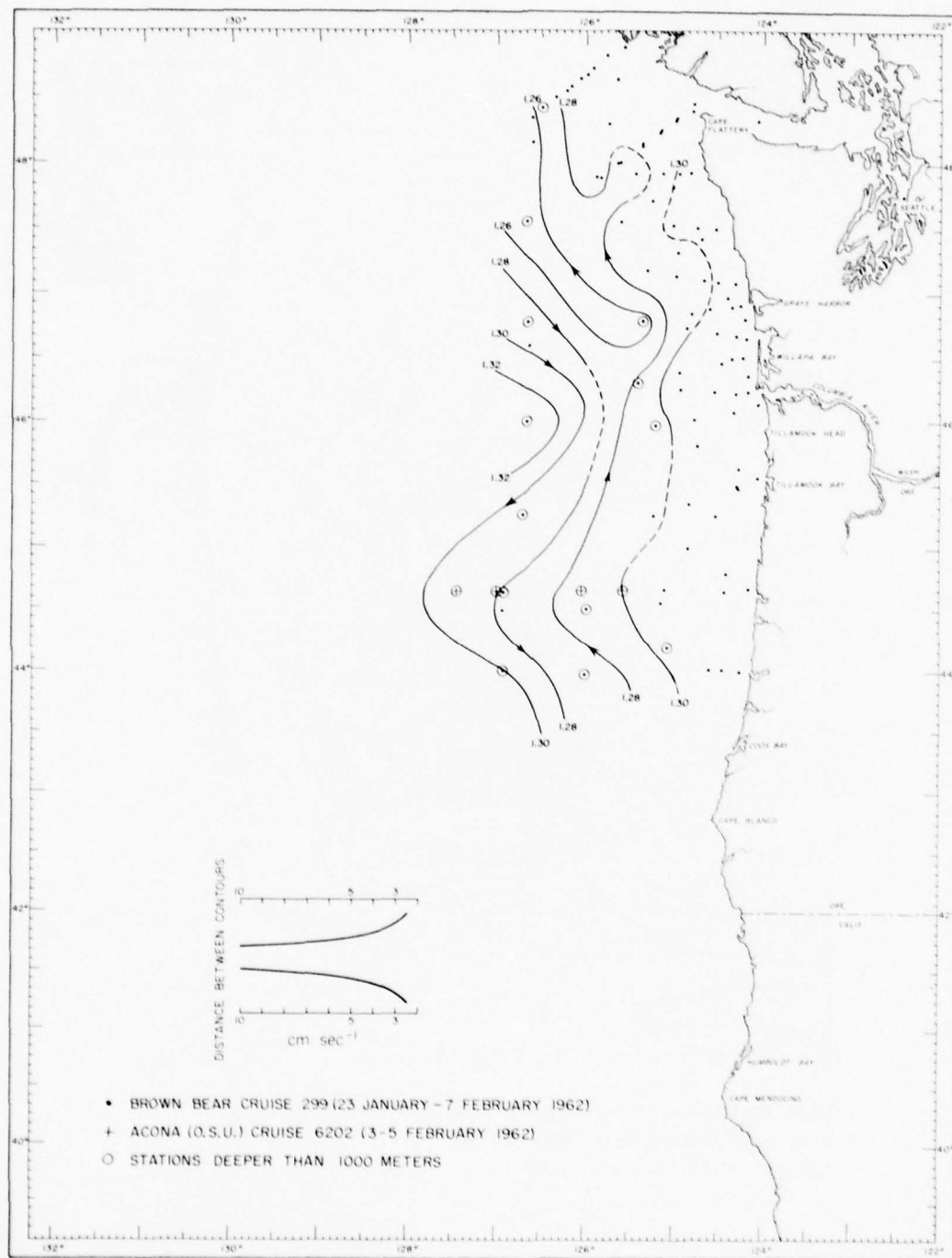


Fig. 12--Geopotential topography,  $^0/1000$  decibars, Brown Bear Cruise 299, 23 January-7 February 1962.

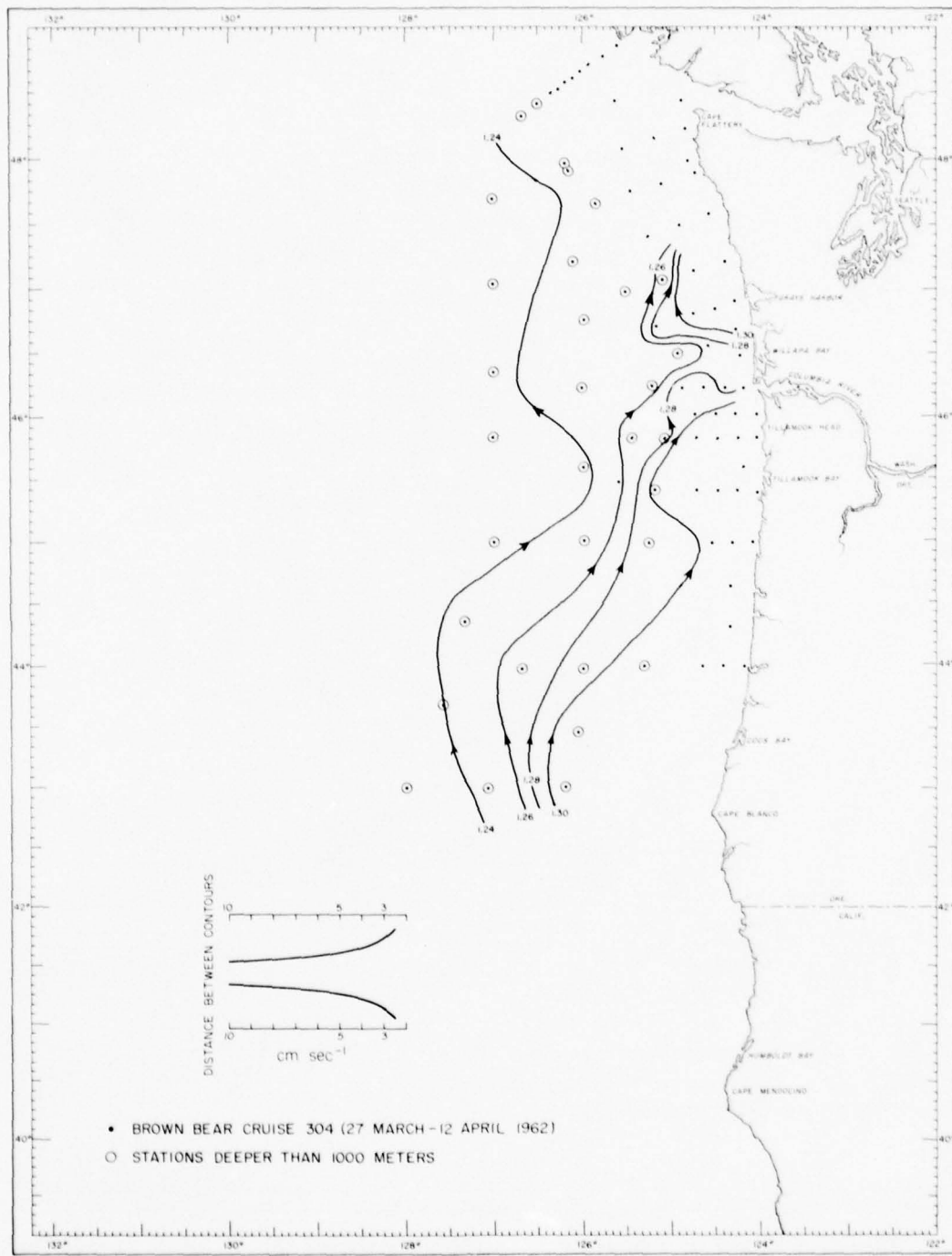


Fig. 13--Geopotential topography,  $^0/1000$  decibars, Brown Bear Cruise 304, 27 March-12 April 1962.

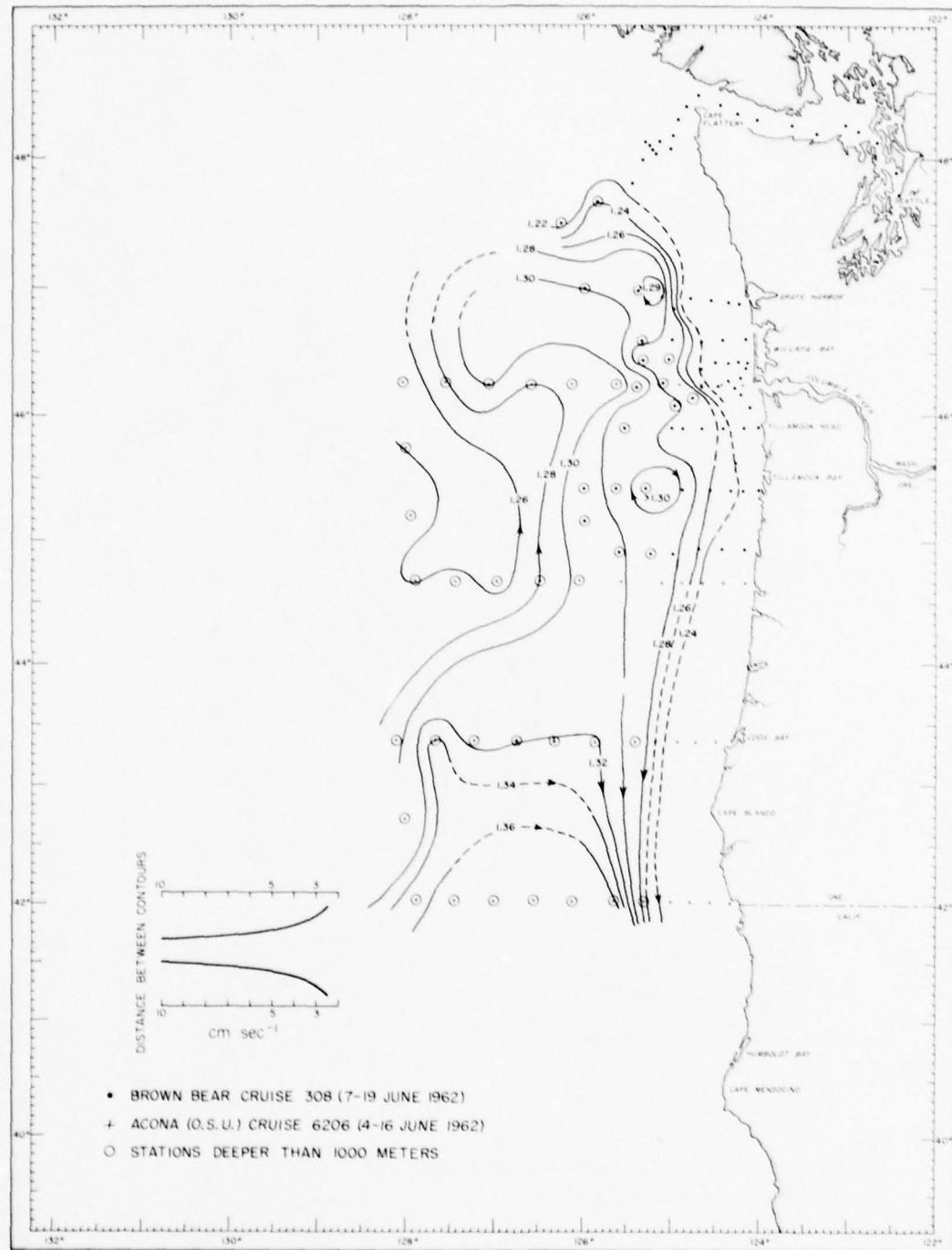


Fig. 14--Geopotential topography, 0/1000 decibars, Brown Bear Cruise 308, 7-19 June 1962.

The interaction between the eddies and the Columbia River water and their combined effect on the mass distribution has not been examined in detail. The currents inferred from the dynamic topography of 0, 50, 100, 200, 300, 500, 700 meters over 1,000 meters give a vertical distribution of velocity with the following general characteristics:

- a) The direction remains constant throughout the column.
- b) Currents at 50 meters are similar in magnitude to those at the surface.
- c) A shear occurs in the halocline such that the current at 200 to 300 m is generally less than  $5 \text{ cm sec}^{-1}$ .

According to Dodimead, Favorite, and Hirano (1963) a northward flow of the deep waters off the Washington-Oregon coasts occurred in 1955, 1956, 1957, and 1959--the California Undercurrent. The presence of this summer current below 200 m is not well documented by their dynamic calculations. Transport of water from the south is inferred from the distribution of variables but this southern water might be that carried by the winter northward flowing current. Our observations show some evidence for a northerly flow below 200 meters during July 1961 north of  $47^{\circ}\text{N}$ , but no other evidence was found and the net summer flow was south at all levels. The month-to-month transport will be computed when the 1963 data are available.

## VI. CHARACTERISTICS OF THE EFFLUENT IN THE OCEAN

### Areal Distribution of the Effluent

The areal distributions of the River effluent for various times during 1961 and 1962 are shown in Figures 15 through 25. As discussed above, the 32.5 ‰ isohaline was found to be a reasonable limit for the delineation of the plume. These charts of surface salinity show quite clearly that during the summer period of predominate northerly winds the river plume streams toward the southwest; and during the winter season of prevailing southerly winds the plume appears as a band of low salinity water adjacent to the Washington coast, blending into the freshwater effluent from the coastal rivers and Strait of Juan de Fuca. Definite limits of the plume as described by a fixed salinity are subject to some error because the surface waters may be contaminated by local precipitation or local land drainage. This is especially true during the winter months, when the coastal rivers are high and the Columbia is low. Only part of the nearshore belt of low salinity water during the winter is due to effluent from the Columbia. Factors such as these should be considered when examining the gross month-to-month changes in the plume as described below. Furthermore, the effluent cannot be detected after three orders of magnitude of dilution by seawater because the limiting precision of the salinometers used in determining the salinity is about .005 ‰.

During the winter cruises of 1961 and 1962 (Figs. 15, 16, 22, and 23), the River's effluent, combined with the local runoff from the coastal rivers extends from approximately 30 km south of the mouth of the Columbia to north of the Strait of Juan de Fuca, in a narrow coastal belt about 50 km wide.

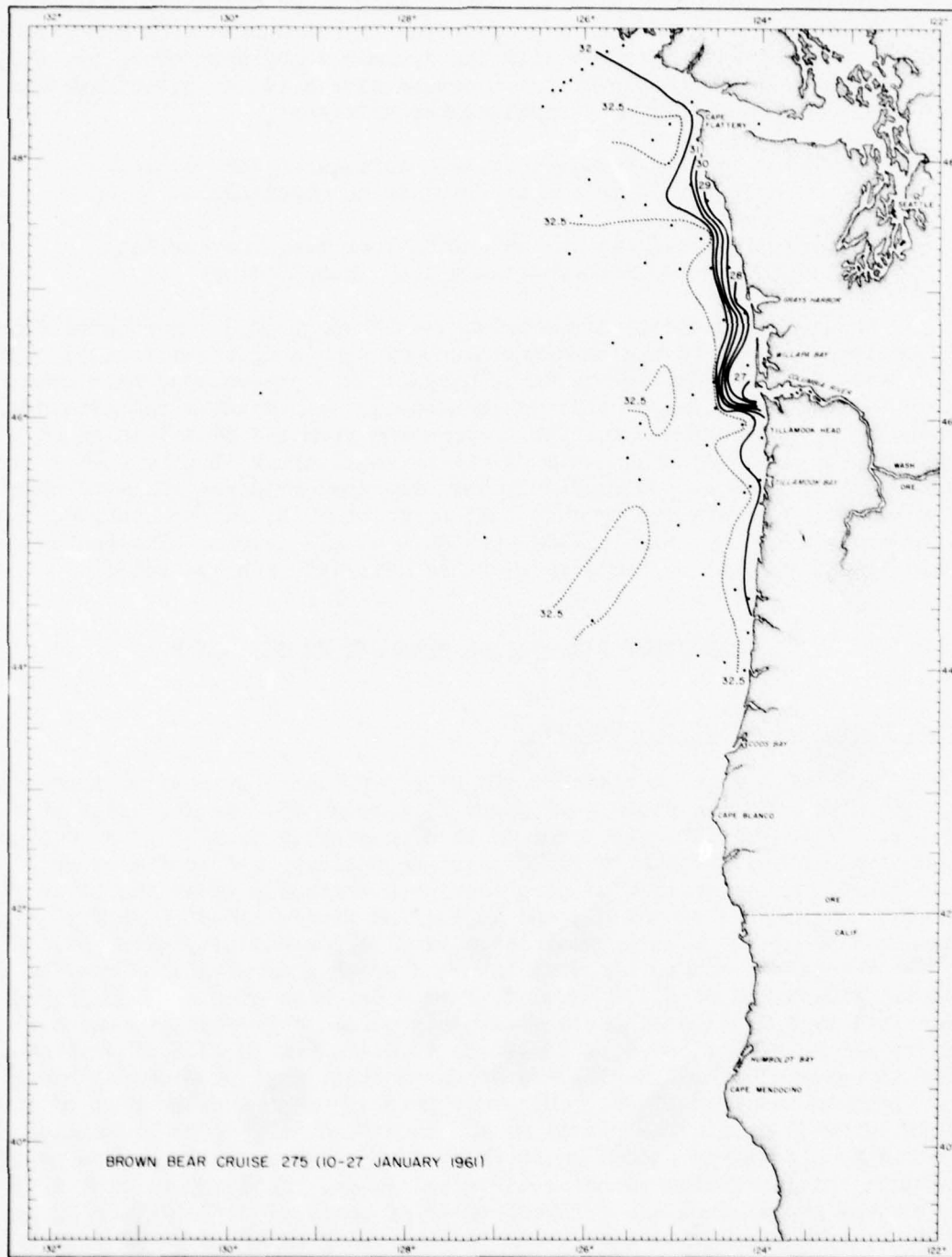


Fig. 15--Salinity ( $^{\circ}/\text{oo}$ ) at surface, Brown Bear Cruise 275, 10-27 January 1961.

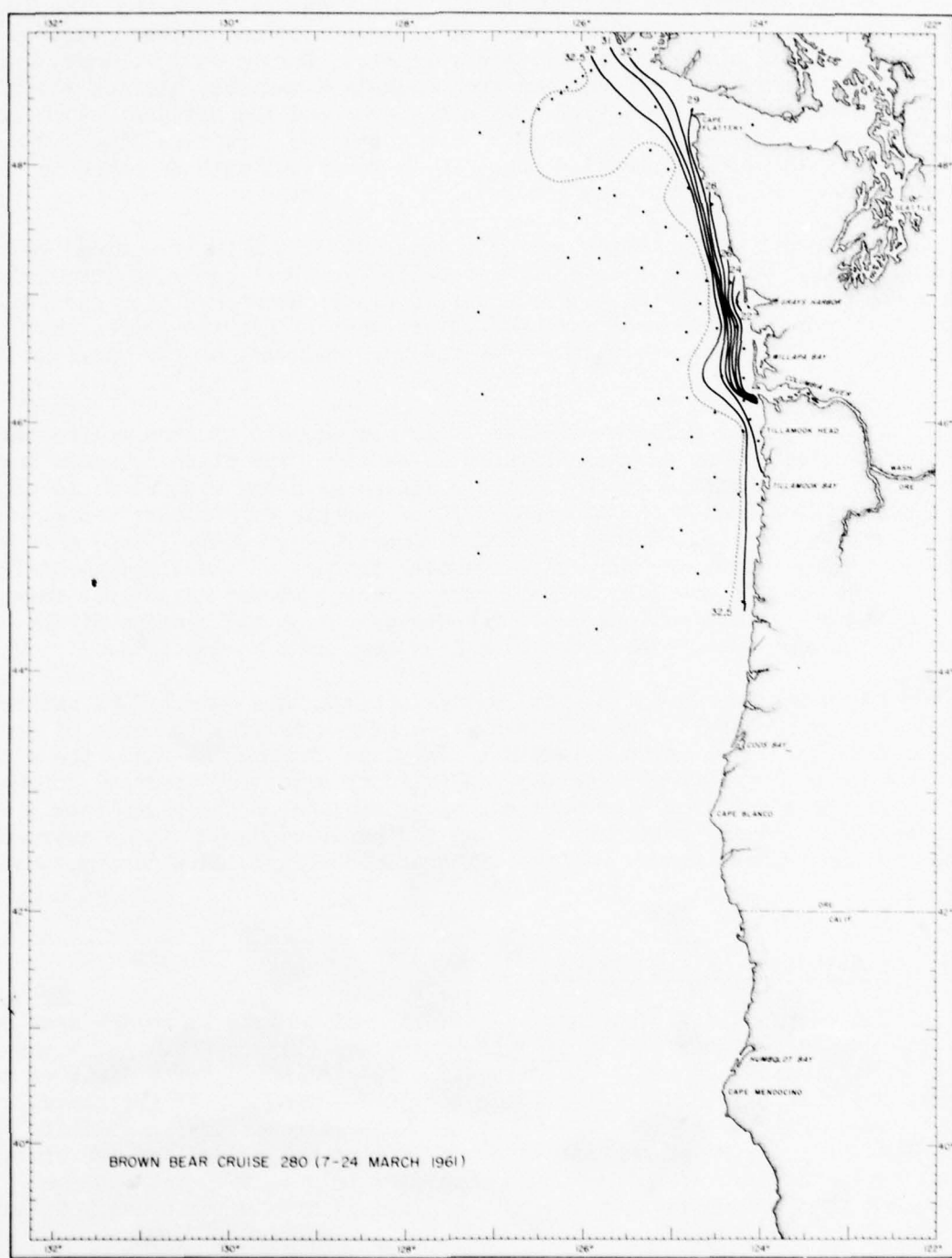


Fig. 16--Salinity ( $^{\circ}$ /oo) at surface, Brown Bear Cruise 280, 7-24 March 1961.

In the spring, May 1961 and April 1962 (Figures 17 and 24), the discharge from the Columbia is no longer so closely confined to the coast by prevailing winter winds and associated currents. During early summer, when the coastal runoff is a minimum and the Columbia a maximum, the low salinity water is readily identified with a single source and the effluent plume is rather sharply delineated by the 32.5 ‰ isohaline. Figures 18 and 25 clearly show the plume extending some 390 km southwest with an offshore boundary about 210 km from the coast.

Just north of the River mouth in June and July there is a broad belt of surface water of less than 32.5 ‰ salinity. This consists largely of the remnants of the diluted coastal belt of winter which has been carried seaward by the same wind and current systems that affect the plume. This less saline water tends to obscure the northern boundary of the plume at this time.

Of particular interest are the localized pockets of less saline water within the river plume shown in Figures 18 and 19. The discrete cells suggest short-term periodic fluctuations in discharge along with wind and tidal influences which lead to a "pinching off" of parcels of effluent water. These parcels are similar to the 'clouds' described by Tully (1949) and Fjarlie (1950). They are probably a regular feature of the effluent distribution in the sea but are less evident during stormy winter conditions when mixing is more effective. As mentioned above, during all seasons of the year the estuary water enters the nearshore area only on ebb tide.

The plume increased in areal extent through late summer 1961 and continued to spread toward the southwest, reaching a maximum distance of about 760 km from the river mouth (Figures 20 and 21). During the fall, the wind system changed to southerly and the low-salinity water was diverted northward. As the river flow slackened a gradual erosion of the plume took place (Figure 22). The intensification of the southerly winds as winter approached restored the typical winter configuration of a confined low salinity coastal belt.

#### Depth Distribution of the Effluent

The vertical distributions of salinity and density along the axes of the plumes are depicted for 10 Brown Bear cruises (Figure 26). As in the areal distribution, the 32.5 ‰ isohaline is used to mark the limit of the plume, which in this case is the lower boundary. The axis of the plume, under summer conditions, is considered to be the line of lowest salinity extending from the River mouth to the terminus of the plume; for the winter conditions, the axis is assumed to be approximately halfway between the coast and the western edge of the belt of low salinity water usually defined by the 32.5 ‰ isopleth.

The Columbia River plume during the summer changes the vertical salinity structure of the ambient ocean water as shown diagrammatically in Figure 4B. Figure 4A illustrates a typical curve of salinity vs. depth outside the plume and Figure 4B shows the modification of the salinity structure brought about by the Columbia River effluent. The effluent layer

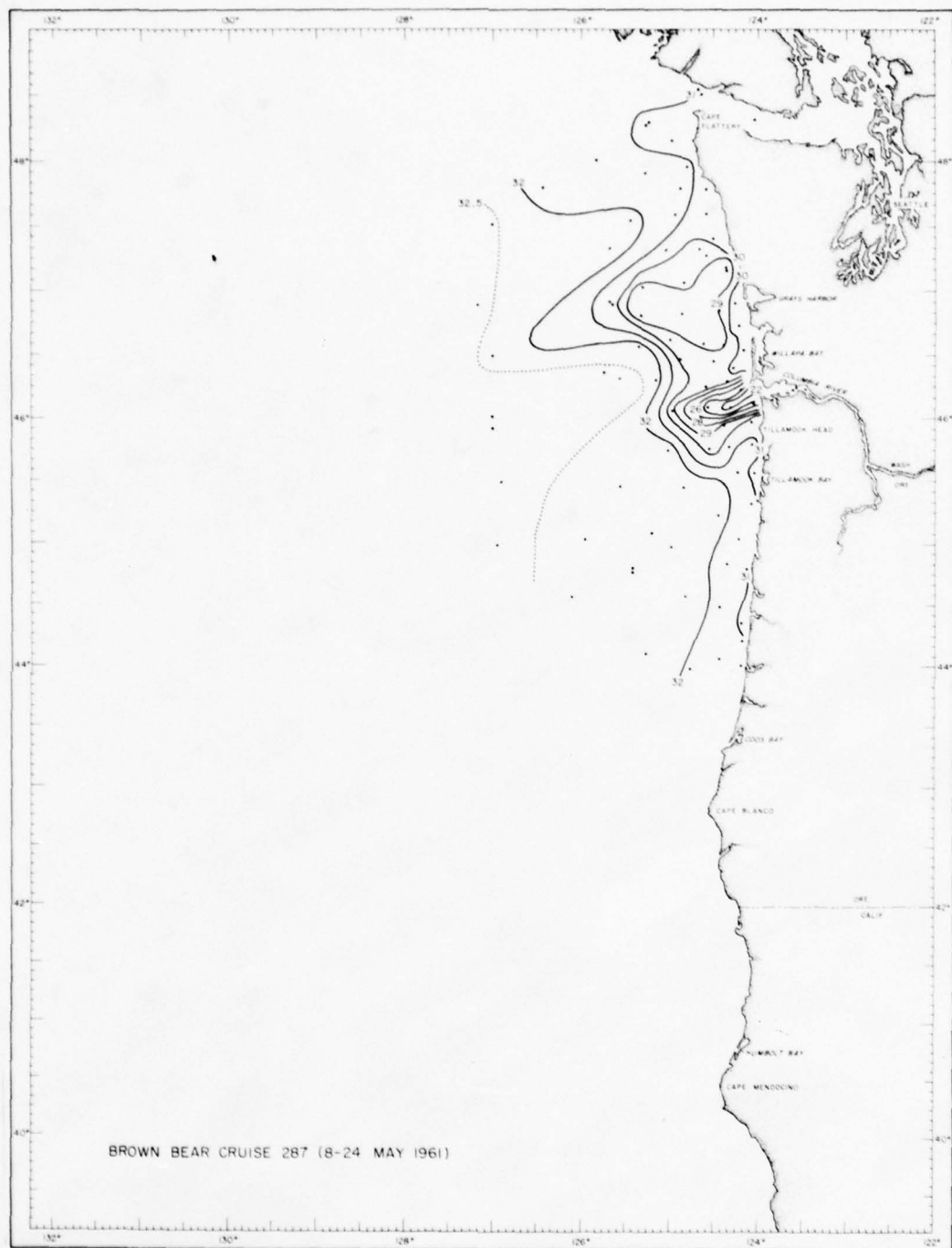


Fig. 17--Salinity ( $^{\circ}/oo$ ) at surface, Brown Bear Cruise 287, 8-24 May 1961.

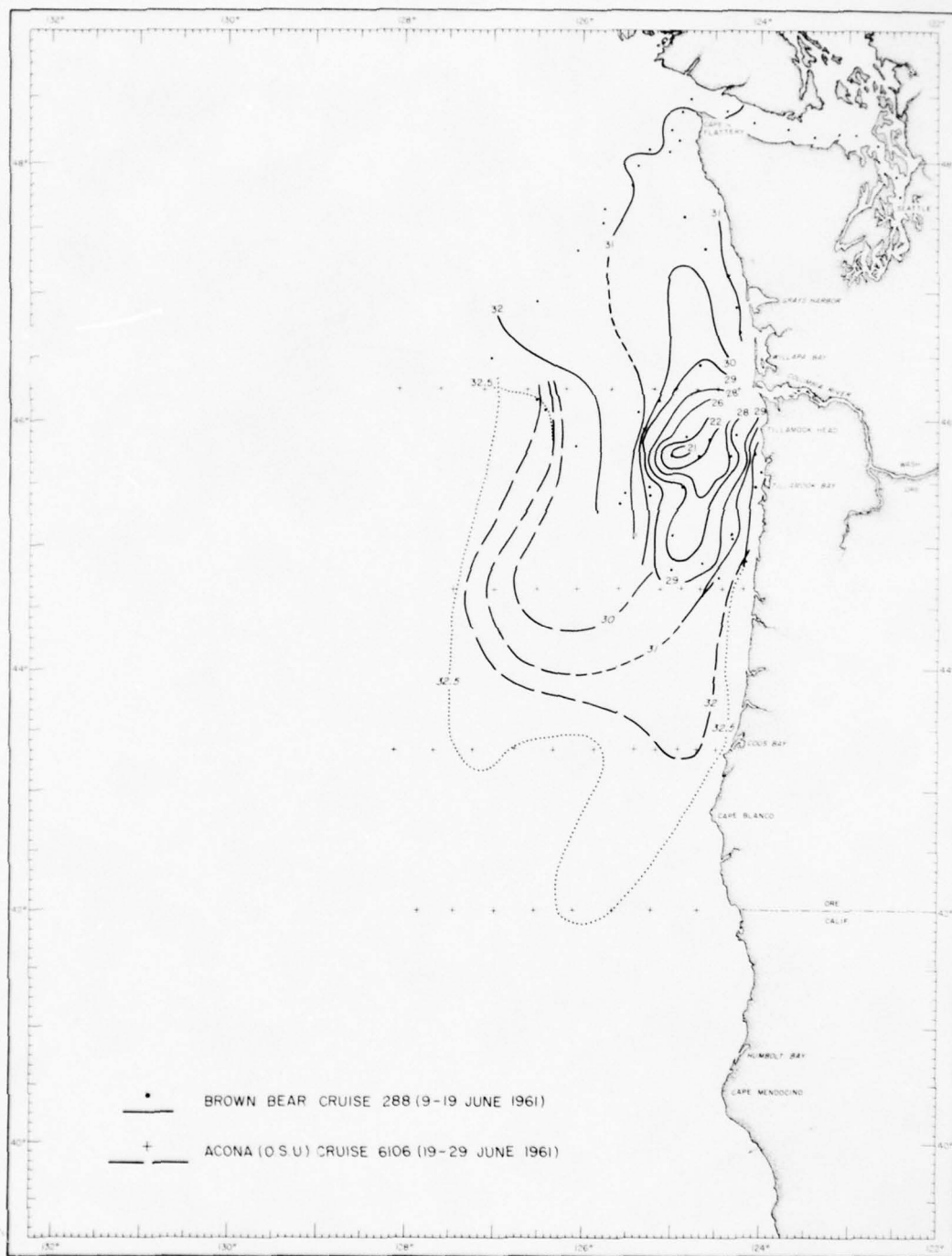


Fig. 18--Salinity ( $\text{o/oo}$ ) at surface, Brown Bear Cruise 288, 9-19 June 1961 and Acona (O.S.U.) Cruise 6106, 19-29 June 1961 (dashed line). The distributions for these two cruises are shown separated to illustrate the effect after about ten days of a strong north-easterly wind ( $16 \text{ m sec}^{-1}$ ) on plume movement.

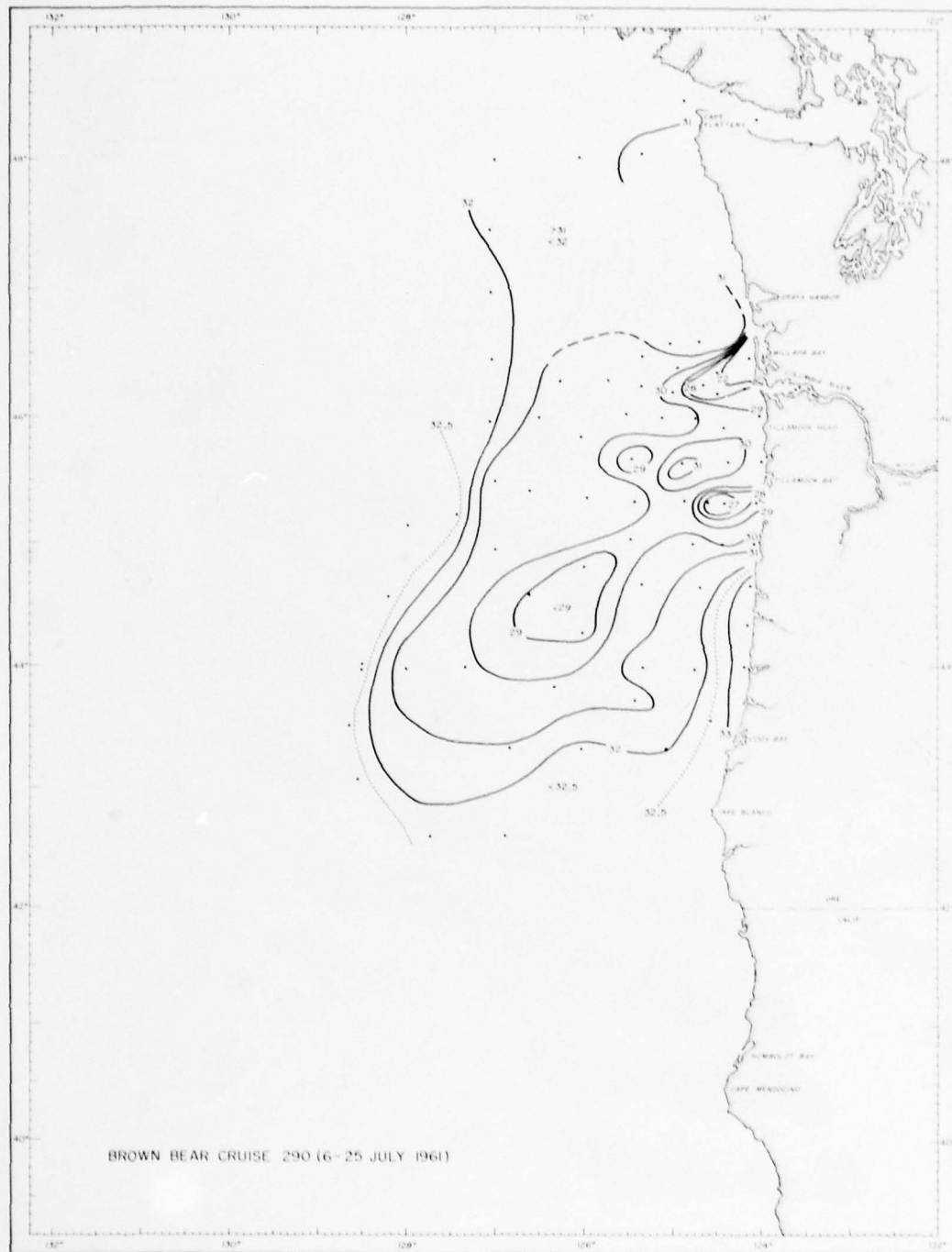


Fig. 19--Salinity ( $^{\circ}/oo$ ) at surface, Brown Bear Cruise 290, 6-25 July 1961.



Fig. 20--Salinity ( $\text{o/oo}$ ) at surface, Brown Bear Cruise 291, 28 July-13 August 1961.

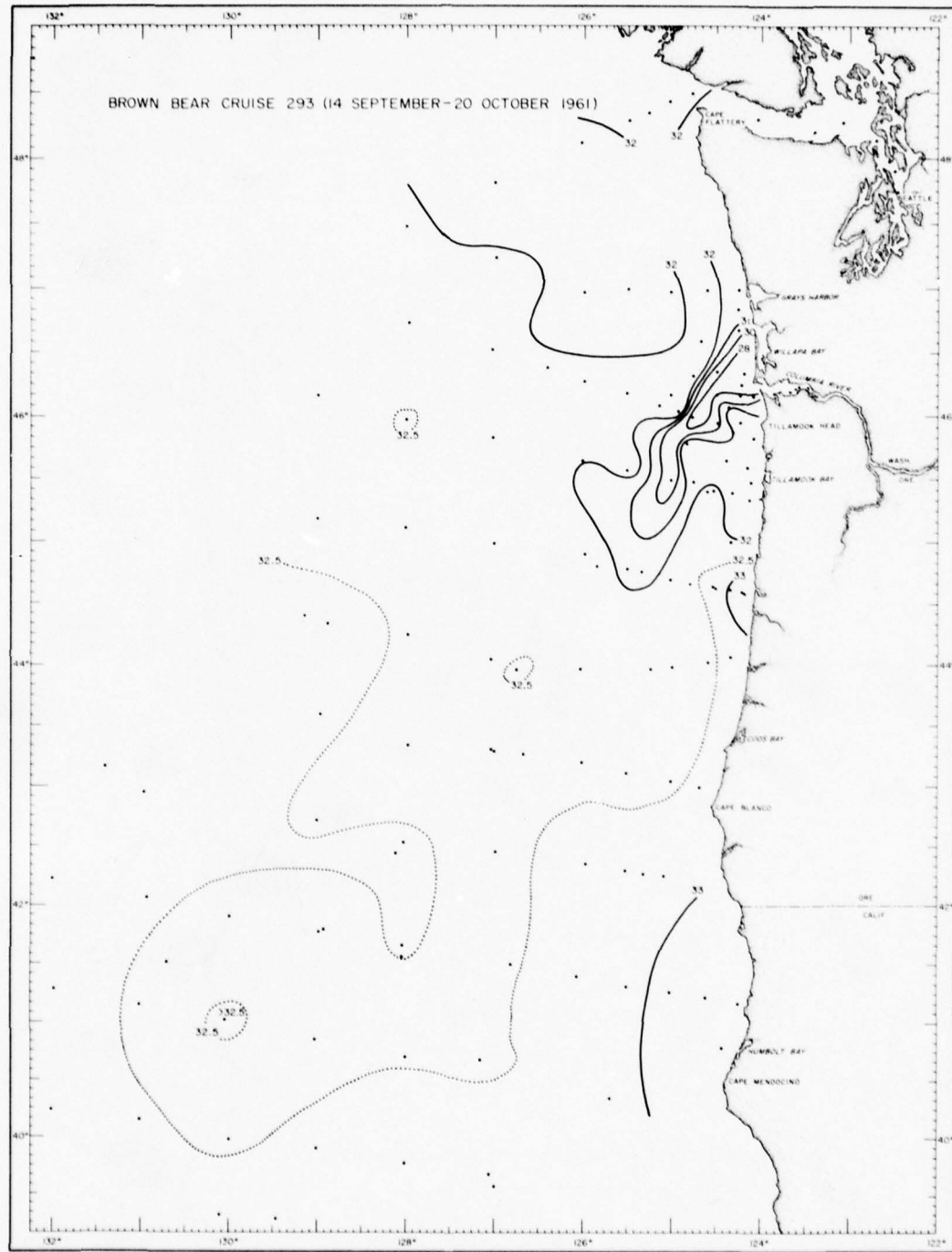


Fig. 21--Salinity ( $\text{o/oo}$ ) at surface, Brown Bear Cruise 293, 14 September -20 October 1961.

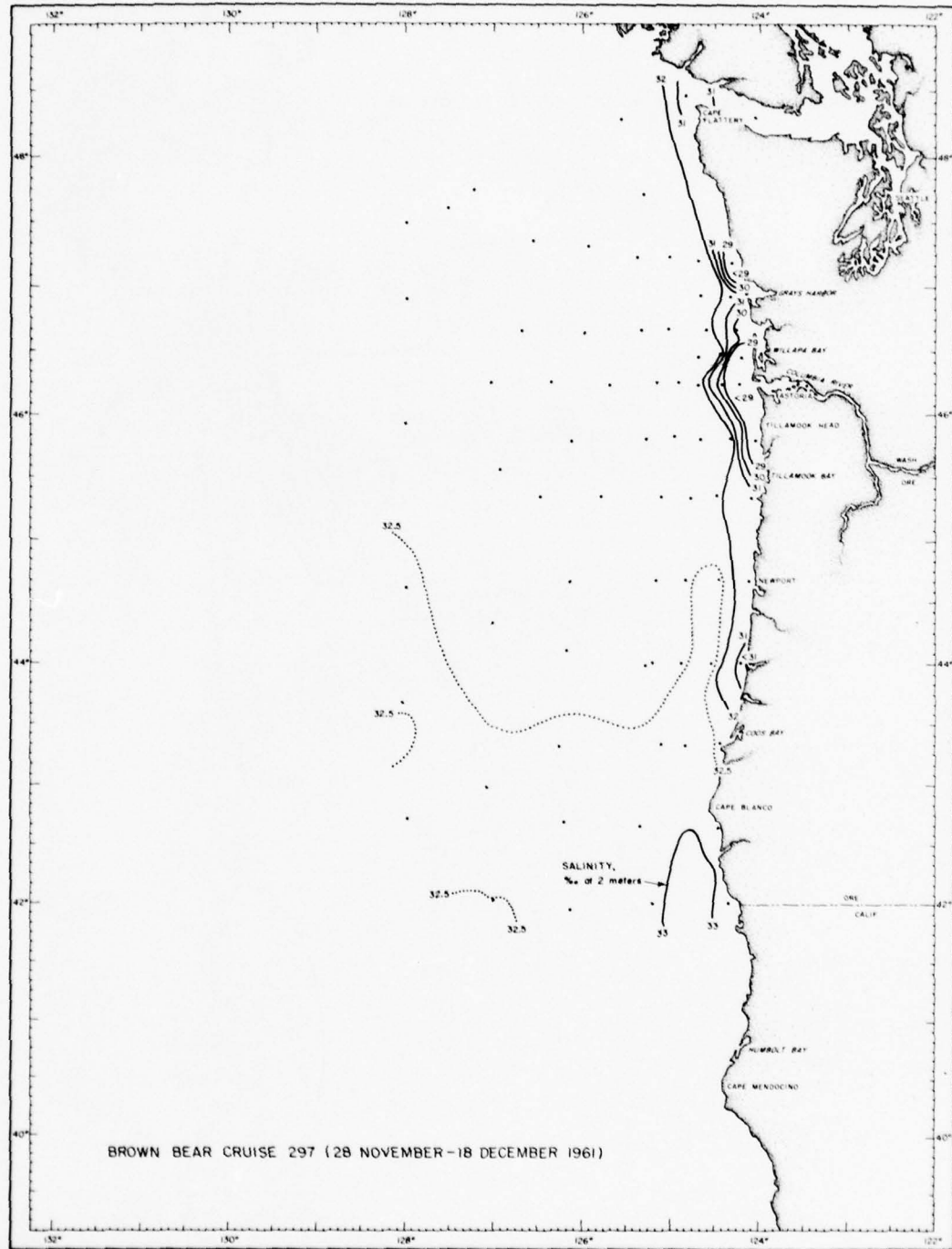


Fig. 22--Salinity ( $^{\circ}/\text{oo}$ ) at surface, Brown Bear Cruise 297, 28 November-18 December 1961.



Fig. 23--Salinity ( $^{\circ}$ /oo) at surface, Brown Bear Cruise 299, 23 January-7 February 1962.

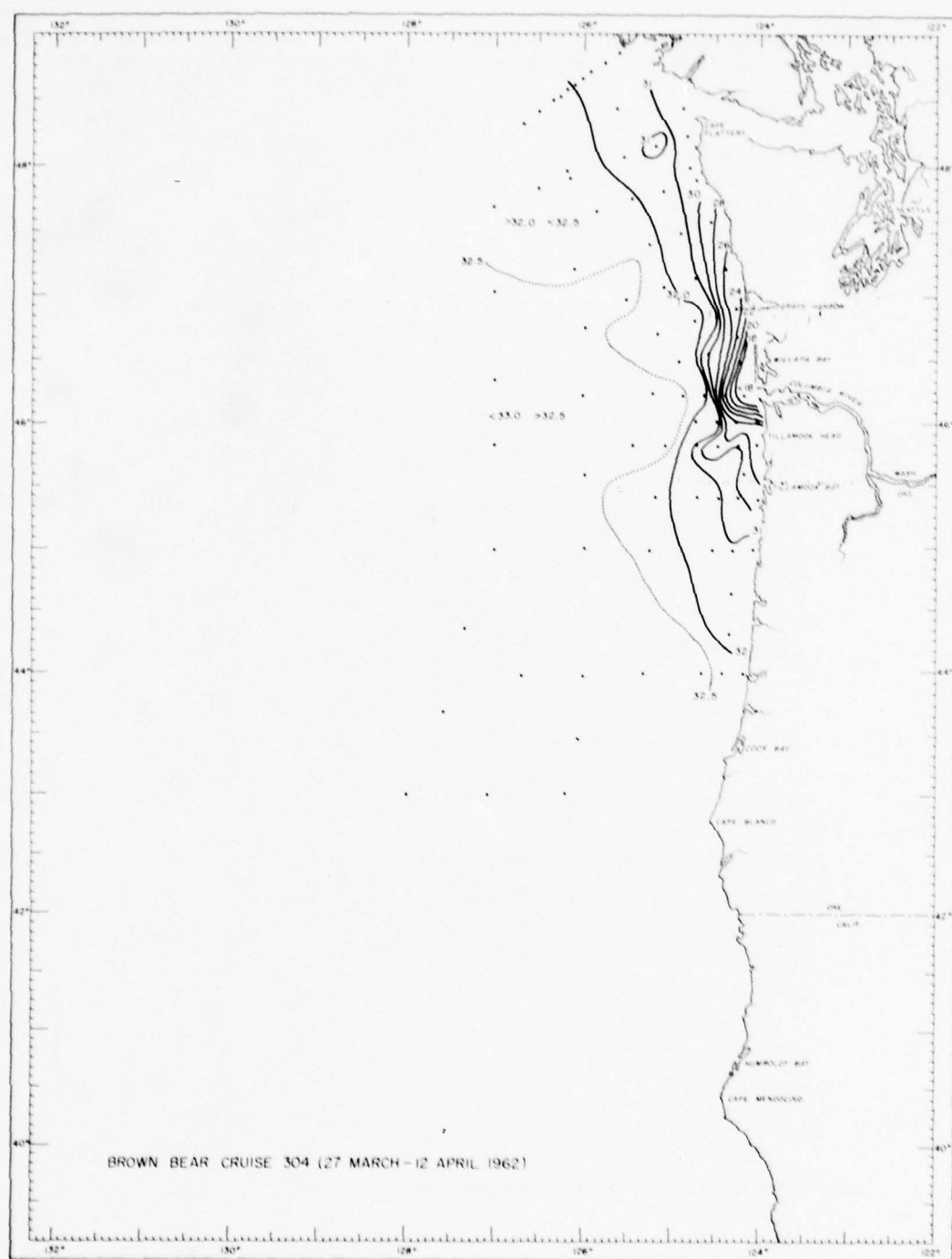


Fig. 24--Salinity ( $^{\circ}$ /oo) at surface, Brown Bear Cruise 304, 27 March-12 April 1962.

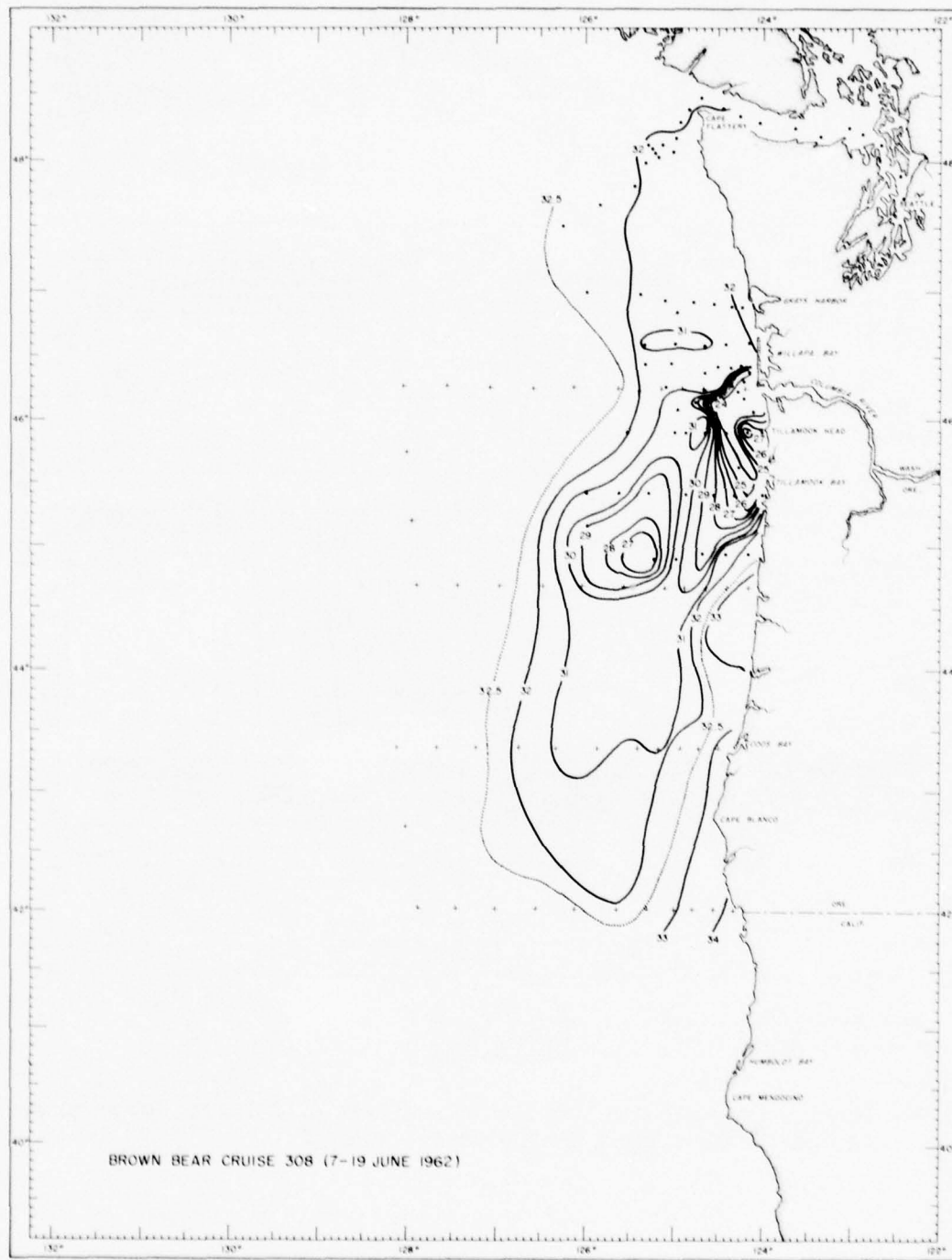


Fig. 25--Salinity ( $^{\circ}$ /oo) at surface, Brown Bear Cruise 308, 7-19 June 1962.

COLLEGE OF LIBRARIES  
UNIVERSITY OF CALIFORNIA  
CONTRACT NO. N-266(84)

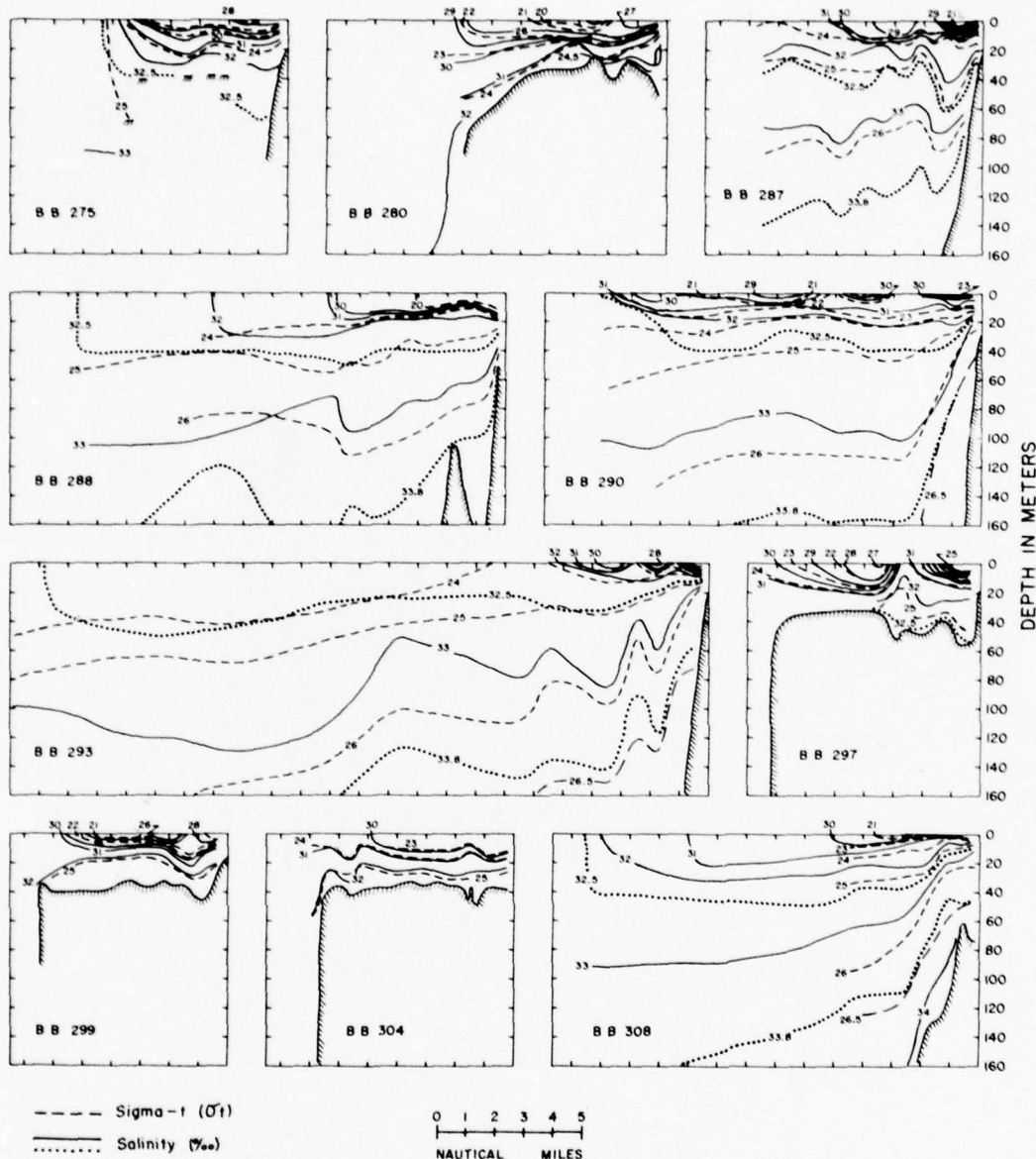


Fig. 26--Density and salinity profiles along axis of Columbia River plume for the various Brown Bear cruises, 1961-62.

(Fig. 26) is seen to be confined to the upper layer at a relatively constant depth. The depth of the bounding 32.5 ‰ isohaline for all cases lay approximately along the 25 sigma-t surface, at between 30 and 60 m depth.

As the water moves away from the River mouth, it is mixed with the surrounding water to a degree which is a function of the wind, tide, discharge, and surf. The depth of the upper mixed layer varies therefore from day to day and season to season. After the effluent leaves the nearshore environment, the open ocean mixing processes predominate and the changes induced by these processes take place more slowly. Undulations of the isopleths that appear in Figure 26 are possibly the result of internal waves or the passage of a local storm.

During Cruise 312, September 1962, a series of closely spaced stations was made on a line extending 90 kilometers on either side of the western edge of the plume (Figure 27). The observed vertical distributions of temperature, salinity, oxygen, and chlorophyll based on stations spaced about 9 km apart are shown in Figure 28.

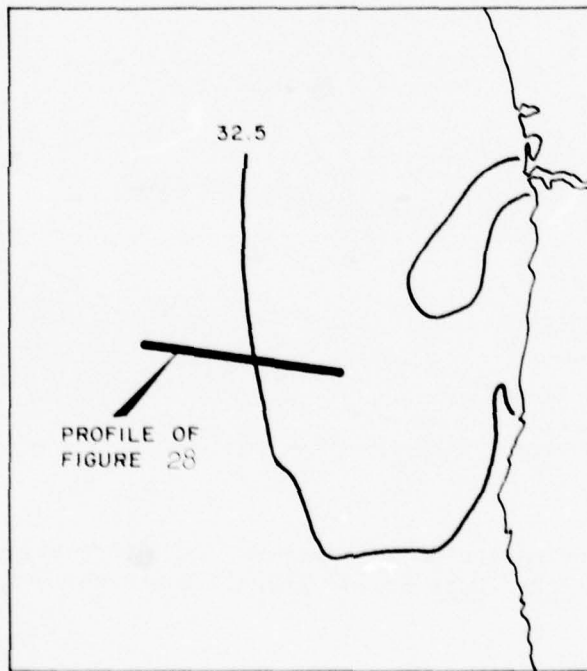


Fig. 27. Location of profile shown in Fig. 28.

Below 30 to 40 m depth in the plume, the location of the 32.5 ‰ bounding isohaline, temperature decreases and the salinity increases rapidly, both contributing to a pycnocline of rapidly increasing density. This boundary between the plume and underlying water is of rather uniform depth and acts as a partial barrier to the vertical exchange of properties between the River effluent and the deeper water. The increase in salinity associated

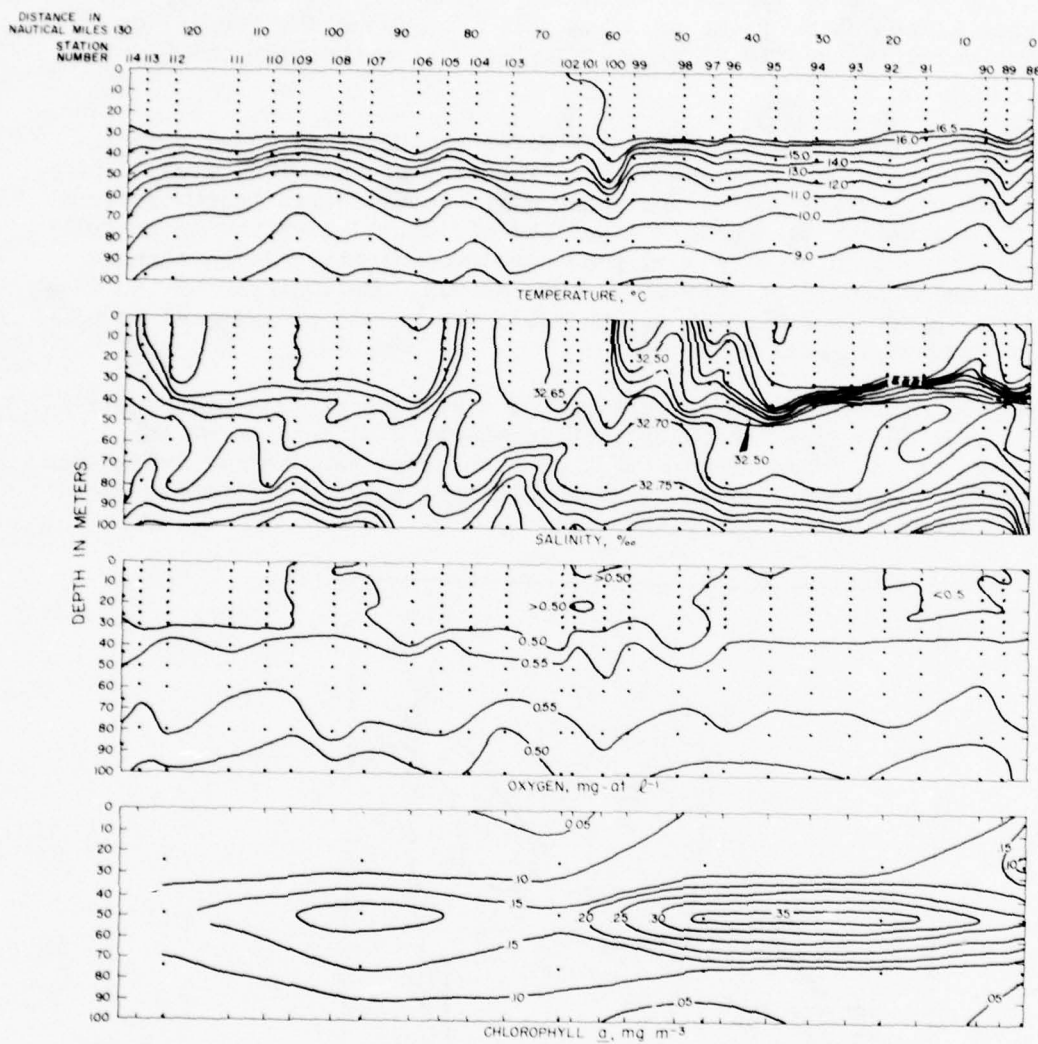


Fig. 28--Vertical distribution of temperature, salinity, oxygen, and chlorophyll, Brown Bear Cruise 312, 14 September-9 October 1962.

with the permanent halocline begins at approximately 80 m depth. The 40 to 70-meter depth interval of dissolved oxygen and chlorophyll a maxima is just below the mixed layer and in the euphotic zone for the region. There are many factors which must be considered when accounting for the vertical distribution of oxygen in this region (Pytkowicz, in press; Stefansson and Richards, in press) and the coincidence of the oxygen and chlorophyll maxima might be fortuitous.

In order to examine qualitatively the mixing of salt water into overlying freshwater, a simple laboratory experiment was performed. Wind stress applied to dyed freshwater overlying salt water resulted in internal waves but no apparent penetration of the dye into the more saline water. When similar stress was applied to clear freshwater overlying dyed salt water, the preferential movement of salt water into the freshwater layer became evident. Figure 29 shows diagrammatically the preferential upward mixing. This phenomenon has been observed and studied in detail by others (Rouse and Dodu 1955; Cromwell 1960) in tanks and is part of the entrainment process described by Tully (1958) when freshwater enters the sea. It can be inferred that the coefficient of vertical eddy viscosity near the pycnocline is less than that near the surface and thus motions generated at the surface result in an upper turbulent layer while there is relatively little disturbance below the pycnocline boundary. A parcel of freshwater carried into the quiet salt water regime is buoyed up again towards the boundary and undergoes relatively less mixing than a parcel of salt water carried into the upper turbulent regime from below. In the ocean, water from below is mixed in the upper layer of River effluent and this mixed layer expands laterally. Dissolved materials in the river effluent will be carried to depths primarily by animals, plants or other particulate matter rather than by mixing processes.

#### Fresh Water Budget of the Plume

The balance between the Columbia River discharge and the apparent disappearance of fresh water from the plume as it mixes with the surrounding seawater was examined. The technique employed is based on the assumption that the background ocean water has a salinity of 32.5 ‰ and that salinities in a water column less than 32.5 ‰ result solely from a mixture of river water and the background water. If this fresh water "fraction" in the water column could be separated from the ocean water, its equivalent height is given by:

$$H = \frac{32.5 Z^* - \int_0^Z S dZ}{32.5}$$

where  $H$  is the height in meters of fresh water,  $S$  the observed salinity, 32.5 the salinity of the ocean background water,  $Z$  the depth and  $Z^*$  the depth of the 32.5 ‰ isohaline. The defects in this approach (a) the salinity of the background ocean water varies a little from 32.5 ‰, and (b) other possible sources of dilution, e.g., precipitation, are ignored; however, it is felt that the technique described above is useful as a first approximation in estimating the volume of river water in the plume. Ketchum and Keen (1955) and Tully and Barber (1960) have used similar approaches in

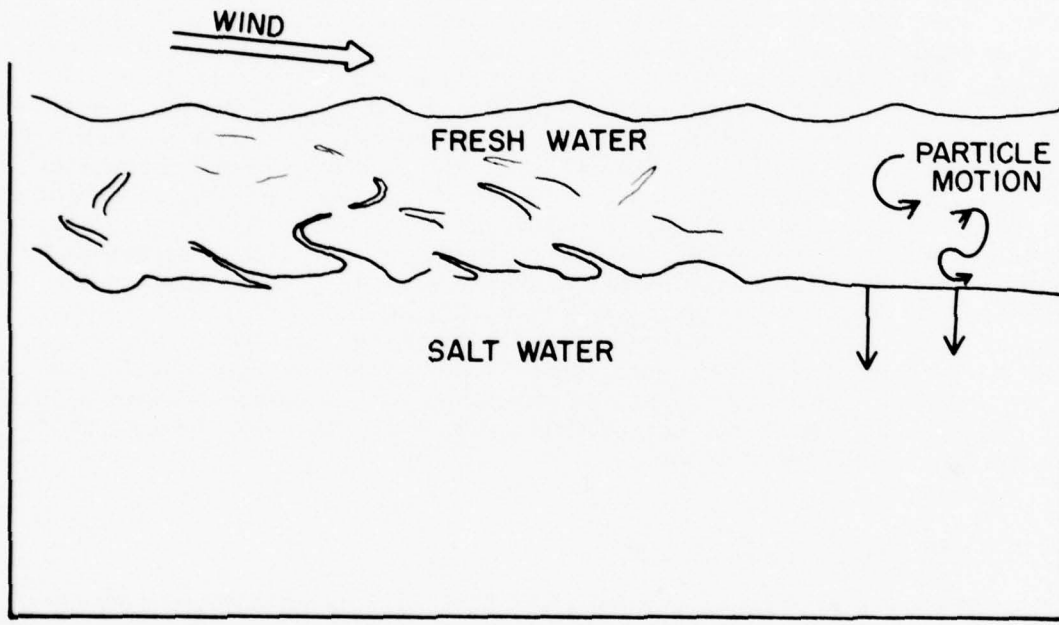


Fig. 29--Model studies of vertical mixing.

studies of the distribution of river and rain water in large areas of the ocean.

The computations described above were completed in the following manner for every station within the plume for 10 cruises listed in Table 4. Large scale plots of the vertical distribution of salinity were made for each station and the value of

$$32.5 Z^* - \int_0^{Z^*} S dZ$$

was obtained using a planimeter. This value was then divided by 32.5 to obtain the equivalent freshwater height in meters. Numerical integration was also carried out for most of the cruises. The difference in heights between the two methods was less than 5 percent and the computer program for determining equivalent fresh water heights is satisfactory.

Contour charts of equivalent fresh water heights were prepared for 10 cruises, and the apparent freshwater volume was determined by planimetry from each of these charts. The results of these computations are shown in Table 4 and contoured charts, which typify winter and summer conditions, are presented for four cruises (Figures 30 to 33). From January 1961 to January 1962, the average daily disappearance or "loss" of freshwater (i.e., mixing of freshwater with seawater until it is no longer detectable by the 32.5 ‰ criterion) was found to be  $6.0 \times 10^8 \text{ m}^3 \text{ day}^{-1}$ , a mean annual loss of plume water of  $6,600 \text{ m}^3 \text{ sec}^{-1}$  ( $232,000 \text{ ft}^3 \text{ sec}^{-1}$ ). If it is assumed that there is no net accumulation of freshwater or increase in salt content in the system surrounding the plume, then the mean annual river discharge should equal this "loss" of freshwater from the plume. The plume "loss" of  $6,600 \text{ m}^3 \text{ sec}^{-1}$  agrees well with the mean annual discharge of  $7,300 \text{ m}^3 \text{ sec}^{-1}$ . This agreement, although perhaps fortuitous, supports the selection of the 32.5 ‰ isohaline as the boundary of the plume. The values shown in Table 4 are from calculations made neglecting precipitation and evaporation and the contribution of coastal streams. The negative value in the "loss" of freshwater volume is probably a result of the combined effects of the rapidly decelerating river runoff in mid-June (Fig. 2) and the wind change shown in Figure 18. The excess apparent freshwater volume during this period might also be attributed to the return southward of the Columbia and coastal river effluent which were previously discharged and lying to the north of the Columbia River mouth. If the average daily "loss" of equivalent freshwater volume is normalized to the area of the plume, it is found to be approximately  $0.1 \text{ cm}^3 \text{ day}^{-1} \text{ m}^{-2}$ . The volumes of freshwater observed for each period of the survey and those for the daily river discharge are presented in Figure 34.

## VII. MAJOR PHYSICAL PHENOMENA AFFECTING THE DISPERSION OF THE EFFLUENT IN THE SEA

### General Description

After initial mixing in the estuary of about 1 part river water with 2 parts seawater, the effluent enters the sea as a "jet" of low salinity

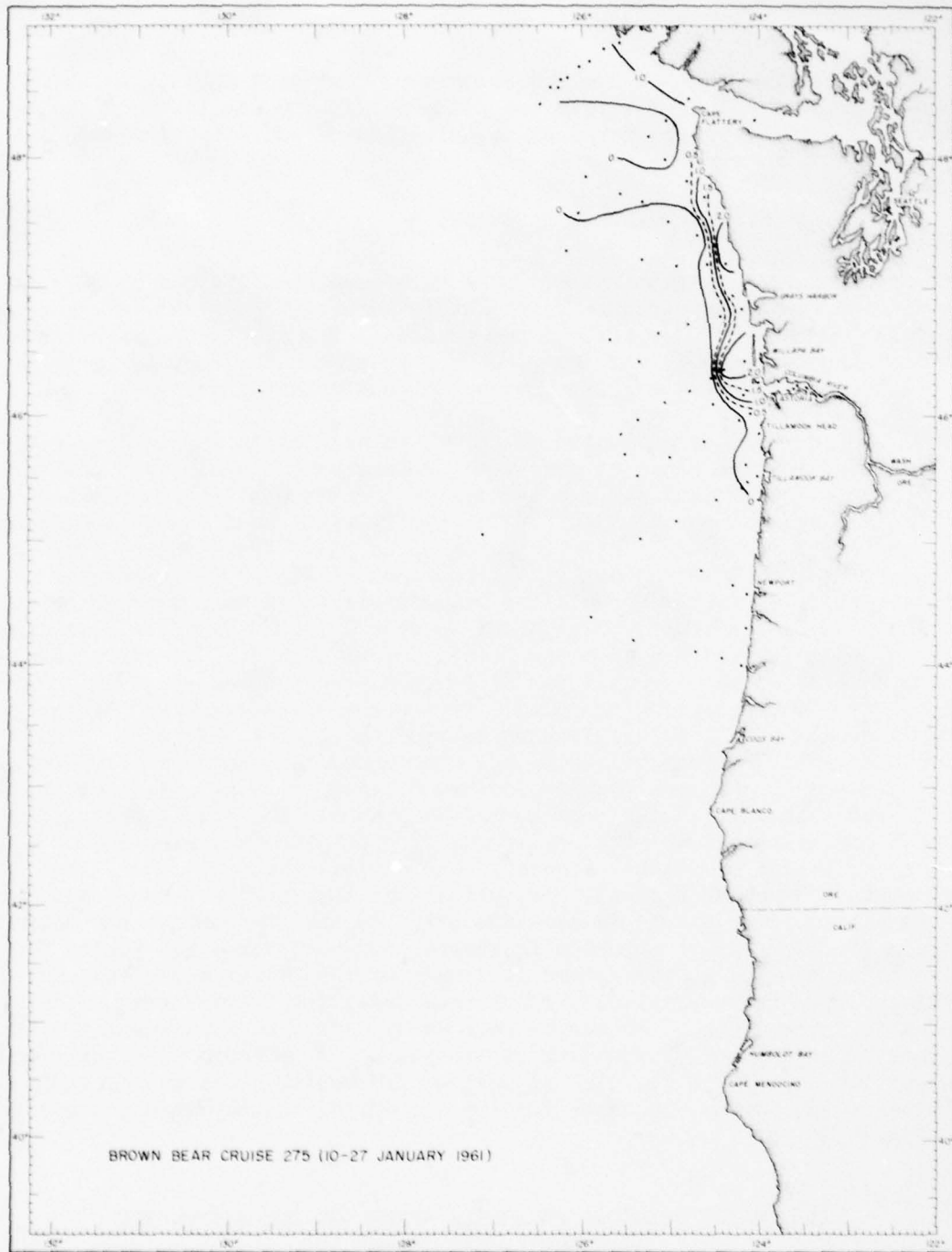


Fig. 30--Equivalent height of fresh water in meters, Brown Bear Cruise 275, 10-27 January 1961.



Fig. 31--Equivalent height of fresh water in meters, Brown Bear Cruise  
290, 6-25 July 1961.

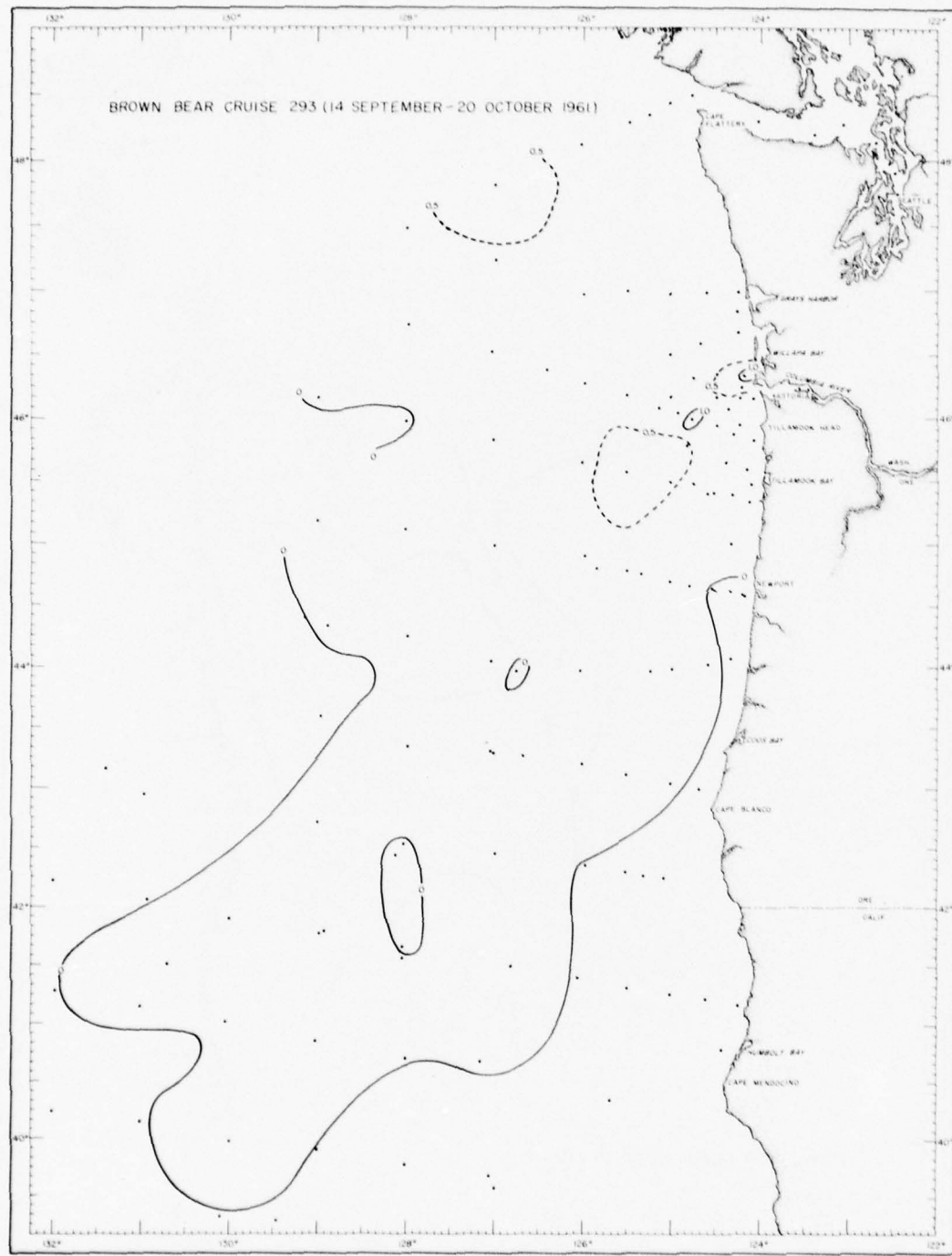


Fig. 32--Equivalent height of fresh water in meters, Brown Bear Cruise 293, 14 September-20 October 1961.

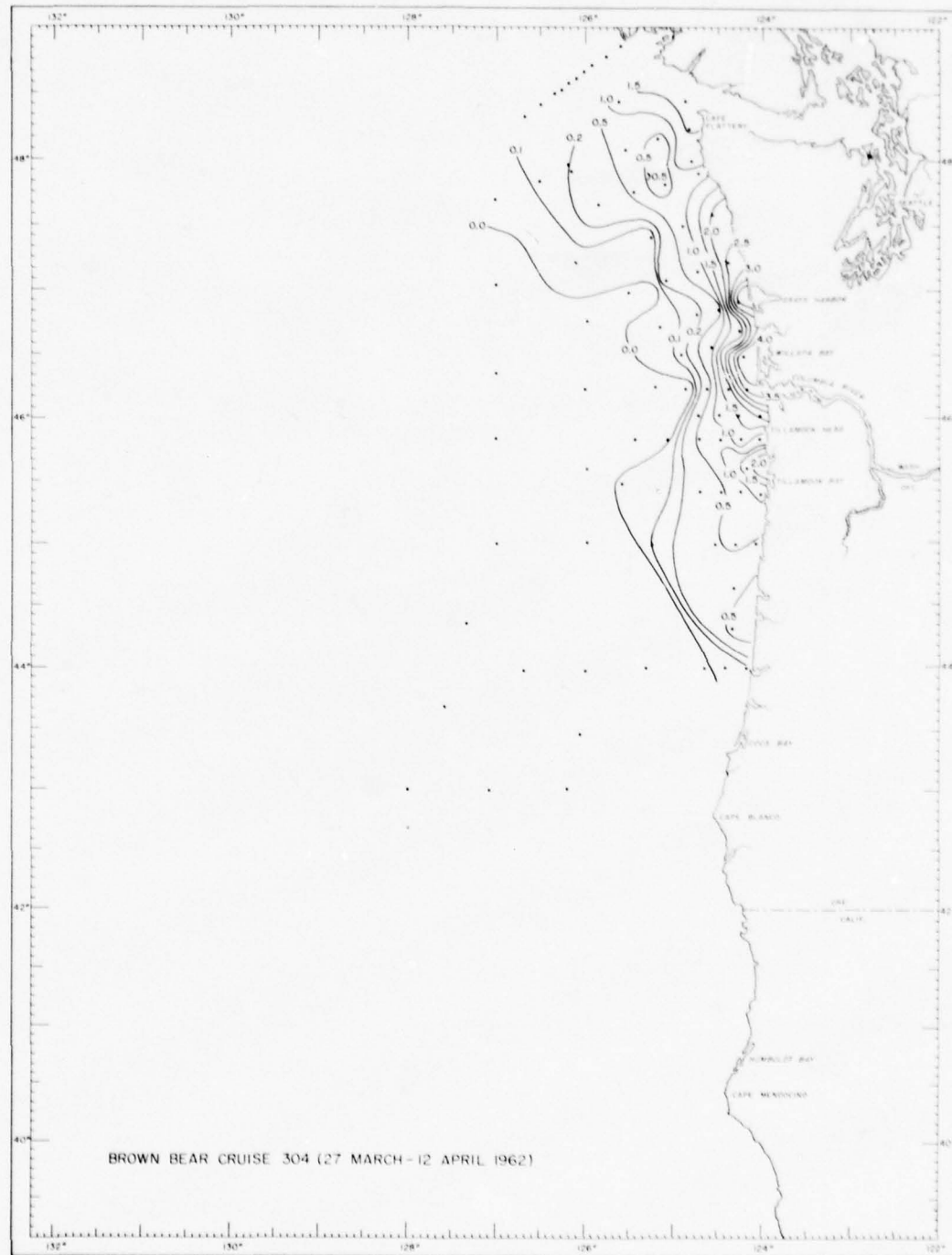


Fig. 33--Equivalent height of fresh water in meters, Brown Bear Cruise 304, 27 March-12 April 1962.

TABLE 4

Cruise Number and Dates	Apparent Fresh Water Volume $m^3 \times 10^{-10}$	Change in Volume between Cruises $m^3 \times 10^{-10}$	No. Days between Cruises	Volume of River Discharge between Cruises $m^3 \times 10^{-10}$		"Loss" of Freshwater $m^3 day^{-1} \times$ $10^{-8} day^{-1}$
				Cruises	50	
BB 275 Jan 1961	0.94	+0.3	58	4.8	7.8	
BB 280 Mar	1.25	+1.9	60	4.2	3.9	
BB 287 May	3.1	+5.0	29	4.5	-1.4	
BB 288 Jun	8.1	+2.3	31	3.2	2.9	
BB 290 Jul	10.4	-6.7	78	2.7	12.1	
BB 293 Sep - Oct	3.7	-1.0	41	2.8	9.2	
BB 297 Nov	2.7	-1.2	53	2.8	7.5	
BB 299 Jan 1962	1.4	+2.3	63	3.0	0.3	
BB 304 Mar - Apr	4.2	+3.2	71	6.8	5.0	
BB 308 Jun	7.4					

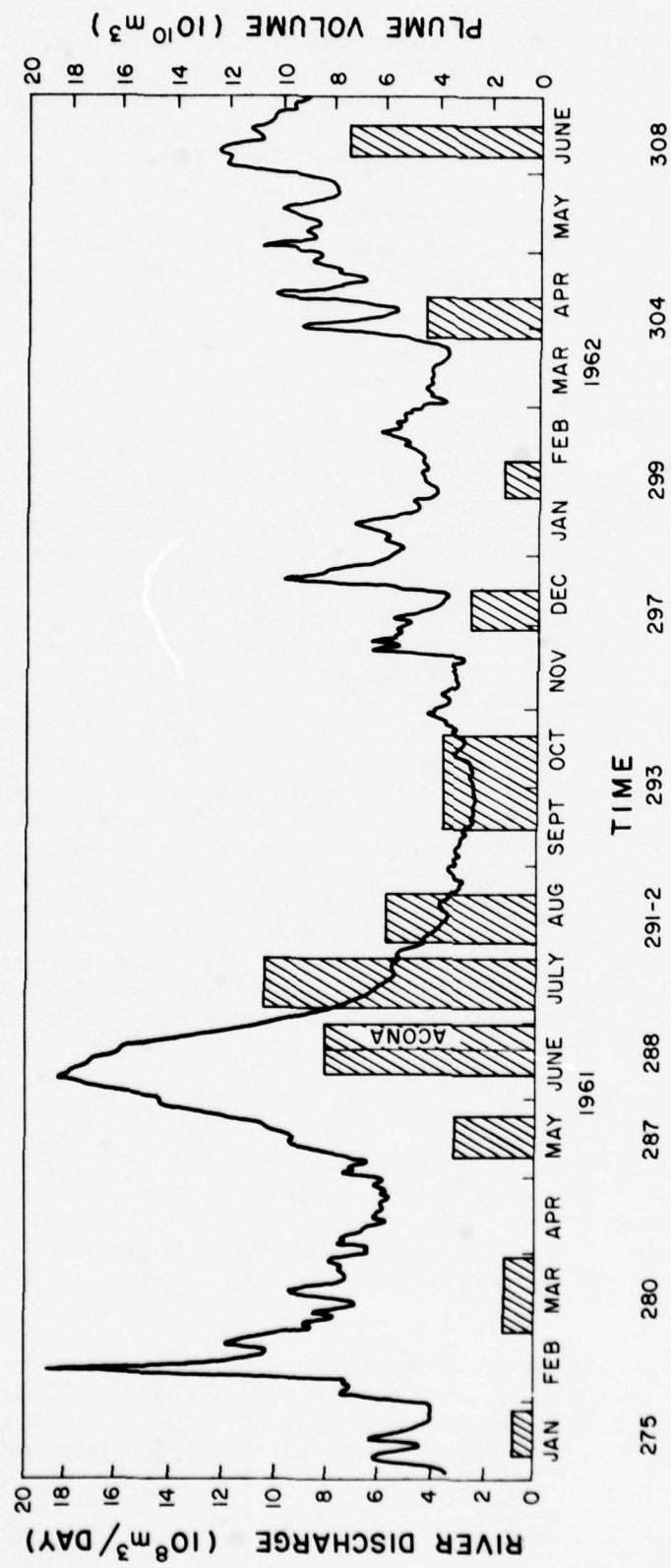


Fig. 34--River discharge curve ( $10^8 \text{ m}^3 \text{ day}^{-1}$ ) and plume volume ( $10^{10} \text{ m}^3$ ) for Brown Bear Cruises 275-308, 1961-62.

water where it continues to be mixed by hydraulic, tidal, and surf-action processes in the nearshore area extending 50 km from the River mouth. In this area lateral and vertical mixing processes create a line source of relatively freshwater, a mixture of about 1 part river water to 10 parts seawater about 40 km in length lying 40 to 50 km seaward of the mouth. As the low salinity mixture of river and salt water accumulates locally on top of denser, more saline ocean water, a surface pressure gradient is maintained which tends to move the freshwater away from the source. The partially mixed effluent enters into the oceanic environment where different processes of mixing and diffusion predominate. In the offshore region advection by wind-induced and geostrophic currents, and eddy diffusion play major roles in dispersing and eroding the plume illustrated diagrammatically for summer conditions in Figure 35.

#### Currents

The currents deduced from the geopotential topography follow a seasonal pattern; they set south both inshore and offshore at 4 to 5 miles per day in the summer and north at about 3 miles per day along the coast during the winter. From the month-to-month details of current direction and speed it is possible to determine the average direction and magnitude of plume movement caused by these currents. In some areas of the region large eddies frequently complicate the pattern and during most periods only a rough average can be estimated. For example, the southerly setting current off the coast of Oregon in the summer of 1961 was about  $8 \text{ cm sec}^{-1}$ ; the range varying locally from 1 to  $20 \text{ cm sec}^{-1}$ . Direction is also variable (cf. Figures 5 to 14). The apparent eddies might be associated with internal waves as mentioned earlier. Geostrophic currents are computed on the assumption of a steady state distribution of mass; whereas transitory effects such as internal waves associated with tides or the passage of local storms; or intrusion of river effluent may cause the local mass structure to depart significantly from steady state conditions and lead to discrepancies in computed currents. Recognizing these limitations, the currents have been computed for various periods of the year and the results used along with wind currents to estimate the resultant movement of the Columbia River water. As an initial approximation the geostrophic current has been estimated to set  $180^\circ T$  at  $8 \text{ cm sec}^{-1}$  in the summer and  $000^\circ T$  at  $6 \text{ cm sec}^{-1}$  in the winter.

#### Wind Transport of the Plume

As mentioned earlier, the seasonal wind patterns of the area off the coasts of Washington, Oregon and Northern California consist of predominantly northerly winds of about  $8 \text{ m sec}^{-1}$  in summer, and southerly winds, frequently of gale force, in winter. The wind drives and mixes the freshwater discharged into the open ocean, greatly affecting the distribution of the Columbia River effluent.

The interaction between the wind and surface waters has been the subject of considerable controversy. A thorough understanding of this interaction has yet to emerge from the numerous studies. The velocity of the surface drift current is a function of the applied surface wind stress and

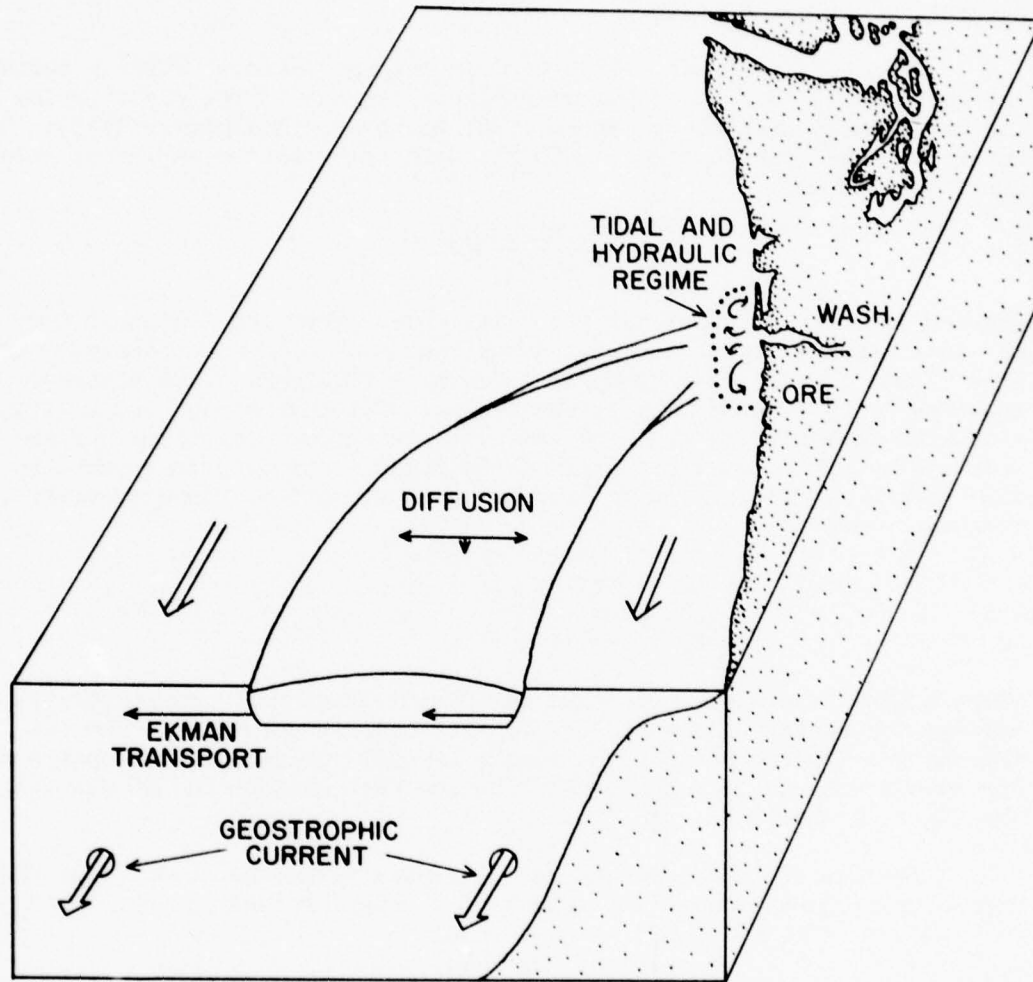


Fig. 35--Major physical phenomena affecting effluent dispersion.

the eddy viscosity of the water. Because of the relatively small eddy viscosity near the shallow sharp pycnocline in the plume area, the momentum input will be confined to a shallower layer in the plume area than outside the plume in the more homogeneous water. The program for computing the wind current is discussed below.

The driving stress of the wind on the sea surface causes a surface current which is directed approximately 45 degrees to the right of the wind in the northern hemisphere (Ekman 1902; Rossby and Montgomery 1935). The water speed is related directly to the wind speed by the empirical relation derived by Ekman:

$$V = \frac{0.0127}{\sqrt{\sin Q}} W \quad (1)$$

where  $W$  is the wind speed and  $Q$  the latitude. The wind factor, 0.0127, has been examined by a number of investigators and a recent analysis of over 77,000 observations supports this value (Budinger, unpublished). The equation is applicable only to the surface wind current and tells little about the transport by wind-induced currents across a vertical surface of unit width. This transport (called the Ekman transport) is related to the wind stress by integration of the equations of motion. In open water the components are

$$\begin{aligned} Ex &= -\tau_y/f, \\ \text{and} \\ Ey &= -\tau_x/f \end{aligned} \quad (2)$$

where  $Ex$  and  $Ey$  are the zonal and meridional Ekman mass transports;  $\tau_x$  and  $\tau_y$ , the surface stresses; and  $f$ , the Coriolis parameter. The net transport is independent of any change in eddy viscosity with depth and the mean transport is directed (in the northern hemisphere) 90 degrees to the right of the wind direction.

The surface stresses can be calculated using the theory that the stress is proportional to the square of the wind velocity:

$$|\vec{\tau}| = \rho_a C_D |W|^2, \quad (3)$$

where  $\rho_a$  is the air density,  $W$  the wind velocity at 10 m,  $C_D$  is a dimensionless drag coefficient, and  $W$  is the wind velocity at 10 m. The validity of this theory and the magnitude of the drag coefficient have been under investigation for many years. Recently, Wilson (1960) examined the results of nearly 50 independent investigations and evaluations of the stress law, and concluded that the mean value of the drag coefficient is 0.0024 for strong winds and 0.0015 for light winds. The two different coefficients have been attributed to an increase in the roughness of the sea surface as the wind increases. The agreement among the authorities quoted was fairly satisfactory for strong winds, but less so for light winds. There is no universal agreement on the velocity or range of velocities demarking strong from light winds in computing drag coefficients. Deacon and Webb (1962) summarized careful observations made under conditions of neutral air stability and found a range of drag coefficient values below

0.002. They suggest that the drag coefficient probably increases linearly with wind speed. This relatively slight increase is described by

$$c_D = (1.00 + 0.07W) \times 10^{-3}$$

where  $W$  is the wind speed in  $m\ sec^{-1}$  at 10 meters. Thus, the drag coefficient for the average winds of  $8\ m\ sec^{-1}$  during the summer would be 0.0016 and for winds of  $20\ m\ sec^{-1}$ , 0.0024. Sheppard's (1958) equation gives 0.0010 and 0.0024, respectively.

The mean stress exerted by a fluctuating wind depends not only on the drag coefficient but also on the value to be used for  $\bar{W}^2$ . Practically, winds must be taken from charts and hence have been smoothed over considerable periods of time (monthly or daily), and as  $(\bar{W})^2$  is always smaller than  $(\bar{W}^2)$ , a larger drag coefficient is necessary to give the same stress value than would be the case if winds were measured continuously. Furthermore, the values of the drag coefficients estimated from different time-averaged observations will vary, and at present there is no means by which wind can be accurately translated into water movement under all conditions. From a review of the work of Taylor (1916), Ekman (1928), Rossby and Montgomery (1935), Palmén and Laurila (1938), and Sverdrup and Fleming (1941) and the results of the use of different coefficients under various natural conditions, a value of 0.0024 for this drag coefficient appears to be the most reasonable for use in the Columbia River effluent area.

The wind speeds in this program were computed from twice daily atmospheric charts. The effect of atmospheric stability will be such as to reduce the drag coefficient for stable conditions and increase the coefficient for unstable conditions; however, the exact relationship has not been determined.

If the wind field is known, its effect on the water can be computed using the equations (1) and (3). It is possible to derive the surface winds and thus the surface stresses from the geostrophic winds, which in turn are a function of the atmospheric pressure field:  $\tau \propto W^2 \propto \Delta P^2$ . The pressures are available from the meteorological reports. This method of determining the surface stresses is similar to that used by Montgomery (1935) and Fofonoff (1960). Fofonoff, applying the theory that total steady-state transport of mass in the ocean depends primarily on the curl of the wind stress acting on the surface of the ocean (Sverdrup 1947; Stommel 1948; Munk 1950), computed the transports in the North Atlantic and North Pacific Oceans. He used monthly means of sea-level pressure (averaged from twice-daily observations) and plotted these on a 10-degree diamond grid. The atmospheric pressures were taken from the observations made by the Extended Forecast Section of the U.S. Weather Bureau. It was found that these data were inadequate for the Columbia River area because day-to-day variations as well as small-scale space variations are important in this problem. To obtain adequate information it was necessary to determine values of atmospheric pressure for eight grid points, shown in Figure 36, from the 0000 and 1200 Greenwich charts of atmospheric pressure prepared by the local weather bureau at the Seattle-Tacoma International Airport.

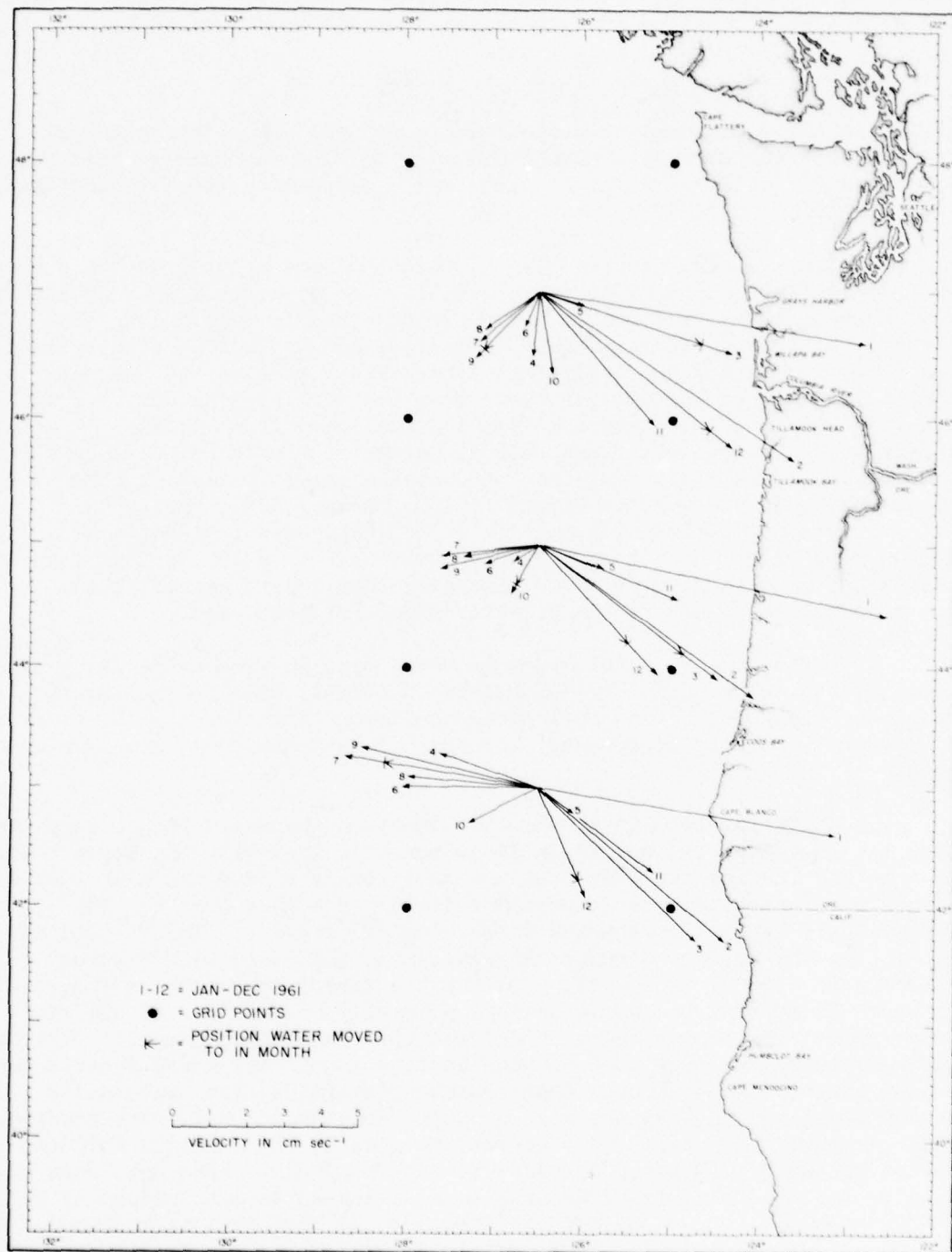


Fig. 36--Monthly averages of Ekman transport, 1961, converted to velocity ( $\text{cm sec}^{-1}$ ) of the water column 0 to 40 meters.

Pressures were recorded for each of the eight grid points for the period of January 1961 through 1962 to present. The University of Washington IBM 709 computer was programmed to compute the meridional, zonal and resultant surface wind, surface drift current, wind stress, and Ekman transport from the twice daily estimates of the pressure field off the Washington and Oregon coasts. The computation scheme entailed determining the geostrophic wind velocity aloft. This wind vector was then rotated 15 degrees to the left (Montgomery 1935) of its downwind direction and reduced by 30 percent (Gordon 1950). The result of this operation is the 10-meter wind (the W applicable to the equations). The meridional and zonal components of this wind were then used to determine the surface current using equation (1). The direction of this current was assumed to be 45° to the right of the surface wind vector.

The surface stress, proportional to the square of the wind speed, was also calculated using the stress relationships:

$$\tau_x = \rho_a C_D U \sqrt{U^2 + V^2}$$

$$\tau_y = \rho_a C_D V \sqrt{U^2 + V^2},$$

where  $U$  and  $V$  are the zonal and meridional components of  $W$ , respectively. The air density,  $\rho_a$ , was taken as  $1.22 \times 10^{-3} \text{ gm cm}^{-3}$ , and the drag coefficients  $C_D$ , as  $2.4 \times 10^{-3}$ . If the wind speeds are in units of  $\text{cm sec}^{-1}$ , the stress is in  $\text{dynes cm}^{-2}$ . The Ekman transport was computed using the computed surface stresses and the Coriolis parameter according to (2).

Because the eddy viscosity becomes very small at the lower boundary of the plume, the depth of frictional resistance of the Ekman layer is assumed to coincide with the bottom of the plume, at about 40 m. Therefore the movement of a water particle within the plume due to the wind-induced Ekman transport can be calculated from:

$$\left| \begin{array}{c} \rightarrow \\ V_E \end{array} \right| = \left| \begin{array}{c} \rightarrow \\ E \end{array} \right| 0.57$$

where  $\left| \begin{array}{c} \rightarrow \\ V_E \end{array} \right|$  is the horizontal displacement of a  $1 \text{ m} \times 40 \text{ m}$  column in nautical miles per 12-hour period and  $\left| \begin{array}{c} \rightarrow \\ E \end{array} \right|$  is the Ekman transport in metric tons  $\text{m}^{-1} \text{sec}^{-1}$ . The resultant monthly averages of Ekman transports are presented in Figure 36 for the year 1961. These vectors clearly show the seasonal variation of the wind effect on the surface transport. The net Ekman transport for 1961 is south. Power spectrum analyses and further studies are planned for the values of Ekman transport.

The period before a steady transport is reached for a particular wind stress has been estimated to exceed 5 pendulum hours and is probably in the order of one day (Ekman 1905; Von Arx 1961). By integrating the transports during each cruise or between mid-times of successive cruises, the magnitude and direction of the wind-induced movement can be obtained. Then the vector sum of the geostrophic current and the Ekman transport current gives the translation of the plume for the period. Figure 37 shows the predicted axes for Cruises 288 (June), 290 (July), and 293 (September-October 1961). A constant  $4 \text{ mile day}^{-1}$  current setting south was used,

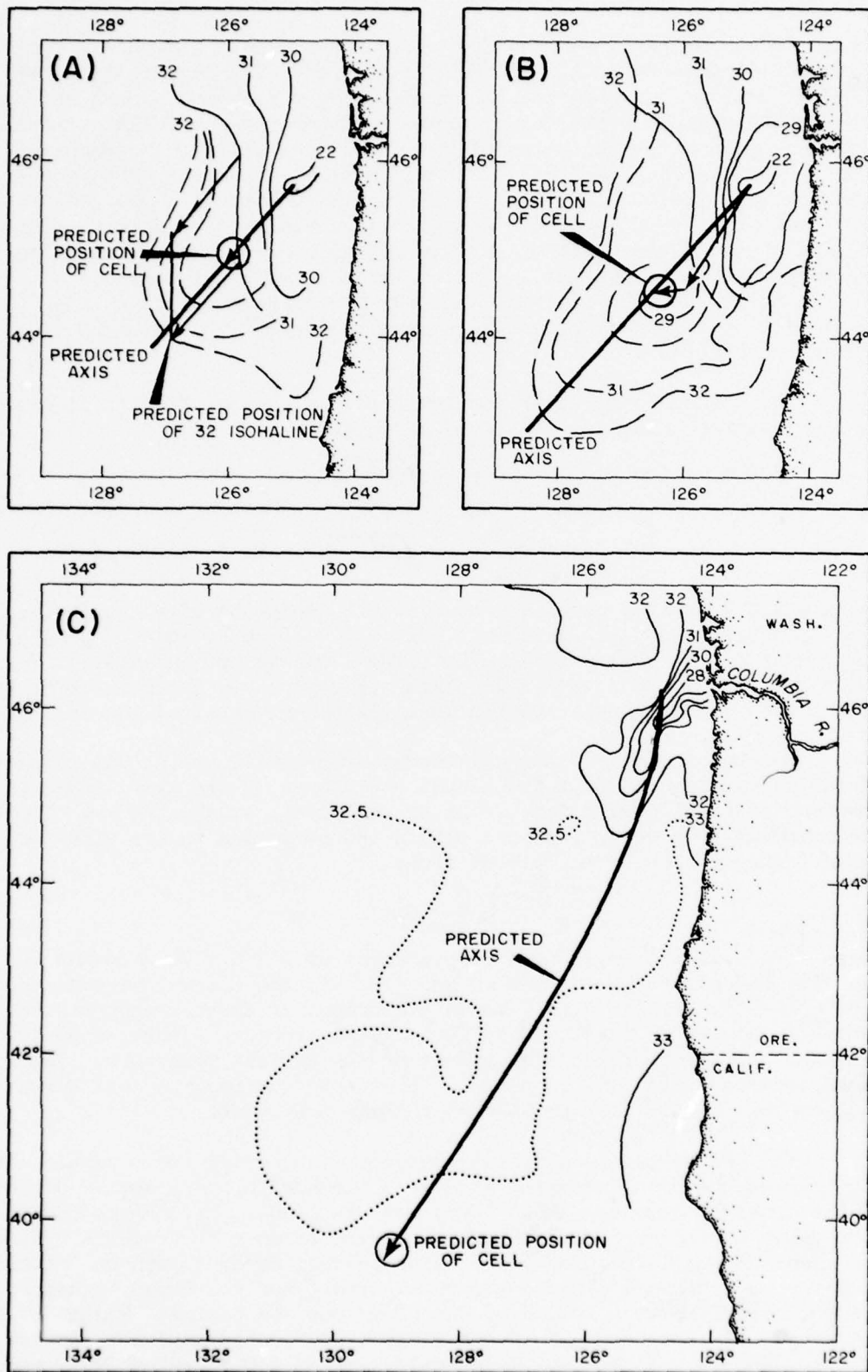


Fig. 37--Predicted axis and outward extent of plume: (A) Brown Bear Cruise 288, 9-19 June 1961, and Acona Cruise 6106, 19-29 June 1961 (dashed line); (B) Brown Bear Cruise 290, 6-25 July 1961; (C) Brown Bear Cruise 293, 14 September-20 October 1961.

except for a period preceding Cruise 290 when there was no current in an area of divergence (Figure 9). During June when the discharge is the greatest an Ekman layer of 20 meters thickness was assumed; for all other periods the layer was assumed to be 40 meters.

Figure 37A shows the observed movement of the plume during a 10-day period in June. The origin for the initial vector was 40 km west of the River mouth. A strong northerly storm ( $16 \text{ m sec}^{-1}$ ) commenced during the later part of Cruise 288 (9-19 June) and abated during the first part of ACONA Cruise 610 (19-29 June). The predicted center of the cell is the resultant of the vector addition of the geostrophic current and wind driven current for the period 10-20 June. The projected  $32^{\circ}/\text{o}$  isohaline was constructed using the same vector. Figure 37B shows the predicted axis of the plume based on the geostrophic and wind currents from Cruise 288 (June) to Cruise 290 (July). The predicted axis for September-October 1961 (Fig. 37C) was prepared by laying out the resultant vectors for the middle and lower grids of Figure 36 with an origin 40 km off the River and on the axis of Cruise 290, respectively. Somewhat better agreement between the actual and predicted axes for the southern section of the plume would be obtained if a grid for Ekman transport had been constructed farther south--the wind current near  $40^{\circ}\text{N}$  was northwest during the latter part of the prediction period from 14 July to 2 October 1961. The predicted axes and water movement are in fair agreement with the observed. It should be stressed, however, that the axes and the cell trajectories are subject to errors in the choice of computation parameters (i.e., layer depth, drag coefficient, averaging period, direction and speed of the geostrophic currents).

## VIII. DIFFUSION OF RIVER WATER IN THE SEA

### General Remarks

Although the vector sum of the geostrophic current and the velocity derived from Ekman transport computations roughly describes the advection of effluent water, the model for analysis and prediction is incomplete unless diffusion is also considered. The yearly average rate of detectable effluent disappearance (mixed beyond recognition by the measuring technique--approximately 1 part of River water to 1,000 parts seawater) was computed as about  $6.0 \times 10^8 \text{ m}^3 \text{ day}^{-1}$ . This figure agrees well with the computed average annual River discharge. It appears that the effluent waters lying on the surface become mixed vertically with seawater from below the upper halocline by a preferential upward movement of deep water, and laterally, as the plume spreads, with background water of  $32.5^{\circ}/\text{o}$ . This results in a slight increase in thickness (about 10 m in 280 kilometers) and width of the pancake-shaped effluent with time and distance from the River mouth.

Vertical and lateral diffusion processes in the sea have proved difficult to describe and analyze, and previous attempts to describe the diffusion of an effluent in the sea are not wholly satisfactory for this system (Takano 1954, 1954a, 1955; Hamada 1959; Gifford 1959; Brooks 1960, and Defant 1961). For most analyses it is necessary to determine the horizontal and vertical coefficients of eddy diffusion,  $K_x$ ,  $K_y$ , and  $K_z$ . These

coefficients are used in a diffusion law of one form or another (Pearson 1960; Waldichuk 1963). Reviews of these coefficients have been given by Okubo (1962) and Ichiye (1962).

As mentioned previously the problem of discharge into the ocean might best be separated into an examination of the nearshore tidal and hydraulic regime (less than 50 km from the estuary) and the offshore wind and current regime. Work has just begun in the more complicated nearshore environment, and no results are as yet available.

#### Vertical Mixing

The river effluent is confined to the first few tens of meters (Fig. 4 and 29) and is mixed with the ambient seawater by upward transport of properties from the deeper water and horizontal turbulence. Three methods were used in an attempt to evaluate the vertical coefficient of eddy diffusion.

**METHOD I--**The vertical salinity section along the plume axis for Cruise 288 (June 1961; Fig. 26) was used to compute  $K_z$  from  $u \frac{\partial S}{\partial x} = K_z \frac{\partial^2 S}{\partial z^2}$ . The ratio  $K_z/u$  was determined at 10-meter depth increments down to 40 meters (the approximate bottom of the plume) for 6 locations 30 km apart along the axis starting 50 km from the source. The values for  $K_z/u$  were not consistent, often changing in sign and magnitude. An average of the positive values of  $K_z/u$  was approximately  $0.3 \text{ cm}$ . Assuming a realistic value of  $10 \text{ cm/sec}$  for  $u$ ,  $K_z$  average is  $3 \text{ cm}^2 \text{ sec}^{-1}$ . A smoothed composite vertical salinity distribution approximating a combination of the profiles from Cruises 288 (June 1961), 290 (July 1961), 293 (September-October 1961), and 308 (June 1962) was then used to compute  $K_z/u$ . It was hoped that the smoothing would remove some of the discrepancies in the values of  $K_z/u$ ; however, the mean value of  $K_z$  of  $3 \text{ cm}^2 \text{ sec}^{-1}$  was averaged from a wide scatter of values.

**METHOD II--**The second method was based on the Fickian equation of diffusion

$$\frac{dM}{dt} = -K_z \frac{dc}{dn}$$

where the mass,  $M$ , of a substance diffusing through a unit area in time,  $t$ , is proportional to the concentration gradient normal to the unit area. The vertical eddy coefficient,  $K_z$ , can be evaluated from this formula if estimates can be made of the change of mass with time within one water mass. During Cruise 309 (September 1961), a series of shallow stations (47A to 47H) was made in a manner which allowed evaluation of the change in mass of the water column above the halocline over a period of time. A 24-foot aviator's parachute was used as a sea anchor and the ship occupied hydrographic stations at approximately 3-hour intervals for a total of 21 hours during which the ship drifted south at  $15-25 \text{ cm sec}^{-1}$ . Figure 38 shows the vertical distribution of salinity at stations 47A to 47H. This figure shows:

- a) a sharp, nearly constant salinity gradient;
- b) an apparent vertical fluctuation of the gradient over a range of 10 m;
- c) a relatively constant value of salinity ( $32.55 - 32.65 \text{ }^{\circ}/\text{o}$ ) at the bottom of the halocline (30 m); and
- d) an increase in salinity in the water column above the halocline between successive pairs of stations.

It would appear that the processes tending to alter the vertical salinity distribution also tend to maintain a steady state in the halocline over the time period of the observations and that salt is being diffused upward across the halocline, steadily increasing the mass of the surface layer. Thus, if the effect of the fluctuations of the halocline is removed, the diffusion equation can be applied directly to calculate  $K_z$  for the halocline.

The changes in depth with time of certain values of salinity in the halocline are shown on the bottom of Figure 38. Both in this figure and in other analyses a regular 11 to 12-hour period suggests that the vertical fluctuations were the effects of tide-generated internal waves. To minimize these effects the vertical salinity distributions were normalized by applying a depth correction calculated from the median values for the depth of the various salinities. After applying the corrections, the vertical salinity distributions for each station were redrawn. The normalized vertical distributions showed remarkable uniformity in the region of the halocline from  $30.7 \text{ }^{\circ}/\text{o}$  at 17 meters to  $32.2 \text{ }^{\circ}/\text{o}$  at 23 meters. These curves are shown in Figure 39, which also illustrates the increase in salt in the water column above the halocline from one station to the next. The diffusion equation was approximated by

$$h(\bar{s}_2 - \bar{s}_1) = -K_z \frac{\Delta s}{\Delta z} (T_2 - T_1)$$

where  $h$  is the depth to the bottom of the halocline, and  $\bar{s}$  is the average salinity over depth  $h$  at time  $T$ . The subscripts signify successive stations. The evaluation given in Table 5 shows the calculated  $K_z$ 's to vary between 2.2 and  $11.3 \text{ cm}^2 \text{ sec}^{-1}$ . Because the stability decreases slightly from A to H, a gradual increase in the eddy coefficient would be expected.

TABLE 5

## COMPUTATION OF VERTICAL EDDY COEFFICIENT FROM DRIFTING STATION 47 BB 309

Sta	$\frac{\Delta s}{\Delta z} \cdot 10^3 \text{ }^{\circ}/\text{o cm}^{-1}$	$\bar{s}_2 - \bar{s}_1 \text{ }^{\circ}/\text{o}$	$T_2 - T_1 \cdot 10^{-3} \text{ sec}$	$h(\bar{s}_2 - \bar{s}_1) \text{ cm} \cdot ^{\circ}/\text{o}$	$\frac{\Delta s}{\Delta z} (T_2 - T_1) \text{ }^{\circ}/\text{o sec cm}^{-1}$	$K_z \text{ cm}^2 \text{ sec}^{-1}$
A-B	2.21	.019	11.8	57	26	2.2
B-C	2.03	.079	10.2	237	21	11.3
C-D	1.92	.016	10.9	48	21	2.3
D-E	1.94	.023	10.5	69	20	3.5
E-F	1.84	.038	11.0	114	20	5.7
F-G	1.89	.041	10.8	123	20	6.2
G-H	1.99	.043	10.0	129	20	6.5

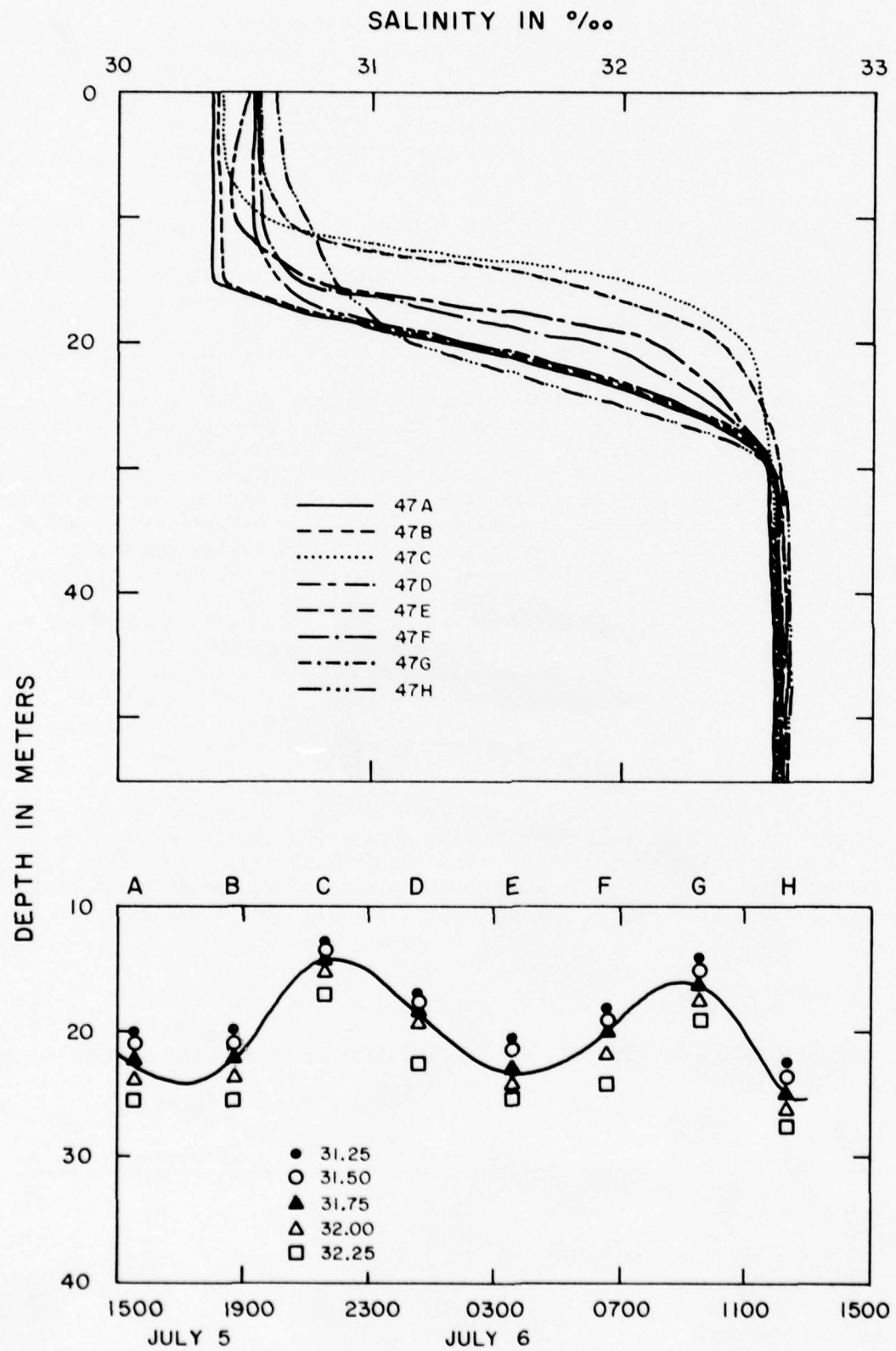


Fig. 38--Vertical distributions of salinity at Brown Bear drifting station 47 during Cruise 309, 20 June-9 July 1962.

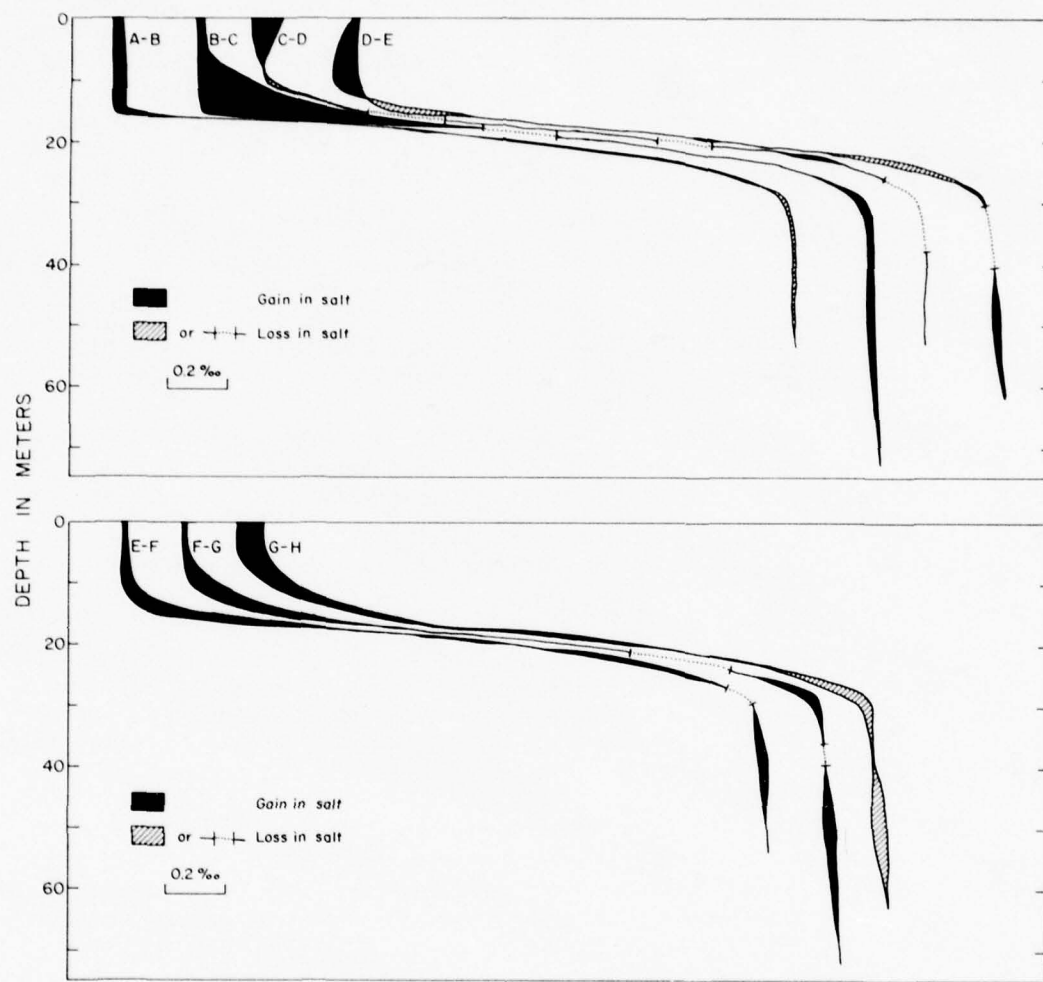


Fig. 39--Normalized salinity distributions of Figure 38 showing salt gain and loss between successive stations.

METHOD III--When the plume is still growing, its volume increases downstream and the change of volume from one section to the next may be converted to an addition of water of salinity 32.5 ‰ per unit time. An apparent upward speed can be computed by dividing this volume addition per unit time by the average surface area of the two sections used to determine the change in volume. The plume near its origin during Cruise 288 (Fig. 18) was divided into three adjacent solid rectangles oriented normal to the axis. The bottom of these adjacent sections was the 32.5 ‰ surface. Assuming that all of the salt was added to each section by advection from below, the mean salinity for the next section can be calculated and compared with the integrated salinity from the observed values. The results of this technique and the vertical speeds are shown in Table 6. The vertical upward speeds decrease with an increase in distance from the mouth of the river. The vertical speed of about 1.5 meters day<sup>-1</sup> ( $1.7 \times 10^{-3}$  cm sec<sup>-1</sup>) is in the order of magnitude of speeds estimated for upwelling in other situations by McEwen (1934), Sverdrup and Fleming (1941), Saito (1951), and by Hidaka's (1954) quantitative conclusions based on a theoretical model.

To compare the results of this method with those from METHODS I and II which give the apparent change as due to diffusion (i.e., in terms of an eddy coefficient), the term for vertical advection ( $w \frac{\partial s}{\partial z}$ ) in the distribution of variables equation was equated to

$K_z \frac{\partial^2 s}{\partial z^2}$ . Assume  $K_z$  is constant and  $w$  from METHOD III is  $1.7 \times 10^{-3}$  cm sec<sup>-1</sup>. Typical values for  $\frac{\partial s}{\partial z}$  and  $\frac{\partial^2 s}{\partial z^2}$  for the area of observation are  $3 \times 10^{-2}$  ‰ cm<sup>-1</sup> and  $4 \times 10^{-4}$  ‰ cm<sup>-2</sup>, respectively. The coefficient  $K_z$  computed by equating the advection term to the diffusion term is  $1.4 \text{ cm}^2 \text{ sec}^{-1}$ . METHODS I and II give coefficients of eddy diffusion between 2 and  $11 \text{ cm}^2 \text{ sec}^{-1}$ . The evaluation of the change of upward velocity with distance from the origin, horizontal advection, and stability is being pursued.

OTHER METHODS--The closely spaced observations shown in Figure 26 and more recent sections through the plume edge provide a basis for the estimation of  $K_z$  and its relation to stability and distance from the river mouth. The undulations in the halocline must be smoothed before computations based on the equation

$$u \frac{\partial s}{\partial x} = K_z \frac{\partial^2 s}{\partial z^2}$$

will be valid. These computations have not been made as yet.

Measurements of horizontal and vertical diffusion of planted dye and radioactive materials are planned and estimation of the coefficients will be made using the techniques outlined by Sutton (1953), Crank (1956), Pritchard and Carpenter (1960), and Okubo (1962).

#### Horizontal Diffusion

Horizontal coefficients of eddy diffusion,  $K_x$  and  $K_y$ , have been shown to vary with a scale of the phenomenon. This scale is sometimes considered to be the distance between neighboring particles or the size of an eddy; or

TABLE 6

## COMPUTATION OF VERTICAL VELOCITIES FROM CONTINUITY

$$\bar{S}_2 v_2 = \bar{S}_1 v_1 + (v_2 - v_1) (32.5) \quad (1)$$

$$W = \left( \frac{\frac{V_2 - V_1}{A_1 + A_2}}{2} \right) \cdot \frac{U}{X} \quad (2)$$

$$\bar{S}_3 v_3 = \bar{S}_2 v_2 + W \left( \frac{A_3 + A_2}{2} \right) \left( \frac{X}{U} \right) (32.5) \quad (3)$$

Subscripts refer to section numbers.

$\bar{S}$	= mean salinity ( $^{\circ}/\text{oo}$ )
$V$	= volume (cu. m.)
$A$	= area (sq. m.)
$W$	= vertical velocity (m/day)
$U$	= mean current, taken to be 5 nm/day
$X$	= translation distance due to $U$ , 10 nm. (width of sections)

Mean Salinities				
Region No.	Integrated from contours	Computed from equation (1)	Computed from equation (3)	$W^{-1}$ m da
1	31.57			1.72
2	31.69	31.68		1.47
3	31.70	31.77	32.31*	0.162
4	31.65	31.71	34.67*	

\* The  $W$  calculated from two preceding volume segments is used to predict the  $\bar{S}$  of the next section; since  $W$  decreases with distance from the source of the freshwater, this  $W$  is too large for the situation existing in the next region, and hence the resulting  $\bar{S}$  is too large.

the size of the water body in more restricted waters (see, e.g., Sverdrup 1946; Stommel 1949). After the scale of phenomenon is defined various "laws" have been used to relate the eddy diffusion coefficients to the length parameter. The relation usually takes the form  $K \propto L^x$  where  $x$  lies between 1 and 4/3 depending on the assumptions and arguments used. An extensive examination of the literature for values of  $K$  calculated from distributions of properties in nature (Coachman and Budinger, unpublished) revealed that a value of  $x$  between 1 and 1.2 best fitted the observations, though there is always considerable variation in this type of calculation. It is obvious that the coefficient will be subject to the choice of the scale of the phenomenon and in many cases this choice is quite arbitrary.

Two techniques were used to calculate  $K_x$  and  $K_y$ :

METHOD I--Over most of the plume beyond 40 to 50 km from the river mouth it can be assumed that advection along the axis is balanced by lateral and vertical diffusion:

$$U \frac{\partial C}{\partial X} = K_y \frac{\partial^2 C}{\partial Y^2} + K_z \frac{\partial^2 C}{\partial Z^2}$$

where  $U$  is the velocity along  $x$ , the axis of the plume;  $C$  is the concentration of freshwater, and  $K_y$  and  $K_z$  are constant eddy coefficients. Approximate solutions for this equation have been given by Roberts (1923). The general solution for a continuous point source introduction of material which is advected in  $x$  and dissipated through non-isotropic mixing is:

$$X = \frac{Q}{4\pi \left\{ K_x K_y K_z \right\}^{1/2} \left\{ \frac{X^2}{K_x} + \frac{Y^2}{K_y} + \frac{Z^2}{K_z} \right\}} \exp \left\{ -\frac{U}{4X} \left( \frac{Y^2}{K_y} + \frac{Z^2}{K_z} \right) \right\}$$

If diffusion in the  $X$  direction is small compared to the advection; that is, if

$$\frac{\left\{ \frac{Y^2}{K_y} + \frac{Z^2}{K_z} \right\}}{\frac{X^2}{K_x}}$$

is negligible, the solution reduces to

$$C \approx \frac{Q}{4\pi (K_y K_z)^{1/2} x} \exp \left\{ -\frac{U}{4x} \left( \frac{Y^2}{K_y} + \frac{Z^2}{K_z} \right) \right\}$$

Values for  $K_y/K_z$  can be obtained from this equation by applying data from various cruises and the river discharge. In order to apply the equation, certain assumptions regarding the quantities  $U$ ,  $C$ , and  $Q$  were necessary. First, the maximum concentration of freshwater on a chart similar to Figures 30 to 33 was taken as the axis of the plume, the  $x$ -axis. The value of  $U$  was estimated from the distance along the axis to the edge of the plume

divided by the number of weeks of accumulated water in the plume. This method leads to advection values which are somewhat lower than those determined from the wind and geostrophic currents; however, the technique used to evaluate  $K_y/K_z$  is not sensitive to the value of  $U$ . The concentration of freshwater in the plume ( $C$ ) was defined as the dimensionless ratio

Equivalent Freshwater Height, and these values were taken directly from the

Depth of 32.5°/oo charts of freshwater distribution. The values for the ratio  $K_y/K_z$  computed in this manner for winter observations of Cruise 287 and the summer observations of Cruise 290 ranged from  $10^5$  near-shore to  $10^8$  offshore. Assuming the scale of the phenomena is described by the r.m.s. of the  $x$  and  $y$  distances, a relationship was found between the eddy coefficient ratios and the scale of the phenomenon (Figure 40:  $K_y/K_z \propto L^{2.6}$ ).

If  $K_z = 1 \text{ cm}^2 \text{ sec}^{-1}$  everywhere, the values of the ratio would also be values for  $K_y$ , but the slope  $K_y/L$  is then significantly larger than has ever been reported. If this is the case we would have to conclude that the simplified equation does not adequately describe the effluent distribution. However, if  $K_z$  were 1 to 2 orders of magnitude smaller near the River mouth than offshore, then the slope of the line in Figure 40 would approach  $K_y L^{1.0}$ . This latter possibility is reasonable in view of the general decrease in stability of the water column with increase in distance from the mouth, as  $K_z$  must increase with a decrease in stability. In either event, the relationship shown in Figure 40 is so consistent that it can be used in an empirical model for predicting the dispersion of the plume water in the offshore environment.

METHOD II--The horizontal coefficients were evaluated using the Eulerian expansion of the distribution of variables equation assuming a steady state and no vertical diffusion. The assumptions are highly questionable and the coefficients calculated are too large, but the technique is presented to show the order of magnitude of the coefficients derived. Data from Cruise 290 were used. The surface salinities from that Cruise (Fig. 19) show distinct pockets of low salinity water. An assumption was made that these cells were generated from the river in a similar manner and thus were originally of the same size. As they move away from the source the volume increases due to addition of surrounding seawater. The horizontal gradient of salinity, assumed to be symmetrical in all directions, was determined for the three cells located approximately along the axis. The one cell remote from the source, but close to the coast, was neglected because of possible reflection from the coastal barrier. The rate of change of the gradient with distance,  $\frac{\partial^2 S}{\partial X^2}$ , was computed by find-

ing the difference between gradients of successive cells and dividing by the distance between the centers of the cells. Assuming a horizontal velocity of  $10 \text{ cm sec}^{-1}$  as a reasonable average resultant for the effects of the geostrophic and wind driven currents,  $K_x$  and  $K_y$  were calculated to be  $K_x = K_y = 4 \times 10^7 \text{ cm}^2 \text{ sec}^{-1}$  and the age of the most remote cell to be 27 days. If the single low salinity cell of Cruise 288 (Fig. 18) is the same as the most remote cell in Figure 19, the calculated age agrees with the actual time interval between Cruise 288 and 290 of 30 days.

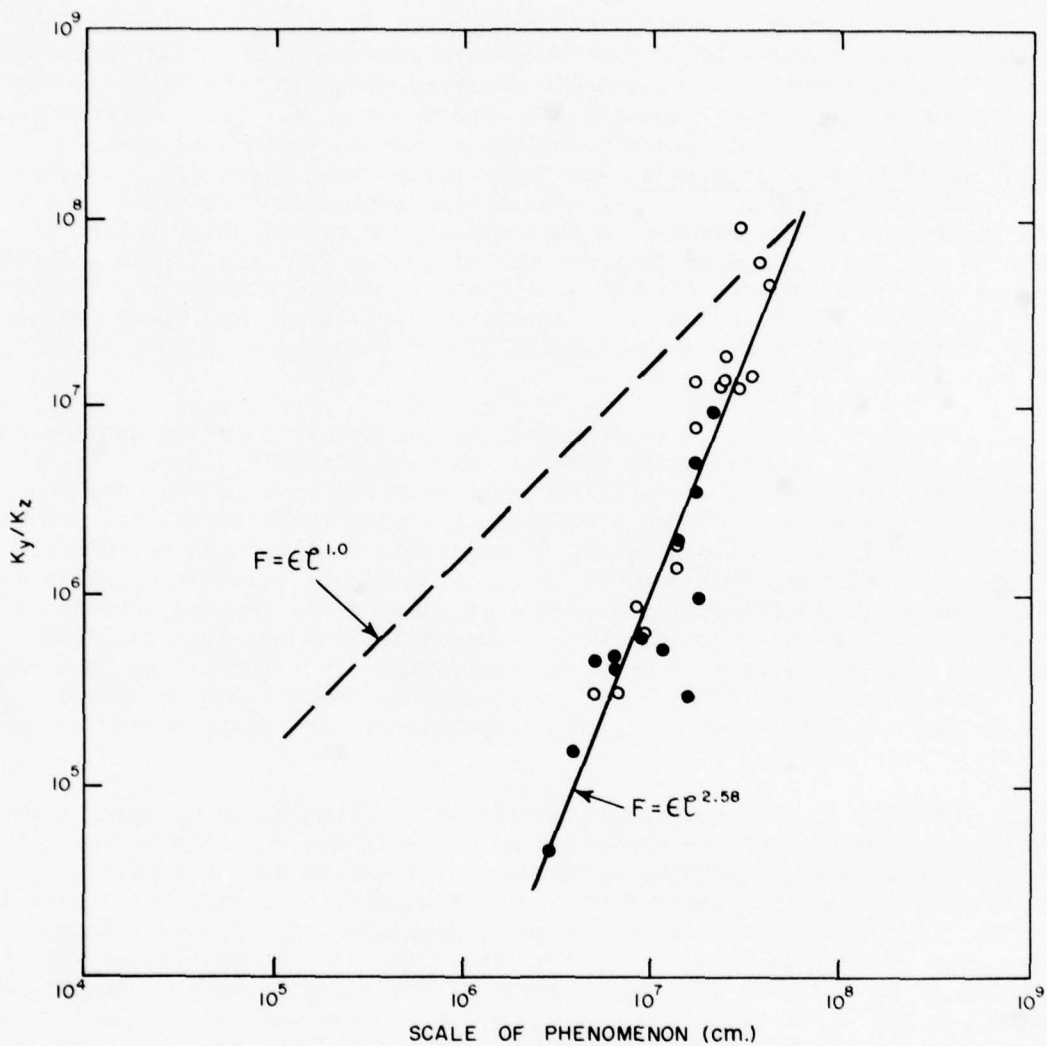


Fig. 40--Relationship between the ratio of horizontal to vertical eddy coefficients of diffusion and the scale of the phenomenon.

From the above two approaches it appears that the horizontal diffusion coefficients are of the order of  $10^7 \text{ cm}^2 \text{ sec}^{-1}$  with a definite tendency in the offshore regions for the values to increase with distance from shore. In the nearshore tidal and hydraulic region (less than 50 km from the river mouth) the coefficient is considerably less. This area is now being studied in more detail.

From these results it would seem that an empirical model could be made which would allow prediction of the distribution of the Columbia River plume. By plotting the weekly trajectories of water movement it is possible to arrive at a predicted axis. Using the solution of Roberts (1923) and the derived eddy coefficients the lateral boundaries of the plume could be predicted from month to month throughout the year. Application of this technique to the dispersion of river water in the open ocean awaits a better evaluation of the changes of the eddy coefficient with distance from the river mouth.

#### SUMMARY

The freshwater flow from the mouth of the Columbia River, located at the boundary between Oregon and Washington, is 14 percent of the annual runoff from the United States and represents the major supply of freshwater to the open ocean along the coast from the Strait of Juan de Fuca to San Francisco Bay. During the spring the peak discharge of nearly  $17,000 \text{ m}^3 \text{ sec}^{-1}$  ( $600,000 \text{ ft}^3 \text{ sec}^{-1}$ ) is associated with the snow-melt of the interior mountains and during winter a secondary peak of about  $7,000 \text{ m}^3 \text{ sec}^{-1}$  ( $250,000 \text{ ft}^3 \text{ sec}^{-1}$ ) corresponds to heavy coastal rainfall. The river freshwater has a significant effect on biological, geological, chemical, and physical characteristics of the adjacent open sea. After the river water is mixed with about 2 parts ambient seawater in the estuary it enters the nearshore environment in 12-hour pulses with each ebb tide where further mixing occurs through hydraulic, tidal, and surf processes. In the area between the mouth and 40 to 50 km seaward, the river water is mixed with about 10 parts of ambient seawater having a salinity of approximately 32.5‰. Thence the effluent enters into the offshore ocean regime characterized by weak north setting currents and winds in the winter and south setting currents and winds in the summer. The effluent is confined to the surface layer; it is rarely found below 40 meters where a sharp pycnocline limits downward mixing but spreads laterally over a large area. In the ocean regime the pancake-like effluent is acted upon by wind stress, geostrophic currents, and turbulent processes. During the summer this water is distributed in the form of a plume extending southwest almost 900 kilometers from the river mouth to near  $40^\circ \text{N}$  latitude. During the winter the effluent lies in a 40 to 55-km wide belt of low salinity water adjacent to the coast from 40 km south of the mouth of the Columbia to north of the Strait of Juan de Fuca.

This description of the dispersion of Columbia River water in the sea is based on 12 oceanographic surveys conducted during 1961 and 1962. A technique of computing wind driven transport of the effluent waters has been developed and this program, along with detailed observations of the geostrophic currents, shows promise as a technique for predicting the axis of the

plume. Studies of the lateral and vertical diffusion of river water by turbulent mixing indicate that the salt flux is preferentially upward and the vertical eddy coefficient in the offshore region is in the range of 1 to  $10 \text{ cm}^2 \text{sec}^{-1}$ . The lateral eddy coefficient was estimated by two techniques and found to be about  $10^7 \text{ cm}^2 \text{sec}^{-1}$ . A model for the diffusion of the effluent waters in the offshore region could be developed from these results, but application of the model awaits the evaluation of the variation of the vertical eddy coefficient with distance from the river mouth.

#### Future Work

It is realistic to divide the study of the effects of the Columbia River water in the sea into three phases. The first phase is the study of the offshore regions. This phase was the major concern during 1961 and 1962, and the major portion of this study is reported in this paper. The second phase is an investigation of the more complicated nearshore environment from the river mouth to the limit of major tidal and hydraulic influences. Stations spaced closely in time and place using more than one ship are necessary to investigate this region of rapid mixing. Exploratory cruises in the nearshore regime were conducted during the summer of 1963 and plans are being made for an intensive investigation of the nearshore region during 1964. Emphasis will be placed on mixing rates, circulation, upwelling, estimations of eddy coefficients and a general three dimensional description by multiship sampling, dye studies, moored current meter studies, and radio beacon current drogues.

A third phase involves the study of estuarine circulation, mixing, sedimentation, and biological transport of suspended and dissolved constituents. Past investigations have been limited to studies by the U.S. Army Engineers in 1959, oceanographic exploratory sampling in the summer of 1963 by the University of Washington, and model studies by the U.S. Army Engineers and U.S. Geological Survey.

Estuary studies by field and model investigations being conducted by others will lead to a better understanding of the nearshore and offshore regimes.

The investigations envisioned for the near future in the offshore area are:

1. Studies of upwelling and divergence areas.
2. Measurements of currents near the Columbia River and Strait of Juan de Fuca.
3. Evaluation of eddy coefficients.
4. Deep and bottom current measurements.
5. Detailed studies on the short-term fluctuations in mass structure.
6. Observations leading toward a better understanding of baroclinic response times.
7. Total transport computations through an extension of the wind program.

## ACKNOWLEDGMENTS

Dr. Alyn Duxbury aided in various phases of this study and made significant contributions to the studies of diffusion of river water. Field observations were conducted under the leadership of Messrs. Eugene Collias, Cuthbert Love, John Stevens, and others from the Department of Oceanography at the University of Washington. The efforts of the many scientists who assisted at sea and the cooperation of the officers and crew of the R. V. Brown Bear are gratefully acknowledged. Mr. Bruce Wyatt and members of the Department of Oceanography at Oregon State University assisted by providing vital data in 1961 and 1962. The observations taken by the Pacific Oceanographic Group also aided in this study. The significant efforts of Miss Helen Koo, Miss Betty-Ann Morse, Mrs. Linley Chapman, Mrs. Monique Rona, Messrs. Don Doyle, Noel McGary, Harvey Peterson, Gerry Schimke, and John Watson are acknowledged.

## REFERENCES

- Anderson, G. C. 1964. Columbia River effluent in the northeast Pacific Ocean 1961-1962: Selected aspects of phytoplankton distribution and production. University of Washington, Department of Oceanography, Tech. Rept. No. 96, Ref. M63-50. 77 p.
- Barnes, C. A., and R. G. Paquette. 1957. Circulation near the Washington coast. Proceedings of the Eighth Pacific Science Congress--Oceanography, 3:583-608.
- Barnes, C. A., and C. M. Love. 1963. Physical chemical and biological data from the northeast Pacific Ocean: Columbia River effluent area, January-June 1961. University of Washington, Department of Oceanography, Tech. Report No. 86, Ref. M63-13. 405 p.
- Bates, C. C. 1953. Rational theory of delta formation. Bull. Am. Assoc. Petrol. Geologists, 37(9):2119-2162.
- Bennett, E. B. 1959. Some oceanographic features of the northeast Pacific Ocean during August 1955. J. Fisheries Res. Board Can., 16(5):565-633.
- Bol'shakov, V. S. 1958. O kontakte rechnykh i morskikh vod v severo-zapadnoi chasti chernogo moria (meeting of river and seawater in the N.W. part of the Black Sea). Akad. Nauk SSSR, Izvestiya, Ser. Geofiz., No. 4. P. 554-557.
- Brooks, N. H. 1960. Diffusion of sewage effluent in an ocean current. In waste disposal in the marine environment. Proc. 1st Int. Conf. on Waste Disposal in the Marine Environment. Univ. of Cal., Berkeley, 22-25 July 1959. Pergamon Press, New York. P. 246-267.

Bureau of Reclamation. 1947. The Columbia River: A comprehensive report on the development of the water resources of the Columbia River basin for irrigation, power production, and other beneficial uses in Idaho, Montana, Nevada, Oregon, Utah, Washington, and Wyoming. U.S. Dept. Interior, 1:393 p.

Chau, Y. K. 1959. The influence of the outflow from the Pearl River on the waters of South China Sea. Intern. Oceanog. Congr., 1st, New York, 1959. Preprints of Abstracts of Papers, Am. Assoc. Advan. Sci., Washington, D.C. P. 678-682.

Crank, J. 1956. The mathematics of diffusion. Oxford University Press, London. 347 p.

Cromwell, T. 1960. Pycnoclines in a Tank. J. of Marine Res., 18(2):73-82.

Deacon, E. L., and E. K. Webb. 1962. Interchange of properties between sea and air, small scale interactions. In The Sea, ideas and observations on progress in the study of the sea, M. N. Hill. Interscience, New York, 1:43-87.

Defant, A. 1950. Reality and illusion in oceanographic surveys. J. Marine Res., 9(2):120-138.

\_\_\_\_\_. 1961. Physical oceanography. Pergamon Press, New York, 1:540-543.

Dobrovolskii, A. D., V. G. Zavriev, and A. N. Kosarev. 1961. Tsvet i prozrachnost', kok preznoki rechnikh vod v more. Okeanologiya, 1(4): 626-629.

Dodimead, A. J. 1958. Report on oceanographic investigations in the northeast Pacific Ocean during August 1956, February 1957, and August 1957. J. Fisheries Res. Board Can., Manuscript Report Series (Oceanographic and Limnological) No. 20. Pacific Oceanographic Group, Nanaimo, Canada. 14 p.

\_\_\_\_\_. 1961. The geostrophic circulation and its relations to the water characteristics in the northeast Pacific Ocean during the period 1955-1960. Abstracts of Symp. Papers Tenth Pac. Sci. Congr., Honolulu. P. 343.

\_\_\_\_\_, F. Favorite, and T. Hirano. 1963. Review of oceanography of the Subarctic Pacific region. Intern. North Pacific Fisheries Comm., Bull. 13, pt. II. 195 p.

\_\_\_\_\_, and H. J. Hollister. 1962. Canadian drift bottle releases and recoveries in the North Pacific Ocean. Fisheries Res. Board Can., Manuscript Report Series (Oceanographic and Limnological), No. 141. 43 figures. Pacific Oceanographic Group, Nanaimo, Canada.

Doe, L. A. E. 1955. Offshore waters of the Canadian Pacific coast. J. Fisheries Res. Board Can., 12(1):1-34.

- Ekman, V. W. 1902. Om jordrotationens inverkan på vindströmmar i havvet. Nat. Mag. Naturvid, Vol. 40. Kristiania.
- . 1905. On the influence of the earth's rotation on ocean currents. Ark. F. Mat. Astr. och Fysik. K. Suf. Vet. Ak., Stockholm, 1905-6, 2(11).
- . 1928. Eddy viscosity and skin friction in the dynamics of winds and ocean currents. Memoirs of the Roy. Meteorol. Soc., 2:161-172.
- Fjarlie, R. L. I. 1950. The oceanographic phase of the Vancouver sewage problem. Manuscript Report, Joint Committee on Oceanography. Pacific Oceanographic Group, Nanaimo, Canada.
- Fleming, R. H. 1955. Review of the oceanography of the Northern Pacific. Intern. North Pacific Fisheries Comm., Bull. 2:1-43.
- . 1958. Notes concerning the halocline in the northeastern Pacific Ocean. J. Marine Res., 17(28):158-173.
- Fofonoff, N. P. 1960. Transport computations for the North Pacific Ocean, 1955. J. Fisheries Res. Board Can., Manuscript Report Series (Oceanographic and Limnological), No. 77. Pacific Oceanographic Group, Nanaimo, Canada.
- . 1962. Mass transport in the North Pacific. Abstracts of Symp. Papers. Tenth Pac. Sci. Congr., Honolulu (1961). 344 p.
- Gifford, F., Jr. 1959. Statistical properties of a fluctuating plume dispersion model. In Advan. Geoph., Academic Press, New York-London. P. 117-137.
- Gordon, A. H. 1950. The ratio between observed velocities of the wind at 50 ft. and 2,000 ft. over the North Atlantic Ocean. Quart. J. Roy. Meteorol. Soc., 76:344-348.
- Gross, M. G., J. S. Creager, and D. A. McManus. 1963. Preliminary report on the sediments and radioactivity in the vicinity of the Columbia River effluent. Univ. of Washington, Dept. of Oceanography, Tech. Report No. 84, Ref. M63-2. 32 p.
- Hamada, T. 1959. Two properties of the stratified density current at a river mouth. Intern. Assoc. Hydraulic Res., 8th Congress, 2:2C1-2C23.
- Holland-Hansen, B. 1934. The Sognefjord Section. Oceanographic observations in the northernmost part of the North Sea and the southern part of the Norwegian Sea. James Johnstone Memorial Volume. Univ. Press of Liverpool, Liverpool. P. 257-274.
- Henry, V. J., and R. B. Elder. 1958. A study of some factors involved in the disposal of radioactive wastes in the sea. Part II. Physical oceanography and sedimentology. The A. and M. College of Texas. Annual Report, Ref. 58-2A. 18 p.

- Hidaka, K. 1954. A contribution to the theory of upwelling and coastal currents. *Trans. Am. Geophys. Union*, 35(3):431-444.
- Ichiye, T. 1960. On the hydrography near Mississippi Delta. *Oceanographical Magazine*, Tokyo. 11(2):65-78.
- \_\_\_\_\_. 1962. Oceanic turbulence. *Oceanographic Institute Florida State University*. Tech. Paper No. 2.
- Jacobs, W. C. 1951. The energy exchange between the sea and atmosphere and some of the consequences. *Univ. of Cal., Scripps Institution of Oceanography Bulletin*, 6(2):27-122.
- Ketchum, B. H., and D. J. Keen. 1955. The accumulation of river water over the continental shelf between Cape Cod and Chesapeake Bay. *In Marine Biology and Oceanography, Supplement to Vol. 3 of Deep Sea Research*. P. 346-357.
- Langbein, W. B., and others. 1949. Annual runoff in the United States. *U.S. Geological Survey Circular 52*, United States Department of the Interior, Washington, D.C.
- Leipper, D. F. 1959. The classical hydrographic procedure and its relation to the physical and chemical properties of seawater. *In Physical and Chemical Properties of Sea Water*. Publication No. 600, National Academy of Science--National Research Council. P. 1-9.
- Leopold, L. B. 1962. Rivers. *Am. Scientist*, 50(4):511-537.
- Marmer, H. A. 1926. Coastal currents along the Pacific coast of the United States. *Department of Commerce, U.S. Coast and Geological Survey*. Special Pub. 121, Washington, D.C.
- McEwen, G. F. 1934. Rate of upwelling in the region of San Diego computed from serial temperatures. *Fifth Pac. Sci. Congress*, 1933, 3:1763.
- \_\_\_\_\_. 1948. The dynamics of large horizontal eddies (axes vertical) in the ocean off southern California. *J. Marine Res.*, 7:188-216.
- Montgomery, R. B. 1935. Transport of surface-water due to the wind system over the North Atlantic. *In Physical Oceanography and Meteorology*. Woods Hole Oceanographic Inst. and M.I.T., 4(3):23-30.
- Munk, W. H. 1950. On the wind-driven ocean circulation. *J. Meteorol.*, 7(2):79-93.
- National Academy of Sciences, National Research Council. 1957. The effects of atomic radiation on oceanography and fisheries. *NAS-NRC study of the biological effects of atomic radiation*. Publication No. 551, Washington, D.C. 137 p.

- \_\_\_\_\_. 1962. Disposal of low-level radioactive waste into Pacific coastal waters. A report of a Working Group of the Committee on Oceanography, NAS-NRC. Publication No. 985. 87 p.
- Okubo, A. 1962. A review of theoretical models of turbulent diffusion in the sea. Chesapeake Bay Institute, The Johns Hopkins University, Tech. Report No. 30. Ref. 62-20. 105 p.
- Palmén, E., and E. Laurila. 1938. Über die Einwirkung eines Sturmes auf den hydrographischen Zustand im nördlichen Ostseegebiet. Societas Scientiarum Fennica, Commentationes Physico-Mathematicae, 10(1):29-31.
- Pearson, E. A. 1960. Proceedings of the first international conference on waste disposal in the marine environment. Univ. of Calif. Pergamon Press, New York. 569 p.
- Pritchard, D. W., and J. H. Carpenter. 1960. Measurement of turbulent diffusion in estuarine and inshore waters. Bull. Int. Assoc. Sci. Hydrol. No. 20. P. 37-50.
- Pytkowicz, R. M. In press. Oxygen exchange rates off the Oregon coast. Deep Sea Research.
- Reid, J. L., Jr. 1960. Oceanography of the northeastern Pacific Ocean during the last ten years. California Cooperative Oceanographic Fisheries Investigations Report, Vol. VII. P. 77.
- \_\_\_\_\_, R. A. Schwartzlose, and D. M. Brown. 1963. Direct measurements of a small surface eddy off northern Baja California. J. Marine Res. 21(3):205-218.
- Reid, R. O. 1959. Influence of some errors in the equation of state or in observations on geostrophic currents. In Physical and chemical properties of seawater. Publ. No. 600, National Academy of Sciences--National Research Council. P. 10-29.
- Richards, F. A., and U. Stefansson. 1963. Silicate-salinity relationships in the Columbia River effluent. Trans. Am. Geophys. Union (abstract), 44(1):213.
- Riley, G. A. 1937. The significance of the Mississippi River drainage for biological conditions in the northern Gulf of Mexico. J. Marine Res., 1:60-74.
- Roberts, O. F. T. 1923. The theoretical scattering of smoke in a turbulent atmosphere. Proc. Roy. Soc. (London), Ser. A, 104:640-654.
- Rossby, C. G., and R. B. Montgomery. 1935. The layer of frictional influence in wind and ocean currents. Papers Phys. Oceanog. Meteorol., Woods Hole and M.I.T., 3(3):12-14.
- Rousse, H., and J. Dodu. 1955. Diffusion turbulente à travers une suite de densités. La Houille Blanche. August-September (4):522-532 (in English).

- Saito, Y. 1951. On the velocity flow in the ocean. *J. Inst. Polytech.*, Osaka City Univ., Ser. B., 2:1-4.
- Scruton, P. G., and D. G. Moore. 1953. Distribution of surface turbidity off Mississippi Delta. *Bull. Am. Assoc. Petrol. Geol.*, 37(5):1067-1074.
- Sheppard, P. A. 1958. Transfer across the earth's surface or through the air above. *Quart. J. Roy. Met. Soc.*, 84:205-224.
- Stefánsson, U., and F. A. Richards. 1963. Processes contributing to the nutrient distribution of the Columbia River and Strait of Juan de Fuca. *Limnol. Oceanog.*, 8(4):394-410.
- \_\_\_\_\_, and F. A. Richards. In press. Distribution of dissolved oxygen, density, and nutrients off the Washington and Oregon coasts. *Deep Sea Research*.
- Stommel, H. 1948. The westward intensification of wind-driven ocean currents. *Trans. Am. Geophys. Union.*, 29:202-206.
- \_\_\_\_\_. 1949. Horizontal diffusion due to oceanic turbulence. *J. Marine Res.*, 8(3):199.
- Sutton, O. G. 1953. *Micrometeorology*. McGraw-Hill Book Co., Inc., New York. 33 p.
- Sverdrup, H. U. 1946. Speculations on horizontal diffusion in the ocean. Scripps Institution of Oceanography, Oceanographic Report No. 1. 3 p.
- \_\_\_\_\_. 1947. Wind driven currents in a baroclinic ocean; with application to the equatorial currents of the eastern Pacific. *Proc. Nat. Acad. Sci.*, 33(11):318-326.
- \_\_\_\_\_, and R. H. Fleming. 1941. The waters off the coast of southern California, March to July 1937. Scripps Institution of Oceanography, Univ. of Calif., *Bull.* 4(10):261-378.
- Sylvester, R. O., and D. A. Carlson. 1961. Lower Columbia River basic water quality data analysis for the year 1960. Dept. of Civil Engineering, University of Washington. 49 p.
- Takano, K. 1954. On the velocity distribution off the mouth of a river. *J. Oceanog. Soc. Japan*, 10(2):60-64.
- \_\_\_\_\_. 1954a. On the salinity and velocity distributions off the mouth of a river. *Ibid.*, 10(3):92-98.
- \_\_\_\_\_. 1955. A complementary note on the diffusion of the seaward river flow off the mouth. *Ibid.*, 11(4):147-149.
- Thompson, W. F., and R. Van Cleve. 1936. Life history of the Pacific halibut. Drift bottle studies. *Rep. Intern. Fish Comm.*, 2:50-61.

- Tully, J. P. 1938. Some relations between meteorology and coast gradient-currents of the Pacific of North America. Trans. Am. Geophys. Union, 19th Annual Meeting, Part I. P. 176-183.
- \_\_\_\_\_. 1942. Surface non-tidal currents in the approaches to Juan de Fuca Strait. J. Fish. Res. Board Can., 5(4):398-409.
- \_\_\_\_\_. 1949. Oceanography and prediction of pulp mill pollution in Alberni Inlet. J. Fish. Res. Board Can., Ottawa. 169 p.
- \_\_\_\_\_. 1958. On structure, entrainment, and transport in estuarine embayments. J. Mar. Res., 17:523-535.
- \_\_\_\_\_, and F. G. Barber. 1960. An estuarine analogy in the Sub-Arctic Pacific Ocean. J. Fish. Res. Board Can., 17(1):92-112.
- \_\_\_\_\_, and A. J. Dodimead. 1957. Canadian oceanographic research in the North Pacific Ocean. J. Fish. Res. Board Can., Manuscript Report Series (Oceanographic and Limnological), Pacific Oceanographic Group, Nanaimo, Canada. File N 7-20-6.
- Uda, M. 1963. Oceanography of the Sub-Arctic Pacific Ocean. J. Fish. Res. Board Can., 20(1):119-179.
- United States Army Corps of Engineers. 1960. Interim report on 1959 current measuring program--Columbia River at mouth Oregon and Washington, vols. I-IV. U.S. Army Engineer District, Portland, Oregon.
- United States Geological Survey. 1955-1961. Surface water supply of the United States 1950-1960. Geological Survey Water-Supply Papers, Parts 11, 12, 14. U.S. Government Printing Office, Washington, D.C.
- \_\_\_\_\_. 1961-1963. Weekly report, Pacific Northwest water resources. Current Records Center, Portland, Oregon.
- Von Arx, W. S. 1962. An introduction to physical oceanography. Addison-Wesley, Massachusetts. 422 p.
- Waldichuk, M. 1963. Vertical diffusion in the sea from a radioactive point source. J. Fish. Res. Board Can. Manuscript Report Series (Oceanographic and Limnological) No. 155. Pacific Oceanographic Group, Nanaimo, Canada.
- Washington (State) Pollution Control Commission, Department of Conservation, U.S. Geological Survey. 1961. Quality of surface waters, June 1959-July 1960. 97 p.
- Wilson, G. W. 1960. Note on surface wind stress over water at low and high wind speeds. J. Geophys. Res., 65(10):3377-3382.

Wooster, W. S., and B. A. Taft. 1958. On the reliability of field measurements of temperature and salinity of the ocean. *J. Marine Res.*, 17:552-566.

Wyatt, B., and N. F. Kujala. 1962. Hydrographic data from Oregon coastal waters, June 1960-May 1961. Oregon State University, Department of Oceanography Data Report No. 7.

UNCLASSIFIED TECHNICAL REPORTS DISTRIBUTION LIST  
for OCEANOGRAPHIC CONTRACTORS  
of the GEOPHYSICS BRANCH  
of the OFFICE OF NAVAL RESEARCH  
(Revised October 1963)

DEPARTMENT OF DEFENSE

- 1 Director of Defense Research & Engineering  
Attn: Coordinating Committee on Science  
Pentagon  
Washington 25, D. C.  
1 Attn: Office, Assistant Director (Research)

- 10 Commanding Officer  
Office of Naval Research Branch  
Navy #100, Fleet Post Office  
New York, New York  
1 Oceanographer  
Office of Naval Research  
Navy #100, Box 39  
Fleet Post Office  
New York, New York

NAVY

- 2 Office of Naval Research  
Geophysics Branch (Code 416)  
Washington 25, D. C.

- Office of Naval Research  
Washington 25, D. C.  
1 Attn: Biology Branch (Code 446)  
1 Attn: Surface Branch (Code 463)  
1 Attn: Undersea Warfare (Code 466)  
1 Attn: Special Projects (Code 418)

- 1 Commanding Officer  
Office of Naval Research Branch  
495 Summer Street  
Boston 10, Massachusetts

- 1 Commanding Officer  
Office of Naval Research Branch  
207 West 24th Street  
New York 11, New York

- 1 Commanding Officer  
Office of Naval Research Branch  
230 N. Michigan Avenue  
Chicago, Illinois 60601

- 1 Commanding Officer  
Office of Naval Research Branch  
1000 Geary Street  
San Francisco 9, California

- 1 Commanding Officer  
Office of Naval Research Branch  
1030 East Green Street  
Pasadena 1, California

- 1 Contract Administrator  
Southeastern Area  
Office of Naval Research  
2110 "G" Street, N. W.  
Washington 7, D. C.

- 1 ONR Special Representative  
c/o Hudson Laboratories  
Columbia University  
145 Palisade Street  
Dobbs Ferry, New York

- 6 Director  
Naval Research Laboratory  
Attn: Code 5500  
Washington 25, D. C.

(Note: 3 copies are forwarded by the above addressee to the British Joint Services Staff for further distribution in England and Canada.)

- 1 Oceanographer  
Chief of Naval Operations  
OP-09B5  
Washington 25, D. C.

- 1 Commander  
U. S. Naval Oceanographic Office  
Washington 25, D. C.  
Attn: Library (Code 1640)

- 1 U. S. Naval Branch  
Oceanographic Office  
Navy 3923, Box 77, F.P.O.  
San Francisco, California

- Chief, Bureau of Naval Weapons  
Department of the Navy  
Washington 25, D. C.
- 1 Attn: FASS  
1 Attn: RU-222
- 1 Office of the U. S. Naval Weather Service  
U. S. Naval Station  
Washington 25, D. C.
- 1 Chief, Bureau of Yards & Docks  
Office of Research  
Department of the Navy  
Washington 25, D. C.  
Attn: Code 70
- 1 Commanding Officer & Director  
U. S. Navy Electronics Laboratory  
San Diego 52, California
- 1 Attn: Code 2201  
1 Attn: Code 2420
- 1 Commanding Officer & Director  
U. S. Naval Civil Engineering Laboratory  
Port Hueneme, California  
Attn: Code L54
- 1 Code 3145  
Box 7  
Pt. Mugu Missile Range  
Pt. Mugu, California
- 1 Commander, Naval Ordnance Laboratory  
White Oak, Silver Spring, Maryland  
Attn: E. Liberman, Librarian
- 1 Commanding Officer  
Naval Ordnance Test Station  
China Lake, California
- 1 Attn: Code 753  
1 Attn: Code 508
- 1 Commanding Officer  
Naval Radiological Defense Laboratory  
San Francisco, California
- 1 Commanding Officer  
U. S. Naval Underwater Ordnance Station  
Newport, Rhode Island
- Chief, Bureau of Ships  
Department of the Navy  
Washington 25, D. C.
- 1 Attn: Code 373
- 1 Officer-in-Charge  
U. S. Navy Weather Research Facility  
Naval Air Station, Bldg. R-48  
Norfolk, Virginia
- 1 U. S. Fleet Weather Facility  
U. S. Naval Station  
San Diego 35, California
- 1 Commanding Officer  
U. S. Navy Air Development Center  
Johnsville, Pennsylvania  
Attn: NADC Library
- 1 Superintendent  
U. S. Naval Academy  
Annapolis, Maryland
- 2 Department of Meteorology & Oceanography  
U. S. Naval Postgraduate School  
Monterey, California
- 1 Commanding Officer  
U. S. Naval Underwater Sound Laboratory  
New London, Connecticut
- 1 Commanding Officer  
U. S. Navy Mine Defense Lab.  
Panama City, Florida
- 1 Commanding Officer  
U. S. Fleet Weather Central  
Navy Department  
Washington 25, D. C.
- 1 Officer-in-Charge  
U. S. Fleet Numerical Weather Facility  
Monterey, California

AIR FORCE

- 1 Hdqtrs., Air Weather Service  
(AWSS/TIPD)  
U. S. Air Force  
Scott Air Force Base, Illinois
- 1 ARCLR (CRZF)  
L. G. Hanscom Field  
Bedford, Massachusetts

ARMY

- 1 Army Research Office  
Office of the Chief of R & D  
Department of the Army  
Washington 25, D. C.
- 1 U. S. Army Beach Erosion Board  
5201 Little Falls Road, N. W.  
Washington 16, D. C.
- 1 Army Research Office  
Washington 25, D. C.  
Attn: Environmental Sciences Div.

OTHER U. S. GOVERNMENT AGENCIES

- 1 Office of Technical Services  
Department of Commerce  
Washington 25, D. C.
- 20 Defense Documentation Center  
Cameron Station  
Alexandria, Virginia
- 2 National Research Council  
2101 Constitution Avenue  
Washington 25, D. C.  
Attn: Committee on Undersea Warfare  
Attn: Committee on Oceanography
- 1 Laboratory Director  
Biological Laboratory  
Bureau of Commercial Fisheries  
P. O. Box 6121, Pt. Loma Street  
San Diego, California
- 1 Commandant (OSR-2)  
U. S. Coast Guard  
Washington 25, D. C.

1 Commanding Officer  
Coast Guard Oceanographic Unit  
Bldg. 159, Navy Yard Annex  
Washington 25, D. C.

1 Director  
Coast & Geodetic Survey  
U. S. Department of Commerce  
Washington 25, D. C.  
Attn: Office of Oceanography

1 Geological Division  
Marine Geology Unit  
U. S. Geological Survey  
Washington 25, D. C.

1 Director of Meteorological Research  
U. S. Weather Bureau  
Washington 25, D. C.

1 Director  
U. S. Army Engineers Waterways  
Experiment Station  
Vicksburg, Mississippi  
Attn: Research Center Library

1 Laboratory Director  
Bureau of Commercial Fisheries  
Biological Laboratory  
450-B Jordan Hall  
Stanford, California

1 Bureau of Commercial Fisheries  
U. S. Fish & Wildlife Service  
Post Office Box 3830  
Honolulu 12, Hawaii

1 Attn: Librarian

1 Laboratory Director  
Biological Laboratory  
Bureau of Commercial Fisheries  
P. O. Box 3098, Fort Crockett  
Galveston, Texas

1 Laboratory Director  
Biological Laboratory, Auke Bay  
Bureau of Commercial Fisheries  
P. O. Box 1155  
Juneau, Alaska

- 1 Laboratory Director  
 Biological Laboratory  
 Bureau of Commercial Fisheries  
 P. O. Box 6  
 Woods Hole, Massachusetts
- 1 Laboratory Director  
 Biological Laboratory  
 Bureau of Commercial Fisheries  
 P. O. Box 280  
 Brunswick, Georgia
- 1 Laboratory Director  
 Biological Laboratory  
 Bureau of Commercial Fisheries  
 P. O. Box 271  
 La Jolla, California
- 1 Bureau of Sport Fisheries & Wildlife  
 U. S. Fish and Wildlife Service  
 Sandy Hook Marine Laboratory  
 P. O. Box 428  
 Highlands, New Jersey  
 Attn: Librarian
- 1 Director  
 National Oceanographic Data Center  
 Washington 25, D. C.
- 2 Defense Research Member  
 Canadian Joint Staff  
 2450 Massachusetts Avenue, N. W.  
 Washington 8, D. C.
- 2 Library, U. S. Weather Bureau  
 Washington 25, D. C.
- 1 Director, Biological Laboratory  
 Bureau of Commercial Fisheries  
 Navy Yard Annex  
 Building 74  
 Washington 25, D. C.
- 2 Director, Bureau of Commercial  
 Fisheries  
 U. S. Fish & Wildlife Service  
 Department of Interior  
 Washington 25, D. C.
- 1 Dr. Orlo E. Childs  
 U. S. Geological Survey  
 345 Middlefield Road  
 Menlo Park, California
- 1 Dr. John S. Schlee  
 U. S. Geological Survey  
 c/o Woods Hole Oceanographic  
 Institution  
 Woods Hole, Massachusetts
- RESEARCH LABORATORIES
- 2 Director  
 Woods Hole Oceanographic Inst.  
 Woods Hole, Massachusetts
- 3 Project Officer  
 Laboratory of Oceanography  
 Woods Hole, Massachusetts
- 1 Director  
 Narragansett Marine Laboratory  
 University of Rhode Island  
 Kingston, Rhode Island
- 1 Bingham Oceanographic Labs.  
 Yale University  
 New Haven, Connecticut
- 1 Gulf Coast Research Laboratory  
 Post Office Box  
 Ocean Springs, Mississippi  
 Attn: Librarian
- 1 Chairman, Department of  
 Meteorology and Oceanography  
 New York University  
 New York 53, New York
- 1 Director  
 Lamont Geological Observatory  
 Torrey Cliff  
 Palisades, New York
- 1 Director  
 Hudson Laboratories  
 145 Palisade Street  
 Dobbs Ferry, New York
- 1 Great Lakes Research Division  
 Institute of Science & Technology  
 University of Michigan  
 Ann Arbor, Michigan
- 1 Attn: Dr. John C. Ayers

- 1 Dr. Harold Haskins  
Rutgers University  
New Brunswick, New Jersey
- 1 Director  
Chesapeake Bay Institute  
Johns Hopkins University  
121 Maryland Hall  
Baltimore 18, Maryland
- 1 Mail No. J-3009  
The Martin Company  
Baltimore 3, Maryland  
Attn: J. D. Pierson
- 1 Mr. Henry D. Simmons, Chief  
Estuaries Section  
Waterways Experiment Station  
Corps of Engineers  
Vicksburg, Mississippi
- 1 Director, Marine Laboratory  
University of Miami  
#1 Rickenbacker Causeway  
Virginia Key  
Miami 49, Florida
- 1 Nestor C. L. Granelli  
Department of Geology  
Columbia University  
Palisades, New York
- 2 Head, Department of Oceanography  
& Meteorology  
Texas A & M College  
College Station, Texas
- 1 Director  
Scripps Institution of Oceanography  
La Jolla, California
- 1 Allan Hancock Foundation  
University Park  
Los Angeles 7, California
- 1 Head, Department of Oceanography  
Oregon State University  
Corvallis, Oregon
- 1 Department of Engineering  
University of California  
Berkeley, California
- 1 Director  
Arctic Research Laboratory  
Barrow, Alaska
- 1 Dr. C. I. Beard  
Boeing Scientific Research Labs.  
P. O. Box 3981  
Seattle 24, Washington
- 1 Head, Department of Oceanography  
University of Washington  
Seattle 5, Washington
- 1 Geophysical Institute of the  
University of Alaska  
College, Alaska
- 1 Director  
Bermuda Biological Station  
for Research  
St. Georges, Bermuda
- 1 Technical Information Center, CU-201  
Lockheed Missile and Space Division  
3251 Hanover Street  
Palo Alto, California
- 1 University of Pittsburgh  
Environmental Sanitation  
Department of Public Health Practice  
Graduate School of Public Health  
Pittsburgh 13, Pennsylvania
- 1 Director  
Hawaiian Marine Laboratory  
University of Hawaii  
Honolulu, Hawaii
- 1 Dr. F. B. Berger  
General Precision Laboratory  
Pleasantville, New York
- 1 Dr. J. A. Gast  
Wildlife Building  
Humboldt State College  
Arcata, California
- 1 Department of Geodesy & Geophysics  
Cambridge University  
Cambridge, England

- 1 Applied Physics Laboratory  
University of Washington  
1013 NE Fortieth Street  
Seattle 5, Washington
- 1 Documents Division - ml  
University of Illinois Library  
Urbana, Illinois
- 1 Director  
Ocean Research Institute  
University of Tokyo  
Tokyo, Japan
- 1 Marine Biological Association  
of the United Kingdom  
The Laboratory  
Citadel Hill  
Plymouth, England
- 1 ASW Information Research Unit  
Building 80, Plant A-1  
Lockheed-California Company  
Burbank, California
- 1 New Zealand Oceanographic Institute  
Department of Scientific and  
Industrial Research  
P. O. Box 8009  
Wellington, New Zealand  
Attn: Librarian
- 1 President  
Osservatorio Geofisico Sperimentale  
Trieste, Italy
- 1 Advanced Research Projects Agency  
Attn: Nuclear Test Detection Office  
The Pentagon  
Washington 25, D. C.
- 1 Chemistry Department  
College of Engineering  
University of Wisconsin  
Madison 6, Wisconsin
- 1 American Biophysical Research Lab.  
P. O. Box 552  
Lansdale, Pennsylvania
- 1 Department of Geology & Geophysics  
~~Massachusetts Institute of Technology~~  
Cambridge 39, Massachusetts
- 1 Institute of Geophysics  
University of Hawaii  
Honolulu 14, Hawaii
- 1 Dr. Wilbur Marks  
Oceanics, Inc.  
114 East 40th Street  
New York 16, New York
- 1 Mr. Neil L. Brown  
Bissett-Berman Corporation  
"G" Street Pier  
San Diego, California